Projecte de Fi de Màster

Ciència i Enginyeria de Materials

Antibacterial properties of antibiotic-loaded PHB grafted on titanium surface for biomedical applications

MEMÒRIA

Autor: Marta González Oller

Director: José Maria Manero Planella

Ponent: Alejandra Rodríguez Contreras

Convocatòria: Juny 2014

Escola Tècnica Superior
d'Enginyeria Industrial de Barcelona

Abstract

With the evolution of human civilization, the field of biomaterials evolved relating different materials with a simple focus: to extend human life and improve the quality of life. Materials used for biomedical applications must exhibit specific properties. Titanium is well-known to be a material used for implants because of its high strength, biocompatibility and high resistance corrosion. It can be used as hard tissue implant, such as artificial bone, hip joint, dental and bone plate. Nevertheless, a relevant aspect of the use of biomaterials is linked with medical device-related and post-operative infections. A promising approach for reducing the occurrences of infections is to provide the surfaces of biomedical devices and implants with features that are unfavourable for bacterial attachment and proliferation.

Therefore, the aim of the present work is focused to develop a new method to combine the antibacterial properties of antibiotic-loaded Poly(3-hydroxybutyrate) (PHB) nano- and micro-spheres, and poly(ethylene glycol) (PEG) as an antifouling agent, with titanium, as the base material for implants, in order to obtain biomimetic surfaces with antibacterial activity.

The titanium surfaces were linked to both PHB particles and PEG by covalent bond. This attachment was carried out by firstly activating the titanium surfaces with either plasma or sodium hydroxide. Further functionalization of the activated surfaces were carried out with two different alkoxysilanes which provided the titanium surfaces different organofunctional groups that allowed the reaction with PHB particles or with PEG. A difunctionalized PEG was used in one last step, which allowed the covalent attachment with the PHB particles. Therefore, the antifouling properties of PEG were related with the antibacterial ones of the PHB spheres. Finally, the different steps of the process were evaluated. The success of the surfaces functionalization as well as the different superficial linkages was confirmed by means of the following characterization methods: contact angle, field emission scanning electron microscopy (FESEM), atomic force microscopy (AFM) and X-ray photoelectron spectroscopy (XPS). The antibacterial properties of the titanium treated surfaces were tested by means of an *in vitro* antibacterial assay using a Gram + and Gram – bacteria.

Finally, it was confirmed that the titanium surfaces achieved the antibacterial properties by combining antibiotic-loaded PHB nano- and micro-spheres, and PEG as an antifouling agent.

SUMMARY

GLOSSARY 6

1. INTRODUCTION 7

1.1. SCOPE 7

1.2. OBJECTIVES 8

1.3. BIOMATERIALS 9

1.3.1. History of biomaterials 9

1.3.2. Implantable materials 10

1.3.2.1.Biocompatibility 10

1.3.2.2.Types of implants 11

1.3.2.3.Categories/Types of biomaterials 12

1.3.2.3.1 Polymers and biopolymers 13

1.3.2.3.2 Metals 14

1.3.2.3.3 Ceramics 15

1.3.2.3.4 Composites 15

1.3.2.4.Biomaterials tissue responses 16

1.3.2.4.1 Toxic 16

1.3.2.4.2 Bioinert 16

1.3.2.4.3 Bioactive 17

1.3.2.4.4 Bioresorbable 17

1.4. TITANIUM AS A BIOMATERIAL 17

1.4.1. Properties of titanium 18

1.4.1.1.Physical properties 18

1.4.1.2.Chemical properties 18

1.4.1.3.Surface charges on hydrated titanium oxide surface 19

1.4.1.3.1 Plasma Cleaning 20

1.4.1.3.2 Sodium Hydroxide treatment 20

1.4.1.4.Corrosion Behavior 21

1.4.1.5.Mechanical properties 22

1.5. POLY 3-HYDROXYBUTYRATE (PHB) 23

1.5.1. Doxycycline (Doxy) 25

1.6. POLYETHILENEGLYCOL (PEG) 26

1.7. TITANIUM SURFACES TRANSFORMATION: APTES (HBTU) AND CPTES .. 27
1.7.1. 3-Aminopropyltriethoxysilane (APTES) 28
1.7.1.1.O-Benzotriazole-N,N,N',N'-tetramethyl-uronium-hexafluoro-phosphate (HBTU) 29
1.7.2. 3-Chloropropyltriethoxysilane (CPTES) 31
1.8. CHARACTERIZATION OF BIOMATERIALS 32
1.8.1. Wettability: Contact Angle 32
1.8.2. Scanning electron microscope (SEM) and field emission scanning electron microscope (FESEM) 34
1.8.3. Atomic force microscopy (AFM) 36
1.8.4. X-Ray Photoelectron Spectroscopy (XPS) 37
1.9. ANTIBACTERIAL CHARACTERIZATION 38
1.9.1. Staphylococcus Aureus 38
1.9.2. Escherichia Coli 39

2. MATERIALS, EQUIPMENT, AND ASSEMBLY PROCESS EXPERIMENTAL ____ 41

SAMPLES PREPARATION 41
2.1.1. Material 41
2.1.2. Sample preparation 42
FUNCTIONALIZATION PROCESS OF TITANIUM 43
2.1.3. STEP 1: SURFACE ACTIVATION 44
2.1.3.1.Plasma Cleaning 45
2.1.3.2.Sodium Hydroxide treatment 45
2.1.4. STEP 2: SILANIZATION 45
2.1.4.1.3-Aminopropyltriethoxysilane (APTES) 46
2.1.4.2.3-Chloropropyltriethoxysilane (CPTES) 47
2.1.5. STEP 3: TITANIUM SURFACES REACTION 48
2.1.5.1.A) Titanium surfaces reaction with Doxy-PHB spheres 48
2.1.5.2.B) Titanium surfaces reaction with PEG 48
IN VITRO ANTIBACTERIAL ASSAY 49
CHARACTERIZATION OF BIOMATERIALS 50
2.1.6. Wettability: Contact Angle 50
2.1.7. Field emission scanning electron microscope 50

2.1.8. Atomic force microscopy (AFM) 51
2.1.9. X-Ray Photoelectron Spectroscopy (XPS) 51

3. EXPERIMENTAL RESULTS 52

SURFACE ACTIVATION 52
3.1.1. Surface morfology 52
3.1.2. Contact angle 52
3.1.2.1.Plasma Treatment 53
3.1.2.2.Sodium Hydroxide Treatment 53
3.1.3. FESEM 54
3.1.3.1.Plasma Treatment 54
3.1.3.2.Sodium Hydroxide treatment 57
3.1.4. In vitro antibacterial Assay 62
3.1.4.1.Staphylococcus aureus (G+) 64
3.1.4.2.Escherichia coli (G-) 65
3.1.5. Atomic force microscopy 65
3.1.6. X-Ray Photoelectron Spectroscopy 66

4. DISCUSSIONS 70

CONCLUSIONS 83

AKNOWLEDGEMENTS 85

REFERENCES 87

ANNEX 91

Glossary

C. p. Ti: commercially pure titanium

NaOH: Sodium Hydroxide

APTES: 3-Aminopropyltriethoxysilane

CPTES: 3-Chloropropyltriethoxysilane

PHB: Poly 3-hydroxybutyrate

Doxy: Doxycycline

PEG: Poly ethylene glycol

HBTU: O-Benzotriazole-N,N,N',N'-tetramethyl-uronium-hexafluoro-phosphate

FESEM: Field emission scanning electron microscope

EDS: Energy Dispersive Spectroscopy

XPS: X-ray Photoelectron Spectroscopy

AFM: Atomic force microscopy

CA: contact angle goniometry

BCC: Body-Centered Cubic

HCP: Hexagonal Close-Packed

DIEA: Diisopropylethylamine

DMF: Dimethylformamide

1. INTRODUCTION

1.1. SCOPE

One of the most common problems after implant surgery is the postoperative bacterial infection. Bacteria attach and proliferate on surfaces of biomedical devices and implants [1]. In this work, antibacterial coatings have been designed to prevent initial adhesion of bacteria and their proliferation onto the implant surface. In order to accomplish these purpose biomimetic surfaces with antibacterial properties were developed with the combination of different materials.

On one hand, metallic materials have been really successful as implants due to its high strength, biocompatibility and high corrosion resistance. They have a significant clinical and economic impact on the biomaterials field, so they are used for different applications throughout the body as implants [8]. On the other hand, a promising approach for reducing the occurrences of infections is to inhibit the initial bacterial adhesion to the surface. PHB is found to be remarkable for its applications in drug delivery due to its excellent biocompatibility and biodegradability [28] and Doxycycline is a well-known broad-spectrum antibiotic, which is effective against both Gram + and Gram - bacteria, protozoa, and various anaerobes. Therefore Doxy-loaded PHB spheres are used to avoid or greatly limit bacteria attachment to the covered surface. This biopolymer was used in a previous work for the formation of Doxy-loaded micro- and nano-spheres [34]. In addition, PEG was also linked together with PHB particles in one last step, relating its antifouling properties with the antibacterial ones of the spheres. The antifouling properties of PEG-based coatings have been widely reported in the literature [2]. Physical adsorption, chemical adsorption, direct covalent attachment, and block or graft copolymerization are some of the techniques that have been used to attach PEG to surfaces [3].

This project is divided in several parts. The first section is the *Introduction*, that it contains a review of biomaterials and the available implantable materials, activation and characterization methods and the antibacterial characterization. The second part is the *Materials, Equipment and Assembly process experimental*. The third section is the *Experimental Results,* which gives all the results and the behavior of the samples treated in contact with different types of bacteria. The next point is the *Discussion* of all the results. And finally, the last parts are the *Conclusion,* the *Acknowledgements* and the *References*.

1.2. OBJECTIVES

The main objective of this study is to develop a new method to combine the antibacterial properties of antibiotic-loaded poly(3-hydroxybutyrate) particles and the antifouling ones of poly(ethylene)glycol with titanium in order to obtain biomimetic surfaces with antibacterial properties.

Then the related secondary objectives of the study were:

- Optimal activation of the titanium surfaces with plasma or NaOH treatments, in order to functionalize the surfaces in a following step.
- Optimal functionalization of the activated titanium surfaces with a specific alkoxylane in order to covalent attaches the antibiotic-loaded PHB spheres.
- Optimal functionalization of the activated titanium surfaces with a specific alkoxylane in order to covalent attaches PEG. In this case, the covalent attachment of PHB spheres with PEG is also desired.
- Covalent attachment of PHB spheres and PEG on the titanium surfaces

1.3. BIOMATERIALS

1.3.1. History of biomaterials

Materials have been used to repair the body for millennia. With the evolution of human civilization, the field of biomaterials evolved involving different materials at multiple length scales from nano-, to micro- to macrolevel with a simple focus to extend human life and improve the quality of life. As long as 4000 years ago the ancient Egyptians used linen threads to close wounds and in the Middle Ages, Europeans used sutures made from catgut. The use of materials to repair the body prior to the era of modern medicine, however, was not limited to sutures. Inca surgeons regularly repaired cranial fractures with gold plates, ancient Mayans used sea shells to create artificial teeth and silver was used as an antimicrobial agent to prevent infection. Different types of surgical procedures can also be found during early stages of civilization. However, probably the most significant developments took place in the field of biomaterials over the years 1901 - 2000.

In the late nineteenth and early twentieth century, scientists and physicians began to examine interactions between the body and materials. They implanted a metal in an animal and then observed the tissue response. But they realized that the body did not tolerate foreign materials well. After the World War II, the scientists began to demonstrate that some materials were tolerated in the body, and they recognized the potential of using artificial materials to treat a variety of problems. The history of the first attempts to implant artificial materials in the body is full of success stories but also horrible failures.

Among the success cases, artificial joints improved the quality of life for millions of people over the past 60 years, resorbable sutures simplified surgical procedures and different cardiovascular devices saved millions of lives. The advent of tissue engineering and organ regeneration is pushing the frontiers of science today to make the years 2001 – 2100 more exciting in the field of biomaterials. However, to appreciate the benefits is important not only the design of biomaterials, but also the device characterization. [1] [5] [6]

1.3.2. Implantable materials

According to the European Society for Biomaterials, a biomaterial is "a material intended to interface with biological systems to evaluate, treat, augment, or replace any tissue, organ, or function of the body" [7]. It may also be used as a delivery system for drug or biological factor. They are designed based on application needs.

An ideal biomaterial must to exhibit properties such as a very high biocompatibility, high mechanical strength and fatigue resistance, a density as low as that of bone, low elastic modulus and good wear resistance. Finding a material that combines all of these properties is not easy. For this reason, it is important to keep on investigating new materials and their combinations in order to fulfill the requirements for an optimal implantable device. [7]

1.3.2.1. Biocompatibility

There are three main factors that are highly dependent for a biomaterial to be successful: the biocompatibility and properties of the implant, the health condition of the recipient and the competency of the surgeon. The first important criterion, that is the biocompatibility, is defined as the ability of a material to perform with an appropriate host response in a specific situation. The engineers can improve this factor finding the right material for each application. [8]

The requirements for a successful implant are:

1. Biocompatibility. Acceptance of the implant to the tissue surface
2. Pharmacological acceptability. (nonallergenic, nontoxic, noncarcinogenic nonimmunogenic, etc.)
3. Chemically inert and stable (no time-dependent degradation)
4. Adequate mechanical strength
5. Adequate fatigue life
6. Sound engineering design
7. Proper weight and density
8. Relatively inexpensive, reproducible and easy to fabricate and process for large-scale production

1.3.2.2. Types of implants

Biomaterial scientists are focused in finding the appropriate, safe, and effective materials for use in the body. There are two types of implants, these which are intended to be implanted in the body for a long lifetime, such as total hip replacements and those that interact with the body for short periods of time, such as soft contact lenses. Different materials are used depending on the type of implant and the properties that must meet.

The following picture Figure 1-1 is an illustration of various implants and devices used to replace or enhance the function of diseased or missing tissues and organs. [8]

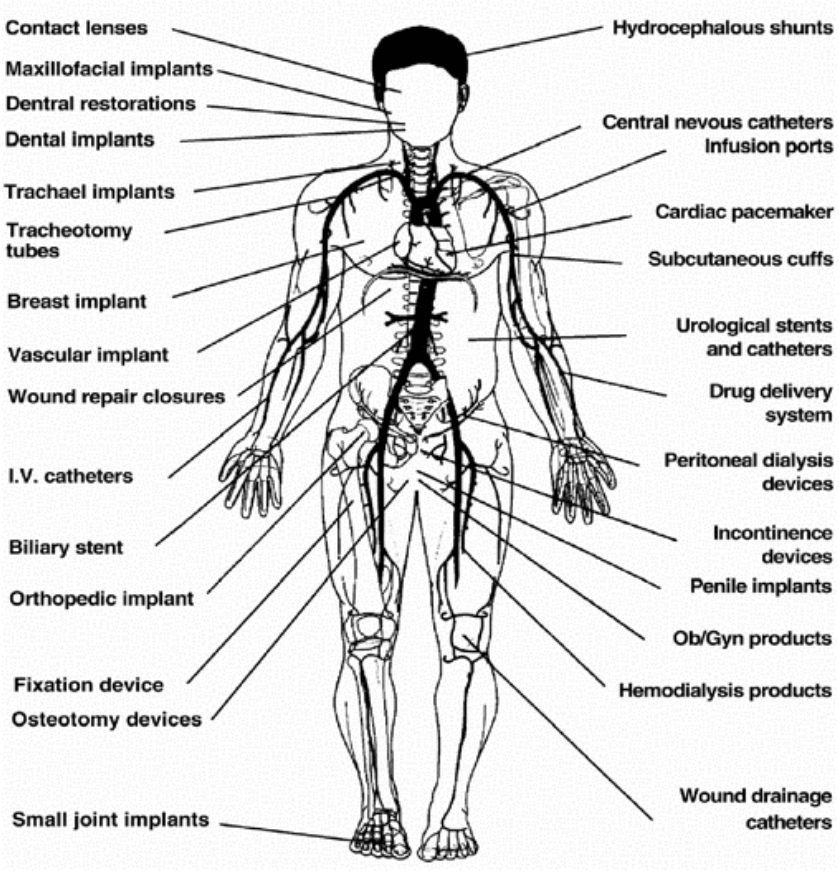

Figure 1-1. Illustrations of implants and devices [8]

The number of medical devices used in humans is increasing every year. The table below *Table* 1-1 shows an estimate of the use of these devices.

Number of Medical Devices	
Intraocular lens	7.000.000
Contact lens	75.000.000
Vascular graft	400.000
Hip and knee prostheses	1.000.000
Catheter	300.000.000
Heart valve	200.000
Stent (Cardiovascular)	>2.000.000
Breast implant	300.000
Dental implant	500.000
Pacemaker	200.000
Renal dialyzer	25.000.000
Left ventricular assist devices	100.000
Millions of lives saved. The quality of life improved for millions more. A $100 billion industry	

Table 1-1. Medical Devices

1.3.2.3. Categories/Types of biomaterials

Biomaterials can be divided into four main groups of materials: polymers, metals, ceramics and composites. The following *Table 1-2* shows a summary of each group [8].

Each group of materials has different structural, physical, chemical and mechanical properties. So they offer specific properties to the different applications in the body.

Materials	**Advantages**	**Disadvantages**	**Examples**
Polymers (nylon, silicone rubber, polyester, polytetrafuoroethylene, etc)	Resilient Easy to fabricate	Non strong Deforms with time May degrade	Sutures, blood vessels other soft tissues, hip socket, ear, nose
Metals (Ti and its alloys, Co-Cr alloys, Au, Ag stainless steels, etc)	Strong, touch ductile	May corrode Dense Difficult to make	Joint replacements, dental root implants, pacer and sutures wires, bone plates and screws
Ceramics (Alumina, zirconia, calcium phosphates including hydroxyapatite, carbon)	Very biocompatible	Brittle Non resilient Weak in tension	Dental and orthopedic implants
Composites (Carbon-carbon, wire or fiber – reinforced bone cement)	Strong Tailor-made	Difficult to make	Bone cement, dental resin

Table 1-2. Class of materials used in the body [8]

1.3.2.3.1 Polymers and biopolymers

Polymers are widely used in biomedical devices. They could be natural such as collagen, cellulose and sodium alginate or synthetic such as silicone rubber, polyester, PMMA. They can be used in both soft and hard tissue applications, which include orthopedic, blood vessels, dental implants, cardiovascular implants etc. and they are also used in drug delivery systems, diagnostic supports and as a reconstructive material for tissue engineering.

Biopolymers are polymeric biomolecules produced by living organisms. They contain monomeric units that are covalently bounded to form larger structures. Biopolymers can be divided into several categories: bio-based plastics and biodegradable or compostable plastics [9]. Bio-based plastics are polymers derived from renewable resources that they can be either biodegradable or non-biodegradable. Compostable plastic is a polymer that undergoes degradation by biological processes during composting to yield CO_2, water, inorganic compounds and biomass, and leaves no toxic residue. [10] The next *Figure 1-2* shows a biodegradable polymer classification.

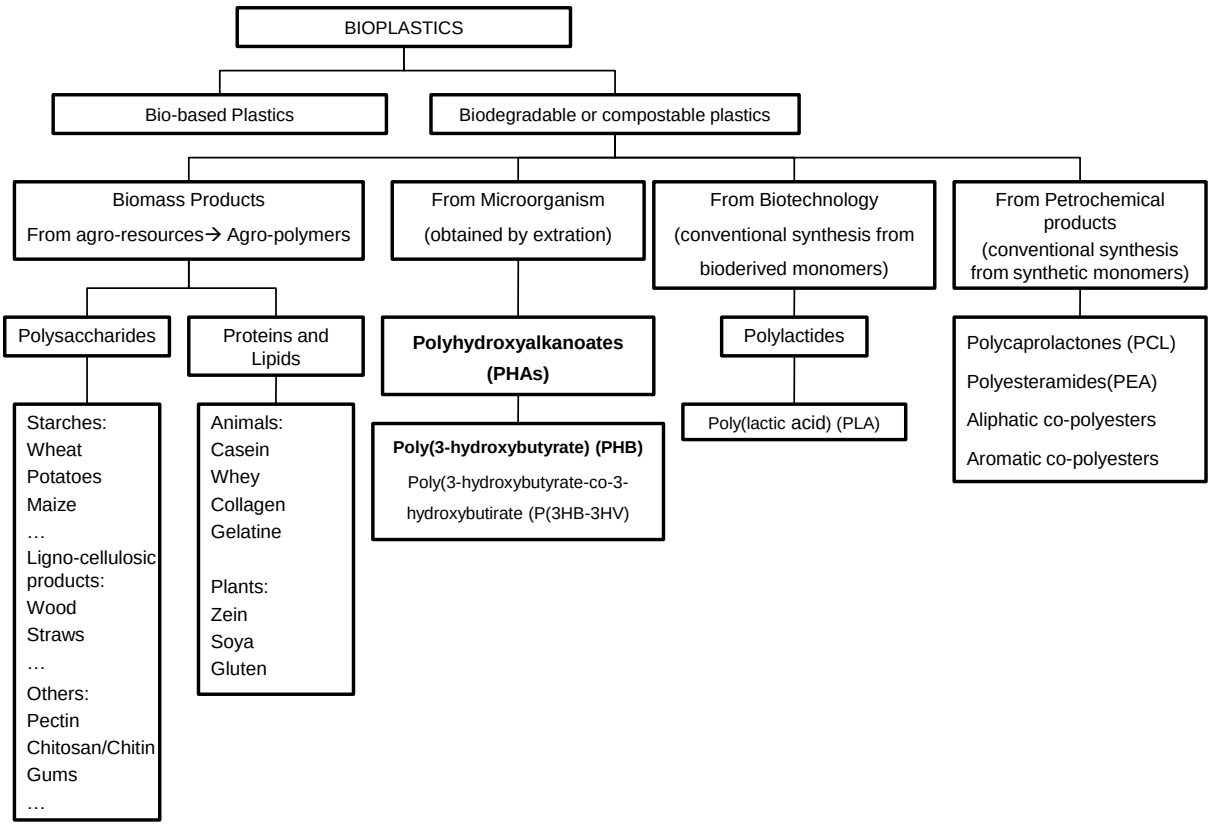

Figure 1-2. Biodegradable polymer classification [9]

In this project, the biopolymers used were the Poly 3-hydroxybutyrate (PHB) as a drug carrier in order to obtain biomimetic surfaces with antibacterial properties and PEG as an antifouling.

Bioengineers increasingly use the polymeric materials alone and in combination with ceramics and metals for the devices used in the body to meet the needs of medical practice. [1][8][13]

1.3.2.3.2 Metals

Metallic materials have been really successful as implants. They have a significant clinical and economic impact on the biomaterials field. Metals are used for different applications throughout the body as implants.

The advantages of the metallic materials are their good properties. They are electrically conductive, they tend to have high tensile strengths, good fatigue resistance, elasticity coefficient, all of these properties of metals and their alloys make them attractive materials for many load-bearing biomedical systems. [1][8][13]

The metallic material has several disadvantages as well. Metals tend to degradation in a corrosion process and it is very concern because the corrosion reactions of releasing some side products such as chemical compounds, ions and insoluble components that may cause adverse biological reactions and the consequences of the loss of material will weaken the implant having undesirable effects. Another disadvantage that also needs to be considered is the toxicity, such as aluminium that it has excellent mechanical properties but it has been associated with toxicity if excessive amounts of it accumulate in the body. [1][8][13]

Sherman Vanadium Steel was the first metal developed for a human use, which was used to manufacture bone fracture plates and strews. Nowadays the metallic systems most frequently used in the body are:

a) Iron-base alloys of the 316L stainless steel.
b) Titanium and titanium-base alloys, such as commercially pure, Ti6Al4V and Ti-Ni.
c) Cobalt base alloys.

Commercially pure titanium was the base material used to do all the experiments throughout this project.

1.3.2.3.3 Ceramics

Ceramics are mainly used in hard tissue repair, regeneration and augmentation, especially in nonload-bearing applications or as coatings on metal implants. The ceramic materials more used in implants are aluminum oxides, calcium phosphates, graphite and apatites.

The advantages of the ceramic materials are their inertness in the body, their high compressive strength, their formability into a variety of shapes and porosities and some cases their excellent wear characteristics. And they are used for several applications such as artificial knees, bone grafts, hip prostheses etc.

In some cases the applications of ceramics are limited by their poor mechanical properties in tension and load bearing. Their poor properties and the fragility are some disadvantages of ceramic materials. [1][8][13]

1.3.2.3.4 Composites

Composite materials contain two or more different materials or phases, on a microscopic or macroscopic size scale. Thus, their properties of composites are strongly influenced by the properties of their constituent materials. Most composite materials are fabricated to provide desired mechanical properties such as strength, toughness, stiffness and fatigue resistance.

They have been used in the field of dental implants and prosthesis. One example of composite used for implants is the combination of fibers such as the carbon ones to reinforce the properties a specific matrix. For the high modulus property of the reinforcing fibers to strengthen the matrix, a sufficient interfacial bond between the fiber and matrix must be achieved during the manufacturing process. This fiber reinforced composite can then be used to make a variety of implants such as intra-medullary rods and artificial joints, in case of carbon fibers.

Composites have unique properties and are usually stronger than any of the single materials from which they are made. [1][8][13]

1.3.2.4. Biomaterials tissue responses

The tissue responses of biomaterials can be grouped into four different types. The four types allow different means of achieving attachment of implants to the muscular skeletal system. These categories are: toxic, bioinert, bioactive and bioresorable. [1] [8] [11]

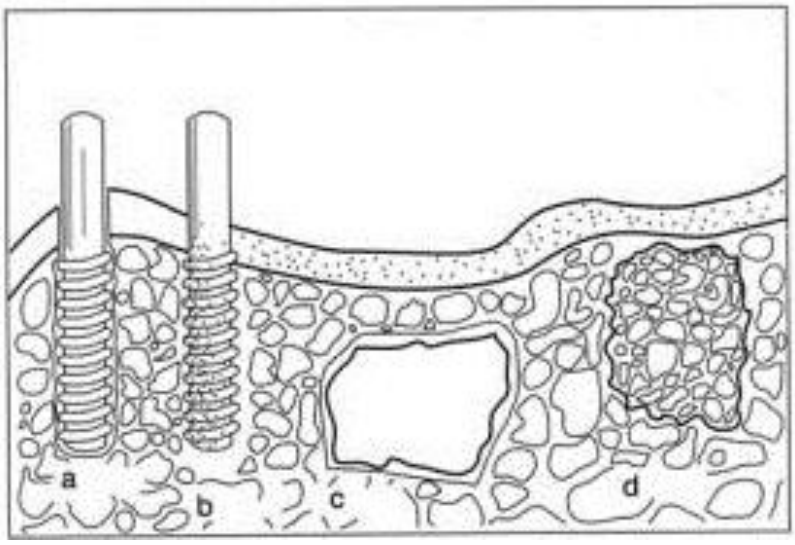

Figure 1-3. Classification of biomaterials according to their bioactivity. a) bioinert, b,c) bioactive, d) bioresorbable

1.3.2.4.1 Toxic

Toxicity of a material describes the ability to damage a biological system by the substances that migrate out the biomaterials. A biomaterial should not be toxic because toxic materials cause death to surrounding tissue. It should not give off anything from its mass unless it is specifically designed to do so. [6]

1.3.2.4.2 Bioinert

A biomaterial bioinert has minimal interaction with the close tissue when it placed into the human body. This type of response is caused by nontoxic but biological inactive materials. Around the bioinert implants, a fibrous capsule is formed that it helps tissue integration (Figure 1-3). Common examples of bioinert materials are titanium, alumina and zirconia. [6]

1.3.2.4.3 Bioactive

Bioactive refers to a material, which when placed within the human body interacts with the surrounding bone and even soft tissues. An interfacial bond forms between the material and host tissue (Figure 1-3*)*. This type of response is seen if the material is nontoxic and biologically active. Examples that fall in this category are bioactive glasses, many types of polymers and most calcium phosphate ceramics. [6]

1.3.2.4.4 Bioresorbable

A biomaterial is bioresorbable when after its placement within the human body, it starts to resorbed and slowly replaced by advancing tissue, such as bone. The nontoxic material dissolves in vivo (Figure 1-3). This is the optimal solution to the problem of biomaterials if the requirements of strength and short-term performance can be met. Examples of bioresorbable materials are calcium sulfate, tricalcium phosphate and bioactive glasses. [6]

1.4. TITANIUM AS A BIOMATERIAL

It was commented before that the titanium was used as a base biomaterial for implants to do all the experiments.

Titanium was discovered as a new and unknown metallic element in England by William Gregor in 1791. Titanium's name appears when Klapproth rediscovered it after the Titans of Greek Mythology in 1795, but he was unable to obtain pure metal. [15]

In spite of its great presence in the terrestrial crust it was not until 1937 when it started being in use in great variety of applications. The efficient separation of the mineral was achieved by Kroll, helped by Siemens and Helske. Nowadays, the obtaining of titanium in big quantities has being achieved by means of technologies more advanced than the ones in 1937, thus being able to satisfy its demand for his commercial use and giving the acquaintance commercial pure titanium or titanium alloy. [8] [15]

1.4.1. Properties of titanium

1.4.1.1. Physical properties

The natural titanium is a common element in the terrestrial bark. It is an element of transition, as the iron, with an electronic structure: 1s2, 2s2, 2p6, 3s2, 3p6, 3d2, 4s2. Titanium forms solid solutions with most substitucional elements thanks to the incomplete shell. Titanium is in group IV and period 4 of Mendeleev's periodic table. Its number atomic is 22 and the atomic weight is 47.9.

Titanium has been classified as a light metal due to his excellent relation between resistance and density. It has high melting point, so it is be able to work in high temperatures, lowers thermal conductivity and low coefficients of thermal and electrical conductivity. [15]

The microstructure of titanium and titanium alloys can be very complex, because titanium undergoes an allotropic phase transformation at 882°C, where alpha (hexagonal close-packed "HCP") transforms to beta (body-centered cubic "BCC"). This is similar to the well-known ferrite to austenite transformation in iron and steel. Thus, depending on processing, the microstructure of titanium can vary widely. For instance, annealed titanium can consist of an equilibrium microstructure with equiaxed grains, whereas titanium that has been rapidly cooled can form metastable phases, such as martensite or bainite, and possess Widmanstätten plates, or have an acicular microstructure. [15]

In this study, pure titanium has been used as a base material in order to do all the experiments.

1.4.1.2. Chemical properties

The titanium is a white and glossy metal, with a low density. It presents an excellent corrosion resistance, an excellent chemical inertness, repassivation ability, and biocompatibility.

Its properties arise from de presence of the surface oxide. When the surface is exposure to air, a native oxide film grows on titanium. The next *Figure 1-4* shows the characteristics of films grown on pure titanium.

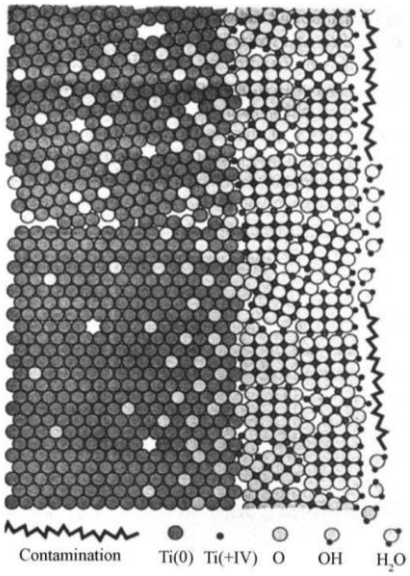

Figure 1-4 Schematic view of the oxide film on pure titanium [15]

The amorphous or nano-crystalline oxide film is typically 3 to 7 nm thick and mainly composed of the stable oxide TiO_2. The TiO_2/Ti interface has an O to Ti concentration ratio that varies gradually from 2 to 1 from the TiO_2 film to a much lower ratio in the bulk. [15]

1.4.1.3. Surface charges on hydrated titanium oxide surface

Hydroxide ions (OH-) attached to metal cations possess acid/base properties depending on the type of the metal cations and the coordinate bonds with the cations. Hydroxides or hydro-complexes of multivalent cations are generally "amphoteric", that is, exhibiting both acid and base properties. The underlining hydrolysis equations of titanium in an aqueous solution can be shown as follows: [15]

$$Ti - OH + H_2O \Leftrightarrow [Ti - O]^- + H_3O^+ \qquad \textbf{Equation 1.1}$$

$$Ti - OH + H_2O \Leftrightarrow [Ti - OH_2]^+ + OH^- \qquad \textbf{Equation 1.2}$$

The first reaction (Eq 1.1) leads to the formation of negative charges on the surface and the second reaction (Eq 1.2) yields positive charges. The titanium oxide surface has two hydroxide groups: acidic and basic types. The two types of hydroxides have been linked to different bonds between the Ti surface cations and basic hydroxide coordinated to one Ti cation leading to increased polarization and electron transfer from the oxygen atom to the Ti cation. As a quantitative measure, the isoelectric point values of titanium oxide vary from 5 to 6.7 and it is often used to investigate the surface charges. [15][16][21]

1.4.1.3.1 Plasma Cleaning

Plasma cleaning is an effective, proven, economical and environmentally safe method for critical surface preparation. Plasma cleaning works by bombarding the material surface with ions that destroy and dislodge surface impurities. Once liberated from the surface, the impurities are drawn away under vacuum in a low pressure plasma system or ejected into the air when using an atmospheric plasma system. In low pressure plasma cleaning, argon is often used as the process gas. Argon is used in these plasma treatment systems because Argon is relatively large in size and is also inert. The large size allows the Argon ions to act as an atomic scale sand blaster. The inert properties of Argon reduce the potential for chemical reactions. [16]

Benefits of Plasma Cleaning

- Clean surfaces with microscale porosity or microchannels not suitable for solvent cleaning due to surface tension limitations.
- Render most surfaces hydrophilic; decrease water droplet contact angle and increase surface wettability.
- Remove organic contaminants by chemical reaction (O2 or air plasma) or physical ablation (argon plasma).
- Clean surface without affecting the bulk properties of the material.
- Promote adhesion and enhance bonding to other surfaces.
- Eliminate the use of chemical solvents as well as storage and disposal of solvent waste.
- Prepare surface for subsequent processing.

Sterilize and remove microbial contaminants on the surface; beneficial for biomedical applications and biomaterials

1.4.1.3.2 Sodium Hydroxide treatment

The treatment of titanium with sodium hydroxide (NaOH) improves the bioactivity and it produces a fine network structure of nanometer scale on the surface of the titanium metal. NaOH treatment can change the crystallinity and surface chemistry of titanium implants. Treatment with a NaOH solution produces a sodium titanate gel layer on the surface of Ti. [19]

After the treatment, a porous surface forms on the surface of titanium. The structural change on the titanium surface during NaOH treatment is described as follows. During the treatment, the TiO2 layer partially dissolves because of the attack by hydroxyl groups.

$TiO_2 + NaOH \rightarrow HTiO_3^- + Na^+$ **Equation 1.3**

This reaction is assumed to proceed simultaneously with hydration of titanium.

$Ti + 3OH^- \rightarrow Ti(OH)_3^+ + 4e^-$

$Ti(OH)3^+ + e^- \rightarrow TiO_2 \cdot H_2O + 1/2\ H_2$ **Equation 1.4**

$Ti(OH)_3^+ + OH^- \leftrightarrow Ti(OH)_4$

A further hydroxyl attack on the hydrated TiO2 produces negatively charged hydrates on the surfaces of the substrates as follows:

$TiO_2 \cdot H_2O + OH^- \leftrightarrow HTiO_3^- \cdot nH_2O$ **Equation 1.5**

These negatively charged species combine with sodium in the aqueous solution to produce a hydrogel layer of sodium titanate. This gel layer has very intricated topography, producing a surface notably high real surface area including a high amount of OH groups. [17][19]

1.4.1.4. Corrosion Behavior

Materials implanted in vivo initially come in contact with extracellular body fluids, such as blood and interstitial fluids, which can contain amino acids and proteins that tend to accelerate corrosion.

The excellent resistance of Ti and its alloys to most environments is the result of the protective surface film, which consists basically of $Ti0_2$. The native titanium dioxide film protects the metal from the corrosion and stabilizes [24]. Although titanium is chemically very reactive, this thin oxide film passivates the base metal, as long as its integrity can be maintained.

Titanium and its alloys corrode either very quickly or extremely slowly depending on the environmental conditions. When in contact with body fluids having close to neutral pH, the materials exhibit corrosion rates that are extremely low and difficult to measure experimentally. Titanium is not corrosion resistant under reducing conditions, in very powerful oxidizing environments or in the presence of fluoride ions, where the protective nature of the oxide film diminishes. The stability and integrity of the film can be improved, however, if inhibiting additions can be added to these environments. [25][26]

1.4.1.5. Mechanical properties

Commercially pure titanium (c.p. Ti) and extra low interstitial Ti6Al4V are two most common titanium base implant biomaterials but obtain pure metal is a difficult work for the high reactivity of titanium. The following *Table 1-3* summarizes the mechanical properties of titanium and its alloys.

Alloy designation	Microstructure	Elastic modulus *E* (GPa)	Yield strength, YS (MPa)	Ultimate strength UTS (MPa)
cpTi	α	105	692	785
Ti–6Al–4V	α/β	110	850–900	960–970
Ti–6Al–7Nb (protasul-100)	α/β	105	921	1024
Ti–5Al–2.5Fe	α/β	110	914	1033
Ti–12Mo–6Zr–2Fe (TMZF)	Metastable β	74–85	1000–1060	1060–1100
Ti–15Mo–5Zr–3Al	Metastable β	82	771	812
	Aged β + α	100	1215	1310
Ti–0/20Zr–0/20Sn–4/8Nb–2/4Ta+ (Pd, N, O)	α/β	N/A	726–990	750–1200
Ti–Zr	Cast α′/β	N/A	N/A	900
Ti–13Nb–13Zr	α′/β	79	900	1030
Ti–15Mo–3Nb–0.3O (21SRx)	Metastable β + silicides	82	1020	1020
Ti–35Nb–5Ta–7Zr (TNZT)	Metastable β	55	530	590
Ti–35Nb–5Ta–7Zr–0.4O (TNZTO)	Metastable β	66	976	1010
Bone	Viscoelastic composite	10–40	–	90–140

Table 1-3. Mechanical properties of some titanium and its alloys [26]

Titanium is very promising in orthopedics due to its high specific strength and low modulus. The modulus of elasticity of these materials is about 110 GPa. This is much lower than stainless steels modulus (210 GPa) and Co-base alloys modulus (230 GPa).

Material	Density (kg/m³)	Young's modulus, E (GPa)	Yield strength, 0.2%(MPa)	Tensile strength, min (MPa)
c.p. Ti grade II	4200	100-110	275	345
Ti-6Al-4V	4500	100-130	870-895	950
Stainless steel 316L	7800	200	280	580-650
Co-Cr alloys	8500	210–230	600-625	880-910

Table 1-4. Mechanical properties of c.p. Titanium grade II and Ti6Al4V. [26]

There are various c.p. titanium grades depending to the amount of interstitial elements present. Titanium is very light with a density of 4.5 g/cm3. The Ti CP is 98.9 - 99.6 % Ti, being the oxygen content (and other interstitial elements such as C and N) the main element influencing

significantly its yield, tensile and fatigue strengths. Interstitial elements strengthen the metal through interstitial solid solution strengthening mechanism, with nitrogen having approximately twice the hardening effect (per atom) of either carbon or oxygen. [26]

The mechanical properties of the Titanium and the Ti6Al4V are different according to the purity.

Property	Grade 1	Grade 2	Grade 3	Grade 4	Ti6Al4V
Tensile strength (MPa)	240	345	450	550	860
Yield strength (MPa)	170	275	380	485	795
Elongation (%)	24	20	18	15	10

Table 1-5. Mechanical properties of Ti CP (ASTM F 67) and Ti6Al4V alloy (ASTM F 136)

When compared by specific strength (strength/density) the titanium alloys exceed any other implant materials. Titanium and titanium alloys, nevertheless, have poor shear strength, making them less desirable for bone screws, plates and similar applications. They also tend to gall or seize in sliding contact with itself or another metal. [26]

1.5. POLY 3-HYDROXYBUTYRATE (PHB)

Polyhydroxyalkanoates (PHAs) are bacterial polymers that are formed as naturally occurring storage polyesters by a wide range of microorganisms usually under unbalanced growth conditions. Poly-3-hydroxybutirate (PHB) and its copolymers with 3-hydroxyvalerate (3HV), poly (3-hydroxybutyrate-co-3- hydroxyvalerate) (PHBV), are the best known representatives of PHA family. These polyesters have attracted widespread attention, as environmentally friendly polymers which can be used in a wide range of agricultural, industrial applications, and for medical devices and systems of sustained drug delivery. Biodegradability and biocompatibility are main characteristics that allow PHAs to be competitive in special market sectors. But not only is their biodegradability the importance of PHAs, but also their thermoplastic and mechanical properties. [29][34]

In the next tables "*Table 1-6 and Table 1-7*" show the properties of some PHAs and a comparison of the thermo and mechanical properties of PHB, 3HV and PP.

	PHB	P(3HB-3% 3HV)	P(3HB-20%3HV)	P4HB	P(3HB-16%4HB)	P(3HO-3HHx)
Melting temperature (T_m) (°C)	177	170	145	60	152	61
Glass transition temperature (T_g) (°C)	4	-	-1	-50	-8	-36
Tensile strength (MPa)	40	38	32	104	26	9
Young´s modulus (GPa)	3.5	2.9	1.2	149	-	0.008
Elongation at break (%)	6	-	50	1000	444	380

Table 1-6. Properties of some PHAs [27]

PHB as a member of the PHAs is produced by microorganisms from renewable resources [27]. It combines three exceptional features: thermoplastic properties, biodegradability under different environmental conditions and excellent biocompatibility, for this reason it is used in drug delivery [34] . The following image shows the chemical structure of PHB.

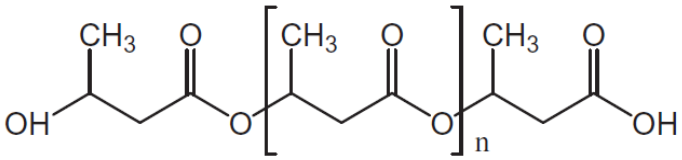

Figure 1-5. Chemical structure of PHB [34]

Among biopolymers, polyglycolic acid (PGA), polylactic acid (PLA), and poly (lactide-co-glycolide) (PLGA) are chemical produced polymers. However, PHB is known for its good properties as a biologically degradable drug carrier. In addition, the biopolymer production via microbial fermentation avoids the presence of toxic products from the synthetic polymerization process. Also, the hydrolytic degradation of PHB leads to obtain the monomer D-3-hydroxybutyric acid which is a common blood constituent [29].

	PHB	P(3HB-3HV) for 4–95% (mol/mol) 3HV	PP
Molecular mass (10^5 g/mol)	1 – 8	3	2.2 – 7

Density (kg/m^3)	1.25	1.20	0.905
T_m (ºC)	171 – 182	75 – 172	176
Crystallinity degree (X_c) (%)	80	55 – 70	70
T_g (ºC)	4 – 10	-13 – +8	-10
O_2 Permeability [(cm^3/(m^{2}atm)]	45	n. d.	1700
UV Resistance	Good	Good	Bad
Resistance to solvents	Bad	Bad	Good
Tensile strength (Mpa)	40	25 – 30	38
Elongation to break (%)	6	8 – 1200	400
Young's modulus (GPa)	3.5	2.9 (3% 3HV); 0.7 (25% 3HV)	1.7
Biodegradability	Yes	Yes	No

Table 1-7. Main thermo and mechanical properties of PHB, 3HV and PP [27]

There are several applications of PHB for its good properties. One of these is medical devices; the perspective area of PHB application is development of implanted medical devices such as bioresorbable surgical sutures, biodegradable screws, wound covering. Another application can be found in drug delivery systems. PHB acts as drug carrier for both films or microspheres and capsules. This improves medical devices opens up the wide prospects in applications with pharmacological activity in medicine. [28][30][31]

1.5.1. Doxycycline (Doxy)

Doxy is a broad-spectrum antibiotic, which is effective against both Gram-positive and Gram-negative bacteria, protozoa, and various anaerobes. *Figure 1-6* shows the chemical structure of PHB and Doxycycline. It shows a long half-life, high lipid solubility, and very good oral absorption. It is used against periodontal infection, for enhancing bone regeneration after periodontal diseases and to prevent bacterial infection related to septic arthritis. However, it has possible side effects such as gastro-intestinal disturbance, esophageal erosion, and photosensitivity when administrated orally. The controlled local delivery of Doxy within a

biodegradable matrix is appealing to reach the infection deep inside the affected tissues with an effective drug concentration and to circumvent the systemic side effects. [34]

In order to reduce this harmful side effects, previous studies have been done trapping Doxy in a biopolymer matrix. Rodriguez-Contreras [34] reports some methods to prepare micro- / nano- spheres to carry Doxy as an antibiotic. In this case, PHB was used as a biopolymer matrix with good properties of biocompatibility and biodegradability to properly entrap this antibiotic.

In this study Doxy-loaded PHB spheres were used to avoid or greatly limit bacteria attachment to the covered titanium surfaces.

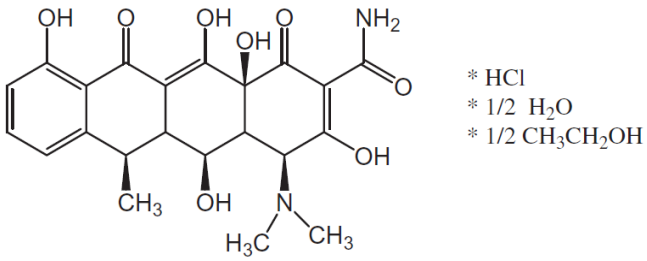

Figure 1-7. Chemical structure of PHB and Doxycycline [34].

1.6. POLYETHILENEGLYCOL (PEG)

Polyethilene glycol (PEG) is a polymeric material used in medicine in drug delivery as conjugates with low solubility drugs and with immunogenic of fairly instable protein drugs, to enhance the circulation times and stabilities of the drugs. It is used either alone or as a surface modifier, for its properties of low cell adhesion and protein adsorption. PEG has also been immobilized on polymeric biomaterial surfaces to make them "nonfouling". [1] Thus, a PEG-modified polymer guarantees low protein adsorption and cell adhesion with its ability to tune adhesive properties through attachment of specific proteins or peptides. [6][35]. Physical adsorption, chemical adsorption, directs covalent attachment, and block or graft copolymerization are some of the techniques that have been used to attach PEG to surfaces.

In this project, the Polyethilene glycol is used as an antifouling on the titanium surface in order to improve the antibacterial character of the surfaces.

1.7. TITANIUM SURFACES TRANSFORMATION: APTES (HBTU) AND CPTES

SILANIZATION

Silane reactions can be used to modify hydroxylated or amine-rich surfaces. An increase in contact angle is a direct evidence for surface modification on the substrates. Silanization is a versatile, cheap and reliable method to link an organic molecule on a metallic, polymeric and ceramic surface. The advantages of silane reactions are their simplicity and stability, which are attributed to their covalent, cross-linked structure. For surface silanization, silane molecules must first be activated and then condensation reactions occur between the Si–OH groups of the silanol and the OH groups of the surface. This leads to the formation of a stable bond with the surface and the release of free alcohols as side products [32]. When the silanization process is finished, the surfaces of the samples are covered by silane molecules that are covalently bound to the surface.

The chemical process allows the alkoxysilanes to bind to the titanium surface. The organosilanes are formed by two functional groups spaced at their ends by a ductile alkyl group. The *Figure 1-8* shows the configuration of a monolayer of silanes attached to a surface, the silane group at one end serves to bind to the surface of titanium oxide and the other functional group at the opposite end serves to bind biomolecules [17].

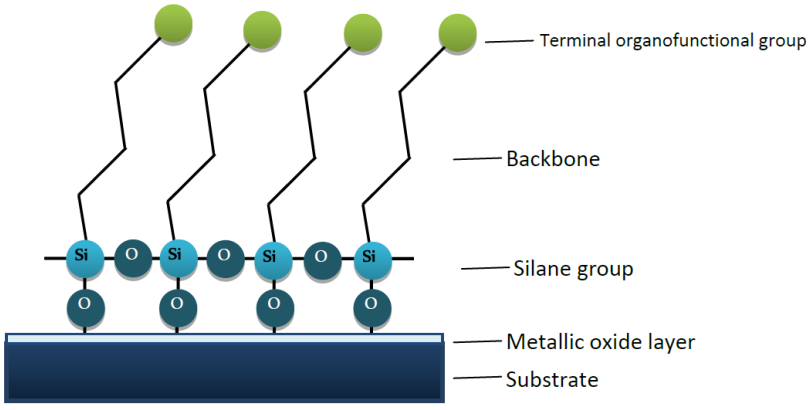

Figure 1-8. Organosilane layer scheme [17]

In the case of this study, two alkoxysilanes were used. 3- Aminopropyltriethoxysilane and 3-Chloropropyltriethoxysilane which show as terminal organofunctional groups a primary amina and a chloro, respectively.

1.7.1. 3-Aminopropyltriethoxysilane (APTES)

Silanization with APTES is related to its intrinsic chemical properties so it is very used for the immobilization of biological molecules and it has an excellent performance on multiple oxide surfaces. [17][33] *Figure 1-9* shows the chemical structure of APTES silane.

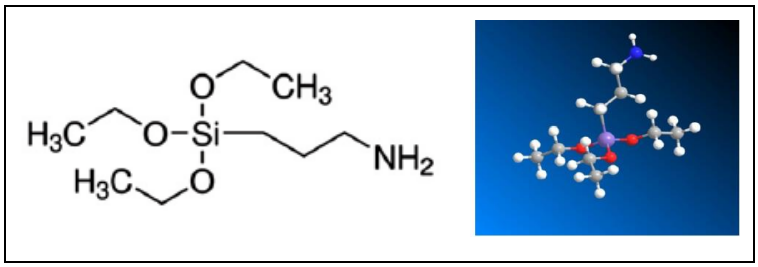

Figure 1-9. chemical structure of APTES silane. Left 2D; Right: 3D [33]

APTES contains a primary amino group at the end of the aliphatic chain. At neutral or basic pH, primary amines contain a free pair of electrons that can be shared to form a new covalent bond.

In this study, the titanium surfaces were covalent linked with Doxy-loaded PHB spheres by means of a silanization reaction with APTES [17] [18][33]. *Figure 1-10* shows the proposed reaction.

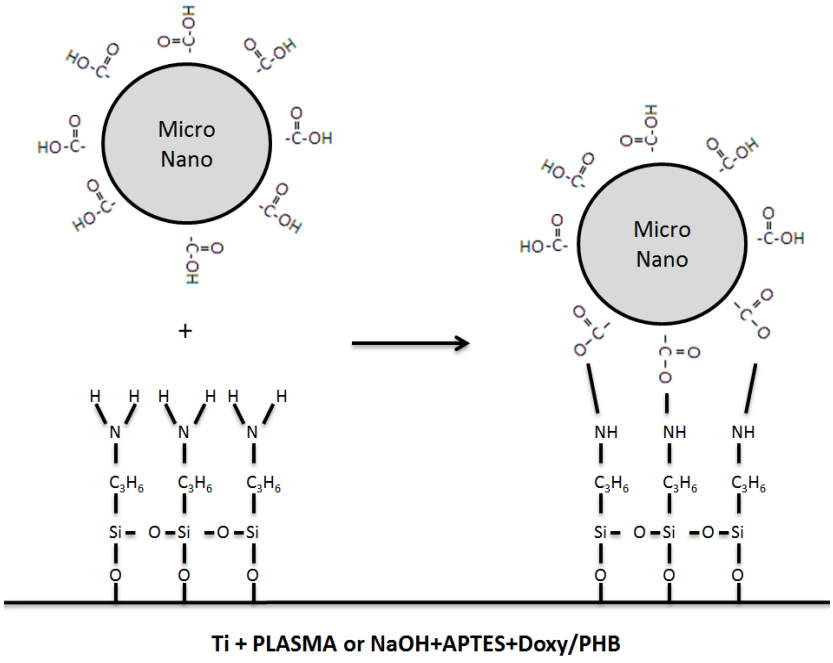

Figure 1-10. APTES reaction

1.7.1.1. O-Benzotriazole-N,N,N',N'-tetramethyl-uronium-hexafluoro-phosphate (HBTU)

In this project, a coupling reagent has been selected to esterify the carboxylic acids of the PHB spheres and to ensure the reaction with the primary amino group of APTES.

HBTU is a popular in situ activating reagent commonly used in solid phase peptide synthesis. Activation with HBTU is cheap and it is much faster and more complete than carbodiimide-mediated reactions and results in shorter cycle times and increased coupling efficiency. It is reported to convert carboxylic acids into azides efficiently and practically. This process may be used with a wide range of carboxylic acids including N-protected amino acids. It has also been reported to be useful in one-pot synthesis of dipeptidyl urea esters, ureas, and carbamates from acids [17] [18][33].

Figure 1-11 shows HBTU's structure and *Figure 1-12* shows the scheme of benzotriazole based ester reaction with a primary amine.

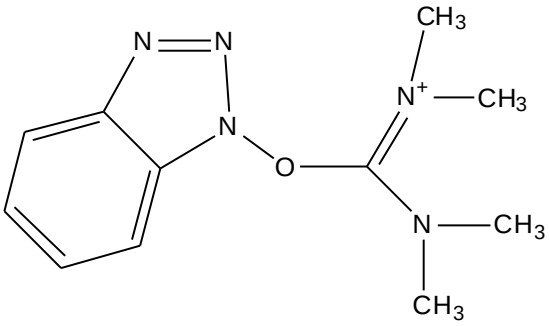

Figure 1-11. Scheme of HBTU [33]

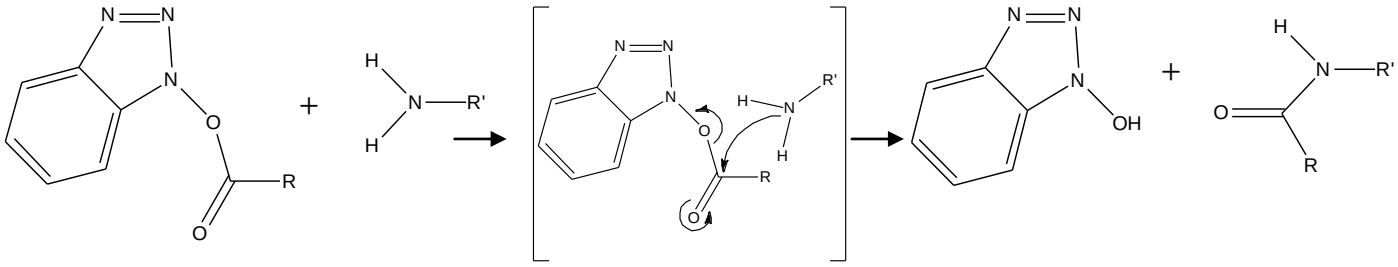

Benzotriazole + Primary amine *Carbodiimide + Amida*

Figure 1-12. Scheme of Benzotriazole based ester reaction with a primary amine

Figure 1-13 shows the scheme reaction of HBTU with a carboxylic acid. When HBTU reacts with a carboxylic acid, the molecule splits into two molecules: a carbodiimide and N-hydroxybenzotriazole. The resulting carbodiimide is unstable and readily reacts with the N-hydroxybenzotriazole formed, leading to an active benzotriazole based ester which can react with a primary amine [17][18] [33].

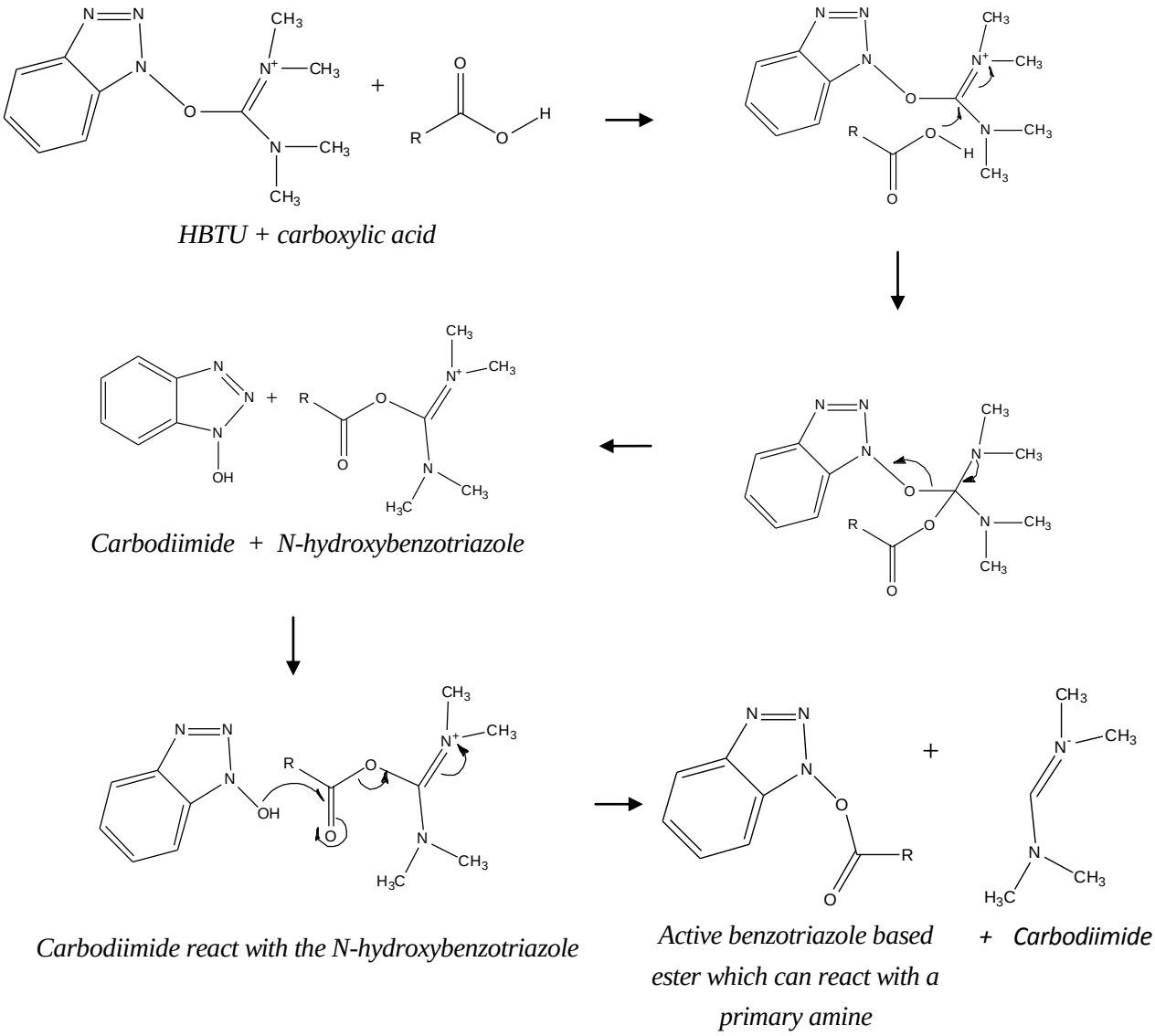

Figure 1-13. Scheme of HBTU reaction with a carboxylic acid

1.7.2. 3-Chloropropyltriethoxysilane (CPTES)

CPTES has the capability to bind nucleophiles such as amines directly in basic conditions. *Figure 1-14* shows the chemical structure of CPTES silane.

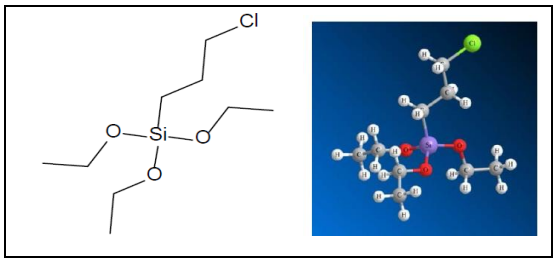

Figure 1-14. Chemical structure of CPTES silane. Left: 2D; Right: 3D [33]

CPTES contains a chlorine atom, a well know electron withdrawing group. Thus, chlorine draws the electronic density from the neighboring C, thereby yielding an electrophilic (electron deficient) -CH_2- group. Peptides and proteins contain free amino groups due to the presence of the N terminus and some amino acid side chains, which have nucleophilic properties and tendency to react with electrophiles. Therefore, the organo-functional group of CPTES will react with peptides and proteins [33][17]. The bond between the chlorine and carbon on CPTES is polarized due to the difference of electro-negativities between carbon and chlorine. The uneven share of electrons in this bond creates a lack of electrons on the carbon atom. As a result, CPTES contains an electrophilic center. The free amine from the N-terminus is a good nucleophile which has a free pair of electrons to share, thus making it a center with an excess of electronic density [33][17] [18].

In this study, neither peptides nor proteins were used, instead PEG containing two amino groups was used to react with CPTES. *Figure 1-15* shows the proposed reaction.

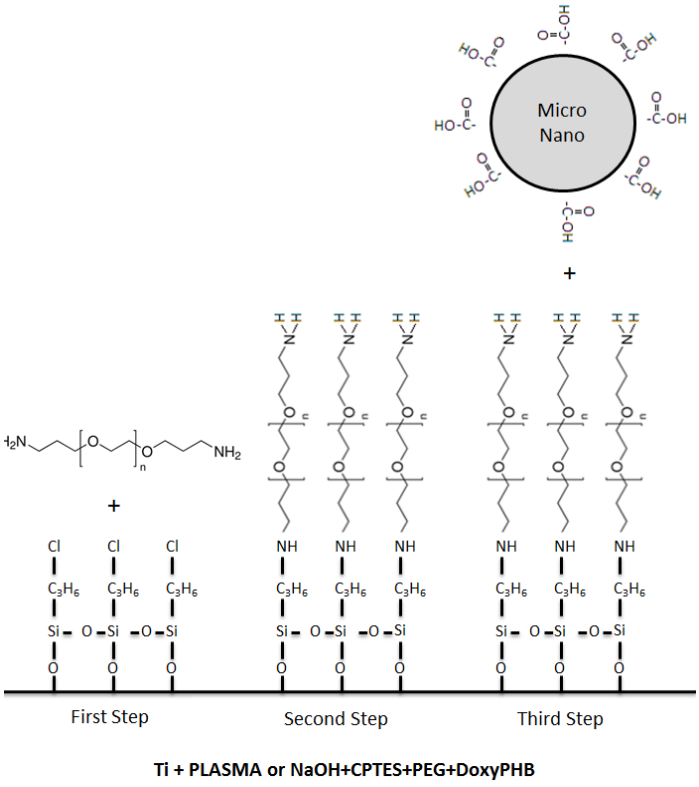

Figure 1-15. CPTES reaction

1.8. CHARACTERIZATION OF BIOMATERIALS

1.8.1. Wettability: Contact Angle

Wettability indicates the behavior of water on a surface. The wettability of a solid with a liquid is usually determined from their contact angle. The contact angle is geometrically defined as the tangent of the interface formed where liquid, solid, and gas phases intersect. The force balance on the far right dictates that the contact angle formed is the resultant of three interfacial tensions: liquid-vapor, solid-liquid and solid-vapor. [1]

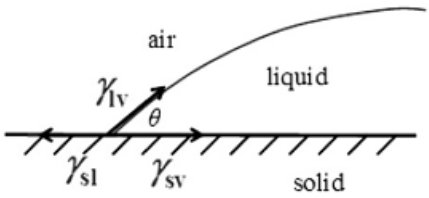

Figure 1-16. Contact angle between liquid and solid surface in air medium [6]

The energy of the surface, which is directly related to its wettability, is a useful parameter that has often correlated strongly with biological interaction. The surface tension can be thought as the energy required for creating a unit area of an interface, the surface energy can be calculated from the Young's equation by measuring the contact angle and the surface tension of the liquid:

$$\gamma sv = \gamma sl + \gamma lv \cdot \cos \theta \qquad \textbf{Equation 1.6}$$

As shown in the *Figure 1-16*, γsl represents the interfacial tension between the two phases while γsv and γlv describe the surface tension components of the solid and liquid phases, respectively. The contact angle θ corresponds to the angle between vectors γlv and γsl and hence, γsv provides the surface energy of the biomaterial. However, to determine the surface energy of solids from contact angle measurements alone, the value of γsl must be known. [12]

Contact angle also signifies physical manifestation of more fundamental concepts of surface tension and surface energy like the chemical bounding of the uppermost surface layers of the biomaterial. Its values give an easy-to-measure indication of this bonding, which determine the wettability, adhesion, surface cleanliness, effect of surface treatments, and properties of coatings. The wettability or wetting is an important characteristic property of the surface for biomaterial applications as it refers to the actual process of spreading of a liquid over the solid surface.[6] If a liquid is dropped on a solid surface, then the liquid droplet will spread (hydrophilic) or make a spherical globule (hydrophobic) *Figure 1-17*. The wetting characteristic can be described as [12]:

θ = 0 → Complete wetting
0< θ<90º → Partial wetting
0>90º → Non-wetting

Contact angle is a quantitative measure of the wetting of a solid by a liquid, for low contact angles, the liquid spreads or wets well, meaning the liquid has a strong affinity for the solid, total wetting, and high contact angles indicate partial wetting conditions. [6]

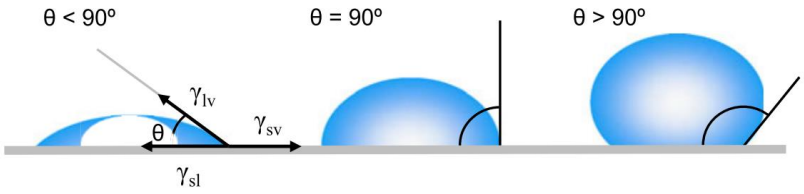

Figure 1-17. Contact angles. Left: Hydrophilic. Right: Hydrophobic. [12]

Overall, contact angle is one of the simple, reliable, sensitive and inexpensive methods for the characterization of the surface as well as physical properties of biomaterials to prepare the biomaterials for specific applications. [6][12]

1.8.2. Scanning electron microscope (SEM) and field emission scanning electron microscope (FESEM)

SEM is a type of electron microscope that produces images of a sample by scanning it with a focused beam of electrons. These images of surfaces have a great resolution and depth of field with a three-dimensional quality. [36] The signals that derive from electron-sample interactions reveal information about the sample including external morphology, chemical composition, and crystalline structure and orientation of materials making up the sample.

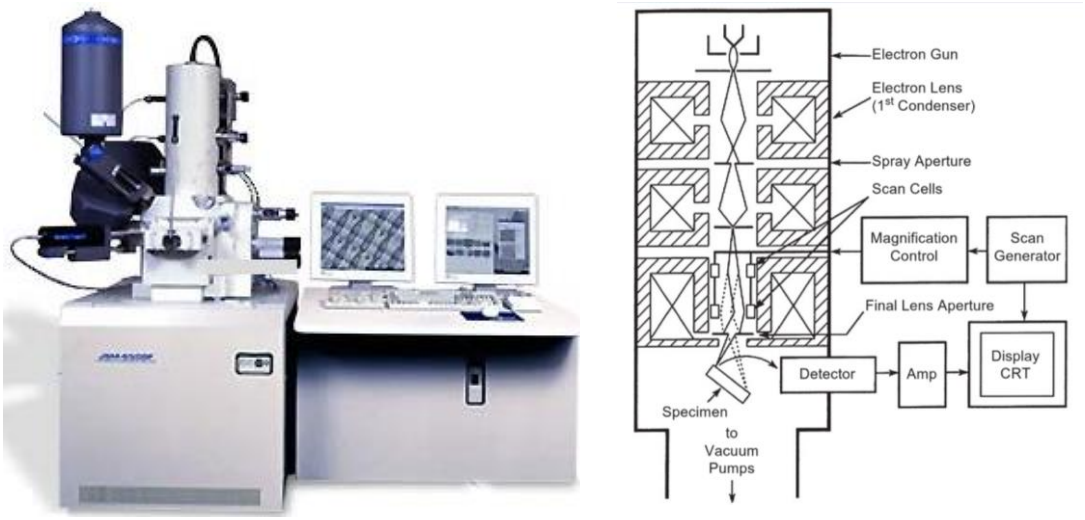

Figure 1-18. Left: Scanning electron microscope. Right: Schematic drawing of the electron column in an SEM showing the electron gun, lenses, the scanning system, and the electron detector [37].

Accelerated electrons in an SEM carry significant amounts of kinetic energy, and this energy is dissipated as a variety of signals produced by electron-sample interactions when the incident electrons are decelerated in the solid sample. These signals include secondary electrons that produce SEM images, backscattered electrons (BSE), diffracted backscattered electrons (EBSD) that are used to determine crystal structures and orientations of minerals, photons that they are characteristic X-rays that are used for elemental analysis and continuum X-rays, visible light (cathodoluminescence-CL), and heat. Secondary electrons and backscattered electrons are commonly used for imaging samples: secondary electrons are most valuable for showing morphology and topography on samples and backscattered electrons are most

valuable for illustrating contrasts in composition in multiphase samples. X-ray generation is produced by inelastic collisions of the incident electrons with electrons in discrete ortitals of atoms in the sample. As the excited electrons return to lower energy states, they yield X-rays that are of a fixed wavelength that is related to the difference in energy levels of electrons in different shells for a given element. Thus, characteristic X-rays are produced for each element in a mineral that is "excited" by the electron beam. SEM analysis is considered to be "non-destructive"; that is, x-rays generated by electron interactions do not lead to volume loss of the sample, so it is possible to analyze the same materials repeatedly. [37]

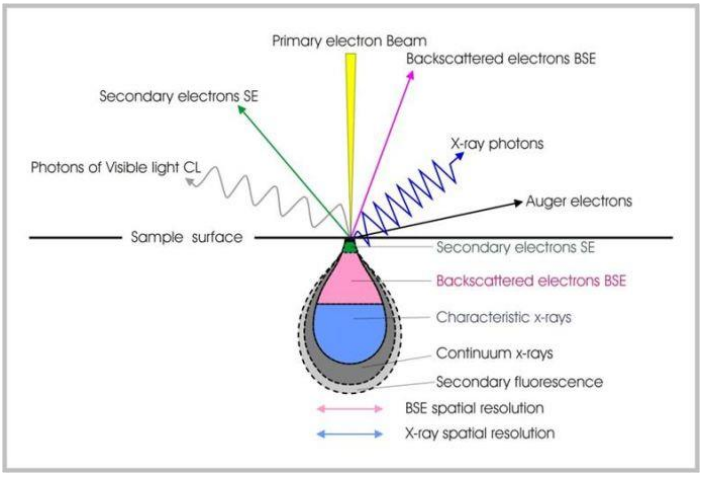

Figure 1-19. Electron-sample interactions[37]

FESEM is electron microscope like SEM that is able to offer a wide variety of information from the sample surface, but with higher resolution and with a range of energy greater than the SEM. The operation is similar to a conventional SEM; an electron beam on the sample surface is scanned while in a monitor information that interests us in terms of available sensors displayed. [38]

The major difference between a FESEM and SEM lies in the generation of electron system. The FESEM used as a source of electrons, a gun that provides electron beams of high and low energy very focused, which greatly improves the spatial resolution and allows working at very low potentials (0.02 to 5 kV); this helps to minimize the effect of non-conductive specimens load and prevent damage to the electron beam sensitive samples. [38]

FESEM was used to obtain high resolution images from the titanium surfaces.

1.8.3. Atomic force microscopy (AFM)

AFM is a technique to obtain images and other information from a wide variety of samples, at extremely high resolution.

AFM provides a 3D profile of the surface on a nanoscale, by measuring forces between a sharp probe (<10 nm) and surface at very short distance, only 0.2-10 nm separation between probe and sample. The probe is supported on a flexible cantilever. The AFM tip gently touches the surface and records the small force between the probe and the surface. [42]

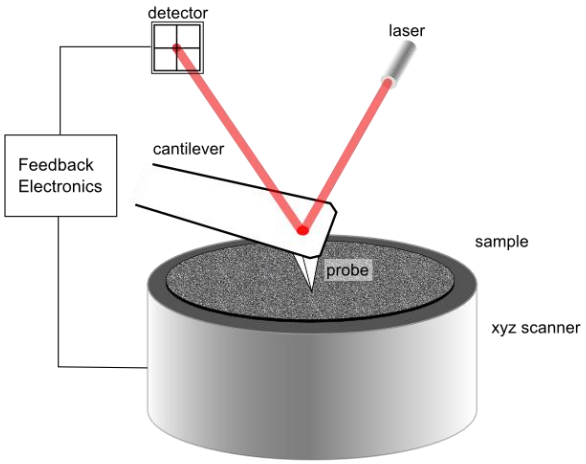

Figure 1-20. Principle of AFM [42]

The basic principle of AFM is that a probe is maintained in close contact with the sample surface by a feedback mechanism as it scans over the surface, and the movement of the probe to stay at the same probe-sample distance is taken to be the sample topography. [42]

Typically, probe radius varies from 5 to 20 nm. The bending of the cantilever normal to the sample surface is usually monitored by an optical lever. The probes gently touches the sample as it moves over the surface, the movement of the probe over the surface is controlled by a scanner. This is normally made from a piezoelectric material, which can move the probe very precisely in the x, y, and z axes. The signal from the photodetector passes through a feedback circuit, and into the z-movement part of the scanner, in order to maintain the probe-sample distance at a set value. [42][43][44]

A great advantage of AFM compared to SEM, is that it is simple to operate in almost any environment, such as aqueous solutions, but also other solvents, vacuum, in air, or other gases.

The resolution can be very high depending on the details of the experiment, to obtain such high resolution work, the state of the sample, the levels of acoustic and electronic noise, and experimental conditions must all be highly optimized.[42][43][44]

1.8.4. X-Ray Photoelectron Spectroscopy (XPS)

XPS also referred to as Electron Spectroscopy for Chemical Analysis (ESCA) is a surface analysis technique based on the photoelectric effect that it is used to determine quantitative atomic composition and chemistry. It uses X-Rays with low energy (1-2 keV) to knock off photoelectrons from atoms of the sample through the photoelectric effect. The energy content of these ejected electrons is then analyzed by a high-resolution electron spectrometer to identify the elements where they came from. [45][46]

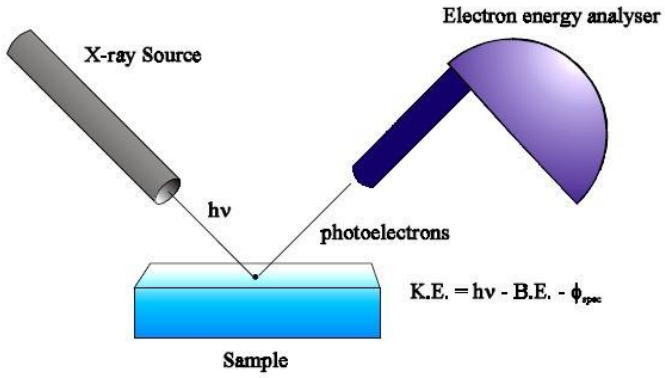

Figure 1-21. Principle of XPS [45]

Each atom in the surface has core electron with the characteristic binding energy that is not strictly, equal to the ionization energy of the electron. When an X-ray beam directs to the sample surface, the energy of the X-ray photon is adsorbed completely by the core electron of an atom. If the photon energy, *hv*, is large enough, the core electron will then escape from the atom and emit out of the surface. The emitted electron with the kinetic energy of *Ek* is referred to as the photoelectron. The binding energy Eb of the core electron is given by the Einstein relationship: [50]

$$Eb = h\nu - Ek \qquad \text{Equation 1.6}$$

The sample analysis is conducted in a vacuum chamber, under the best vacuum conditions achievable, typically ~10-10 torr. This facilitates the transmission of the photoelectrons to

the analyzer but more importantly minimizes the re-contamination rate of a freshly cleaned sample. [50]

Applications of XPS

- Examination for and identification of surface contaminations
- Evaluation of materials processing steps (cleaning, plasma etching, thermal oxidation, silicide thin-film formation etc.)
- Failure analysis for adhesion between components (air oxidation, corrosion etc.)
- Evaluation of thin-film coating or lubricants
- Tribological or wear activity
- Effectiveness of surface treatment of polymers or plastics
- Surface composition differences of alloys

1.9. ANTIBACTERIAL CHARACTERIZATION

Bacteria come in many varieties. Different species of bacteria can be very different from each other in their shape, mobility, range of habitat, and even the process by which they generate energy. Two types of bacteria used in antibacterial assay are studied; they are *Staphylococcus Aureus* and *Escherichia Coli* [39] [40].

1.9.1. Staphylococcus Aureus

S. aureus is one of the most common causes of life-threatening bacterial infections. Every year in the United States, roughly 400,000 hospital patients are infected by *S. aureus* is one of about 32 species in the Staphylococcus genus of bacteria. Most of the other species are found only in other mammals and do not infect humans. The origin of *S. aureus* is not well understood, but current theories suggest that it evolved from prehistoric soil bacteria. [39] This bacterium is not capable to move and it grows in clusters like grapes. The cells are about 1 micrometer in diameter, so 1000 cells lined up next to each other would cover a distance of only 1 millimeter.

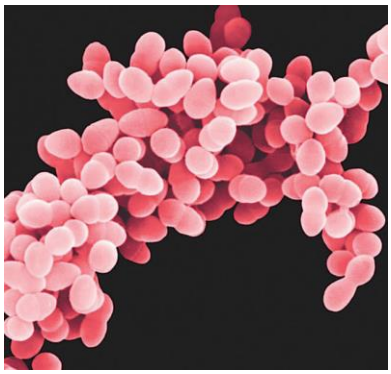

Figure 1-22. An electron micrograph of Staphylococcus aureus [39]

S. aureus lives on the skin and mucous membranes of warm-blooded animals, humans are one of its primary carriers. The spherical bacteria grow in distinctive grape-like clusters and it is extremely durable that it grows in a wide temperature range of 15º – 45ºC. If conditions for growth are not favorable, *it* can be inactive and lie in wait for a good time to begin growing. Later, the bacteria can start growing again when conditions are more favorable. The cell wall of *S. aureus* is very thick compared with the cell walls of other bacteria, it is the reason of its resiliency, and this thickness allows *S. aureus* to exist with the highest internal pressure of any type of bacteria. *S. aureus* infections are difficult to treat because the high internal pressure and the thick cell walls make it very difficult for antibacterial drugs to get inside *S. aureus* cells and kill them [39]. This bacteria cause many human diseases ranging from minor skin infections to life-threatening heart valve infections.

1.9.2. Escherichia Coli

E. coli is a bacterium that lives in the lower intestines of warm blooded animals, including humans. Fossil remains of bacteria are found in rocks that are billions of years old. *E coli* is very small, its cells are shaped about 2.5 µm long by about 0,8 µm in diameter, with hemispherical end caps. It has not a nucleus, other membrane-enclosed organelles, or any cytoskeletal elements typical of higher cells, such as those composing the human body. However, some elements of this kind are built into the cell wall. And *E. coli* has external organelles, thin straight filaments that enable it to attach to specific substrata, and thicker, longer helical filaments that enable it to swim. Cells of *E. coli* can live with or without oxygen, and thus survive until they find another host.[40]

E. coli is a facultative anaerobe capable of fermentative and respiratory metabolism. Its optimum temperature is 37ºC and it grows readily on a wide range of simple culture media and on simple synthetic media. Under anaerobic growth conditions there is an absolute requirement for fermentable carbohydrate. Glucose is fermented to pyruvate, which is converted into lactic, acetic and formic acids. Part of the latter is converted into hydrogen and carbon dioxide by formic hydrogenlyase but some strains do not produce gas. [41]

E. coli swims and it modifies the way in which it swims to move toward regions in its environmental that it deems more favorable. Each flagellum is driven at its base by a reversible rotary motor, driven by a proton flux. The cell's ability to migrate in a particular direction results from the control of the direction of rotation of these flagella. This control is affected by intracellular signals generated by receptors in the cell wall that count molecules of the interest that impinge on the cell surface. [40]

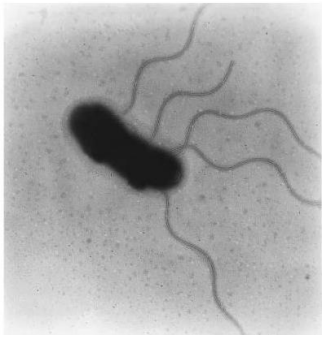

Figure 1-23. Electron micrograph of E. coli negatively stained [41]

2. MATERIALS, EQUIPMENT, AND ASSEMBLY PROCESS EXPERIMENTAL

SAMPLES PREPARATION

2.1.1. Material

Pure titanium grade 2 bars was used as the base material for the experiment part of the study. The solvents used to wash the samples were cyclohexane, ethanol, acetone, water and isopropanol. Poly (ethylene glycol) bis (3-aminopropil) (Mn ~1,500) (Reference 452572-5g) (PEG) was supplied by Sigma-Aldrich. Doxy-loaded PHB micro-and nano- spheres were obtained from a previous work [34]. The spheres used in this study were the corresponding ones named US/TU13 and US/TU14 for micro- and nano-spheres respectively (Figure 2-1). *Table 2-1* shows the drug loading, entrapment efficiency (EE) and PHB-based particle sizes, corresponding to the previous work of Doxy/PHB particles synthesis.

Sample	% Loading (w/w)	EE %	Diameter size (µm)
US/TU13	1.93	11.56	17.43±6.01
US/TU14	2.90	14.84	0.32±0.16

Table 2-1. Micro- and nano- spheres [34]

A) 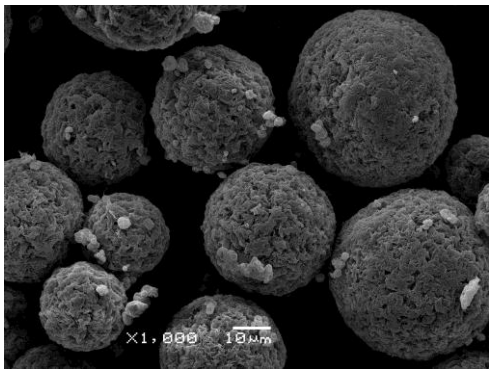

B) 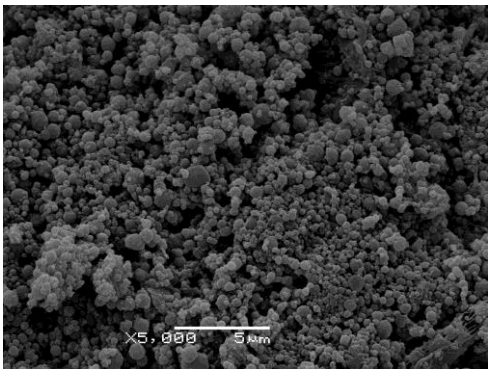

Figure 2-1. SEM micrographs of the Doxy-loaded PHB particles used in this study: A) Micro-particles (US/TU13), B) Nano-particles (US/TU14)

2.1.2. Sample preparation

Titanium disks of 3 mm thick were obtained by cutting an 8 mm diameter bar using a cutting equipment (Isomet, low speed saw, Buehler, Germany). Disks surfaces were devastated and polished (automatic polishing *Ecomet4*, Buehler, Germany). Mirror-like, smooth surfaces were achieved by grinding with SiC papers of decreasing grit size (from P240, P400, P600, P1200, P2500, P400 European P-grade standard). Then, alumina suspension of 1 µm and 0,05 µm were used. Water was used as a lubricant except for the final polishing where alumina with distilled water was used instead. The disk rotated at 180-200 rpm counter to the wheel rotation. *Table 3-1* shows a summary of the polishing process and the *Figure 2-2* shows the automatic polishing Ecomet 4 from Germany.

Figure 2-2. Automatic polishing Ecomet4 (Germany)

ABRASIVE	TIME (min)	FORCE (LBS)	MOTOR (rpm)	LUBRICANT
240	120	6	180	Water
400	30	6	180	Water
600	100	8	180	Water
1200	120	10	200	Water
2500	60	12	200	Water
4000	30	15	200	Water
1 µm	60	20	200	Alumina + Distilled Water
0,05 µm	60	20	200	Alumina + Distilled Water

Table 2-2. Polishing process

Table 2-2 shows a summary of the values of the polishing process that it is described below. The samples linked with "Loktite" in a metallic disc. The first abrasive paper was 240, this paper is used to grind all samples at the same level. Once the samples were at the same level, the abrasives papers were changed. The change of the paper did not do until most of the previous grinding marks were removed. The final polishing stage with 1 and 0,05 micron suspended alumina oxide particles should be carried out on a separate cloth polishing wheel. The wetness of the cloth used for the final polishing has a great influence on the end result. If the cloth is too wet the sample will show pits; if too dry, buffing and/or smearing will result.

The cleaning of the samples followed a general protocol, to ensure an exhaustive cleaning of metallic samples. It combines both apolar and polar solvents in order to remove the maximum number of impurities. The beaker was cleaned with H_2O and acetone and the samples were placed at its bottom. All the samples were fully covered with ciclohexane and they were sonicated in an ultrasonic bath for five minutes. The ciclohexane was changed to a total of three washings. After the ciclohexane, the process was repeated with different solvents. Isopropanol, water, ethanol and acetone were used three times, five minutes each other. Finally, the samples were dried with N_2 and they were stored in a multi-well plate.

Figure 2-3. Sonicate (UPC)

FUNCTIONALIZATION PROCESS OF TITANIUM

This section describes a reliable functionalization process. The first step of the process was the activation of the surface, once the titanium surfaces were activated they were silanized, and finally the PHB spheres were added together with the PEG. The study can be separated in different steps, which table 2-3 summarizes:

Step 1: Surface activation

- Plasma cleaning

- Sodium Hydroxyde treatment

Step 2: Silanization
- APTES
- CPTES

Step 3 *A)* Titanium surfaces reaction with Doxy-PHB spheres
- Doxy-LOADED PHB: micro- and nano- size
- O-Benzotriazole-N,N,N',N'-tetramethyl-uronium-hexafluoro-phosphate (HBTU)

B) Titanium surfaces reaction with PEG

Activation	Silanization	PHB Spheres	
Plasma	Ti + APTES	HBTU	Micro
			Nano
		-	Micro
			Nano
	Ti + CPTES + PEG	HBTU	Micro
			Nano
		-	Micro
			Nano
NaOH	Ti + APTES	HBTU	Micro
			Nano
		-	Micro
			Nano
	Ti + CPTES + PEG	HBTU	Micro
			Nano
		-	Micro
			Nano

Table 2-3. Classification of all the samples.

2.1.3. STEP 1: SURFACE ACTIVATION

In order to activate titanium surface for further binding to alkoxysilane, the titanium discs were treated with two methods: plasma cleaning and sodium hydroxide treatment.

2.1.3.1. Plasma Cleaning

The samples were introduced into the chamber on a glass surface (Plasma Cleaner, Sterilizer PDC-002, Harrick Scientific Corporation, USA), this chamber generated vacuum and the argon was injected inside for five minutes. The plasma cleaning was generated for 10 minutes. After this time plasma switched off and the vacuum broke. The activation of the surface was finished and the samples were extracted from the chamber. The next step and the characterization have to do quickly because the plasma activation lost properties during the time [6].

Figure 2-4. Plasma cleaning equipment (UPC)

2.1.3.2. Sodium Hydroxide treatment

Titanium disks were immersed in readily prepared sodium hydroxide 5 M in closed polypropylene flasks. They were introduced in a furnace at 60ºC for 24h. Once the treatment was completed, the samples were immersed in Milli-Q water for 30 minutes two times. Finally the samples were cleaned with different solvents; water, acetone, ethanol and then they dried with nitrogen [17].

2.1.4. STEP 2: SILANIZATION

Silanization is the most widely used method for the immobilization of biological molecules on model surfaces. 3-Aminopropyltriethoxysilane and 3-Chloropropyltriethoxysilane were

applied as organosilane on the activated metal surfaces in order to attach the loaded PHB particles in a following step.

2.1.4.1. 3-Aminopropyltriethoxysilane (APTES)

The magnetic stirrer was switched on and set at 90ºC to warm the surface. The samples were placed at the bottom of an Erlenmeyer, which was previously cleaned with H_2O and acetone, and dried with nitrogen. A magnetic stir bar was put inside the Erlenmeyer jointed with the samples, and closed with a rubber stopper. Erlenmeyers was completely closed with vacuum and purged nitrogen gas. Then, 10 ml of anhydrous toluene and 0,2 ml of APTES (0.04M) were added. The reaction mixture was leaved under agitation for one hour at 70ºC.

Figure 2-5. Silanization with APTES

Afterwards, the samples were transferred to a beaker that contains toluene, and were sonicated in an ultrasound bath for five minutes in order to eliminate the loosened silane from the surface. Subsequently, the samples were washed with toluene three times, acetone one time, isopropanol, ethanol and acetone three times, and were dried with nitrogen. Once the samples were washed, they were placed in a petri dish and the silanes were cured at 120 ºC for five minutes. Finally, the samples placed into a new beaker. Thus, the samples were ready for reaction with Doxy-loaded PHB micro- and nano-spheres.

Figure 2-6. Samples cured at 120ºC for 5 minutes.

2.1.4.2. 3-Chloropropyltriethoxysilane (CPTES)

The magnetic stirrer was switched on and set at 90ºC to warm the surface. The samples were placed at the bottom of an erlenmeyer, which was previously cleaned with H_2O and acetone, and dried with nitrogen. A magnetic stir bar was put inside the Erlenmeyer jointed with the samples, and closed with a rubber stopper. Erlenmeyers was completely closed with vacuum and purged nitrogen gas. Then, 10 ml of anhydrous toluene, 0,1 ml of diisopropylethylamine 0.06 M (DIEA), and 0.2 mL CPTES 0.08 M were added. The reaction mixture was leaved under agitation for one hour at 70 ºC. Afterwards, the samples were washed with toluene, isopropanol, water, ethanol and acetone three times with each solvent and dried with nitrogen. Thus, the samples were prepared for the reaction with PEG.

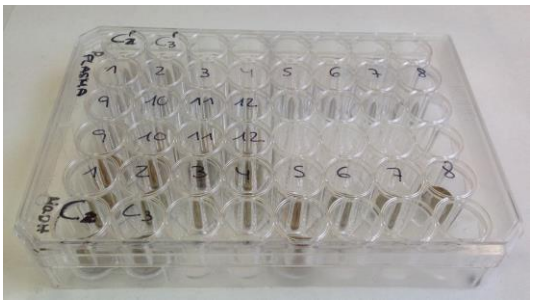

Figure 2-7. Silanized samples

2.1.5. STEP 3: TITANIUM SURFACES REACTION

2.1.5.1. A) Titanium surfaces reaction with Doxy-PHB spheres

- *Doxy-LOADED PHB: micro- and nano- size and O-Benzotriazole-N,N,N',N'-tetramethyl-uronium-hexafluoro-phosphate (HBTU)*

The magnetic stirrer switched on and it set the hot plate at 30ºC to warm the surface. Three samples were placed at the bottom of each erlenmeyer, which were previously cleaned with H_2O and acetone and dried with nitrogen.

Four different studies were carried out: the combination of micro- and nano-spheres with or without HBTU as a coupling agent. The PHB spheres (nano- and micro-) and HBTU were separately introduced inside each erlenmeyer jointed with the titanium surfaces. Micro- and nano-spheres were added in the amount to obtain a concentration of 15 mM, and 45 mM for HBTU. Then, 0,2 ml of DIEA and 20 ml of dimethylformamide (DMF). The reaction was carried out at 30 ºC temperature for 2 hours with orbital agitation. Afterwards, the samples were washed in DMF twice, rinsed in water, acetone and dried with nitrogen. The samples were then used or stored in vacuum for further experiments.

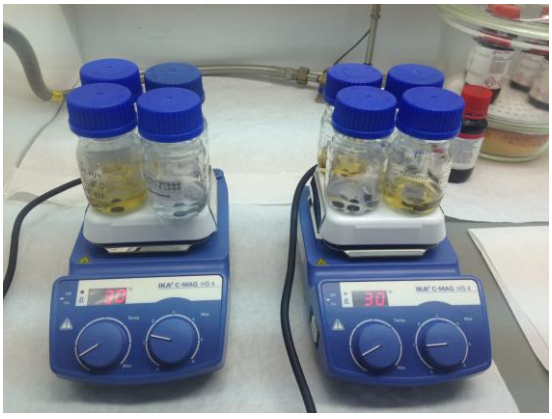

Figure 2-8. Titanium surfaces reactiun with Doxy/PHB spheres

2.1.5.2. B) Titanium surfaces reaction with PEG

Following the silanization of the titanium surfaces with CPTES, the samples were placed with a magnetic stirrer into a hermetically sealed beaker. Then, 0,26 g PEG, 0,01 g sodium carbonate, and 40 ml mille-Q water were added. The reaction was leaved for 24 hours at 200 rpm and at room temperature. Thus, the samples were ready for reaction with Doxy-loaded PHB micro- and nano-spheres.

IN VITRO ANTIBACTERIAL ASSAY

Figure 2-9 shows the material requires to carry out the in vitro antibacterial assay.

Figure 2-9. Material used in bacterial assay

Titanium treated surfaces were in vitro tested with *Escherichia coli* and *Staphylococcus aureus* as a Gram – and Gram + bacteria, respectively. The strains were cultivated for 24 hours in each specific solid media. From them, precultures were incubated overnight in 10 mL tubes containing 5 mL of TSB at 37 ºC. Then, a bacterial solution was prepared with TSB, adjusting the OD to 0.2 at 600 nm (bacterial concentration about 10^8 cfu/ml). Prior to use the samples, they were washed with distilled water, ethanol and acetone and dried at room temperature. For sample sterilization, they were sterilized under UV light for five minutes. Then, they were introduced in a multi-well plate with 1 mL of the bacterial suspension and incubated for 2 h at 37 ºC. To quantify bacterial cells adhered to the c.p.Ti samples, they were washed twice with PBS and then introduced in an Eppendorf tubes containing 1 ml solution. Upon continued vortexing (5 min) viable cell counts in the supernatant were determined by cultivating them in the respective solid media for 24 h at 37 ºC, and counting the colonies formed in a 10^{-3} and 10^{-5} dilution [51].

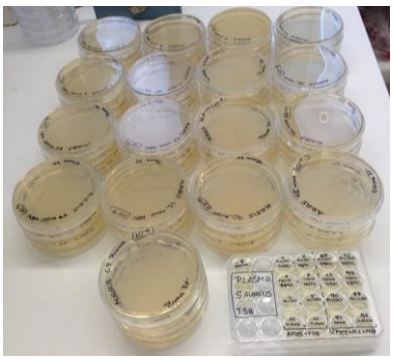

Figure 2-10. Solid media

CHARACTERIZATION OF BIOMATERIALS

2.1.6. Wettability: Contact Angle

The sessile drop method is the most common and convenient method used to measure the contact angle. The contact angle goniometer used was "Contact Angle System OCA 15plus, Germany" and the software to analyze the contact angle was "SCA20, Dataphysics, Germany. The equipment consists of a horizontal stage to mount a solid sample, a micrometer pipette to form a liquid drop, an illumination source, a camera and a telescope equipped with a protractor eyepiece. The sample was placed on a stage and through the software, a drop of liquid of about 5 µl was dropped on the solid surface and the measurement was achieved by simply aligning the tangent of the sessile drop profile at the contact point with the surface and reading the protractor through the eyepiece. The camera takes photographs of the drop profile so as to measure the contact angle with more precision and accuracy. Several measurements were taken with the same sample to compare the results.

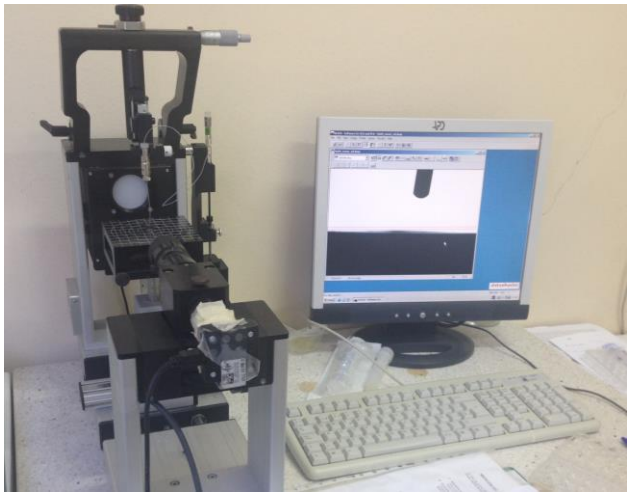

Figure 2-11. Contact Angle System OCA (Germany)

2.1.7. Field emission scanning electron microscope

FESEM was used to observe the morphology of the surface (JSM 7001 F, Japan). Titanium surfaces were platinium/paladium coated (coating thickness between 10-15 nm) under vacuum by means of a BAL-TEC (SCD 005, Germany) cool sputter coater and their scanning electron micrographs were obtained using a Jeol (JSM-7001F, Japan) scanning electron microscope,

operating at 15 KV. Energy Dispersive X-ray Spectroscopy (EDS) was also used for the elemantal analasis of the surfaces.

2.1.8. Atomic force microscopy (AFM)

AFM of the titanium surfaces was performed using a Dimension 3100 Microscope from Bruker, working in tapping mode. All the AFM images were processed with the WSxM software.

2.1.9. X-Ray Photoelectron Spectroscopy (XPS)

XPS was used to analyze the chemical composition of the samples surface. XPS spectra were acquired with an XR50 Mg anode source operating at 150W and a Phoibos 150 MCD^{-9} detector (D8 advance, SPECS Surface Nano- Analysis GmbH, Germany). High resolution spectra were recorded with pass energy of 25 eV at 0.1 eV steps and a pressure below $7.5 \cdot 10^{-9}$ mbar. Two samples were studied for each working condition.

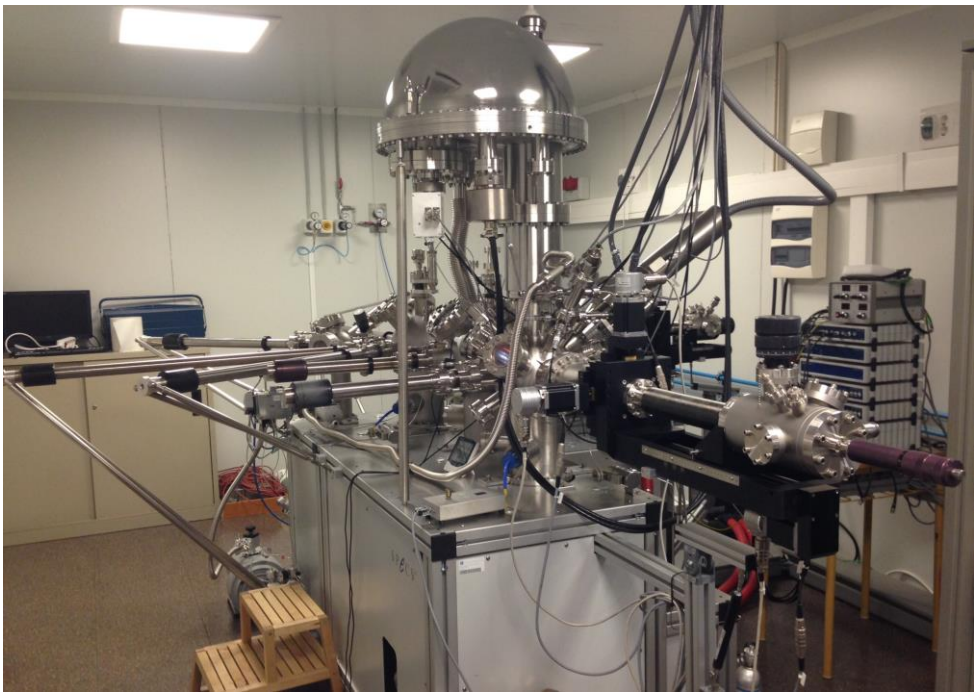

Figure 2-12. XPS located in UPC Barcelona

3. EXPERIMENTAL RESULTS

SURFACE ACTIVATION

3.1.1. Surface morfology

The plasma cleaning and the sodium hydroxide treatment were used in order to obtain different roughness on the surfaces of the samples. Micrographs in *Figure 3-1* show the morphology of the untreated titanium surfaces, and the surfaces with each activation treatment. The *image C* from *Figure 3-1* shows that the samples with sodium hydroxide treatment have more roughness with nanoporous on the surface than the samples with plasma treatment.

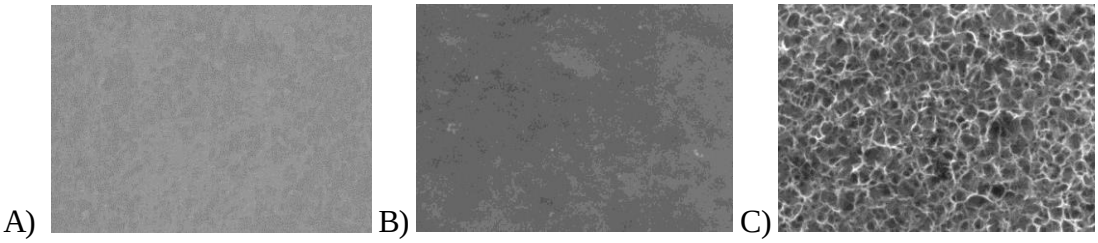

Figure 3-1. FESEM images x30000. A) c.p. Titanium; B) Plasma cleaning; C) NaOH

3.1.2. Contact angle

Contact angle was measured on the surface of each superficial treatment, minimum six times. The contact angle of the commercially pure titanium (c.p. Ti) was 42.8±4.9º. Plasma treatment reduced the contact angle as well as the NaOH treatment. Thus, the wettability and the hydrophilicity on the titanium surfaces changed for each activation treatment. Figure 3-2 shows the wettability of the surface treated with different methods.

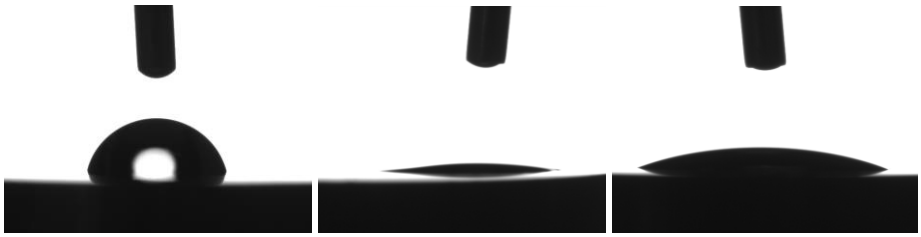

Figure 3-2. Contact angle. Left) Titanium; Middle) Titanium + Plasma; Right) Titanium + NaOH

Each activation treatment was silanized with different methods: APTES and CPTES. The contact angle was also measured for these surface treatments. Following, the comparison of the contact angle results are described separated by the activation treatment.

3.1.2.1. Plasma Treatment

Plasma treatment reduced the contact angle of the titanium surface from 42º to 8,9º, so it increased the hydrophilicity. When the samples were silanized, water contact angle increased, especially when APTES was used to silanized the c. p. Ti surfaces. APTES increased the hidrophobicity since the contact angle increases in 37º and CPTES reduced 7º in comparison with APTES treatment. Thus, all the silanized samples were more hydrophobic than the samples treated with only plasma. However, there is a variation of the hydrophobicily if the surfaces with CPTES and CPTES+PEG are compared. The presence of the PEG increased the hidrophilicity. Figure 3-3 shows the contact angle graphic with the average angles and the images of the samples with each treatment.

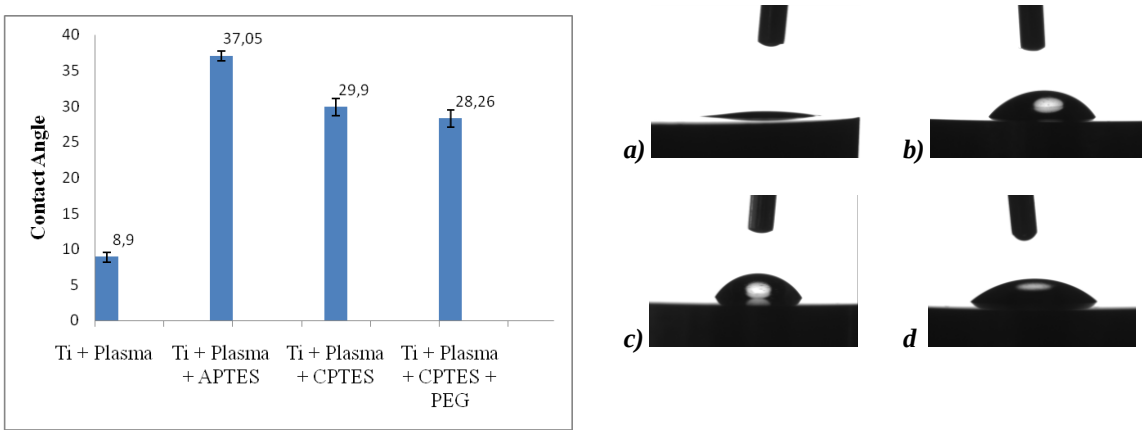

Figure 3-3.Left: Contact angle graphic. Right: a) Titanium + Plasma. b) Titanium + Plasma + APTES. c) Titanium + Plasma + CPTES. d) Titanium + Plasma + CPTES + PEG

3.1.2.2. Sodium Hydroxide Treatment

Sodium Hydroxide treatment reduced the contact angle of the titanium surface to 23º. The activation with APTES increased the hydrophobicity to 29.5º on the titanium surface. CPTES silanization increased the contact angle as well, but slightly less than the other silanization. When PEG was added, the contact angle reduced.

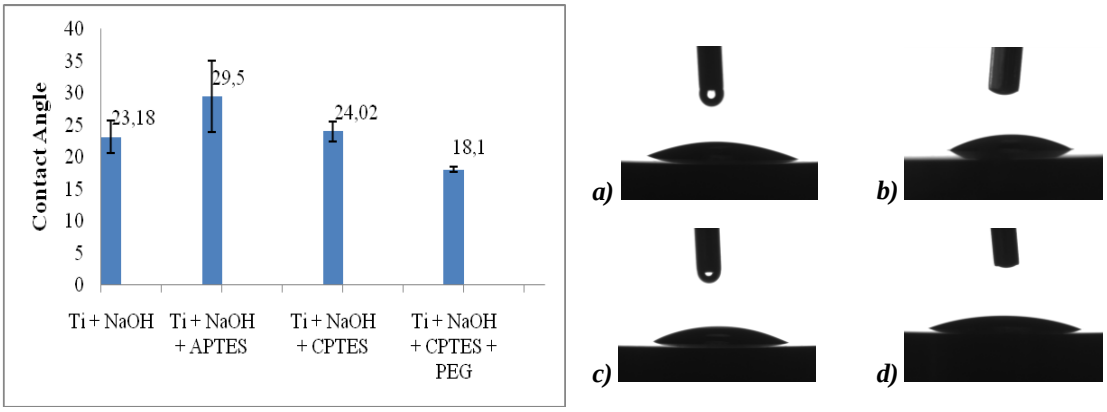

Figure 3-4.) Left: Contact angle grahic. Right: Titanium + NaOH. b) Titanium + NaOH + APTES. c) Titanium + NaOH + CPTES. d) Titanium + NaOH + CPTES + PEG

3.1.3. FESEM

All samples were observed under electron microscopy in order to study the morphology of the titanium surfaces first, and second to ensure the attachment of the Doxy/PHB spheres.
In general, different morphologies were observed between the surfaces treated with plasma and with NaOH. PHB spheres have been observed in practically all the titanium surfaces treated.

3.1.3.1. Plasma Treatment

Figure 3-6 shows the FESEM micrographies of the samples tested. When the micro- and nano-spheres have been added, only the smaller spheres have been attached to the titanium surface. In the case of the micro-spheres, this could be possible due to the high particle size dispersion. In general, all samples where the Doxy-loaded PHB spheres were linked using HBTU show slightly better results compared to the samples were no coupling agent was used. It is observe that higher amount of spheres were attached where the surface showed major irregularities and the tendency of them is to group together (see *Ti + Plasma + CPTES + PEG + Nano- PHBa* Figure 3-5.B).

A) Titanium + Plasma + APTES

Ti + Plasma + APTES + Micro- PHB + HBTU

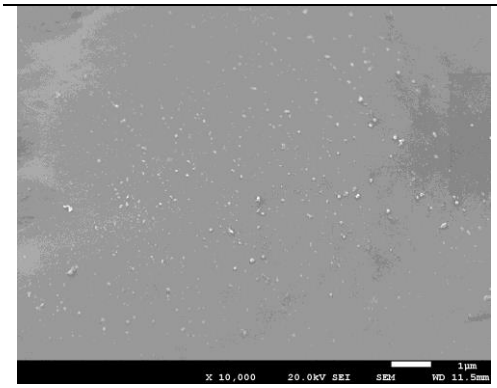

X10000 X30000

Ti + Plasma + APTES + Micro- PHB

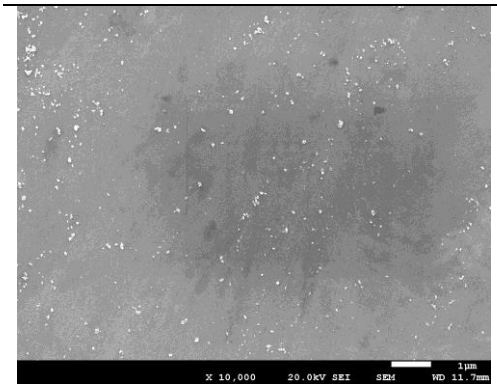

X10000 X30000

Ti + Plasma + APTES + Nano- PHB + HBTU

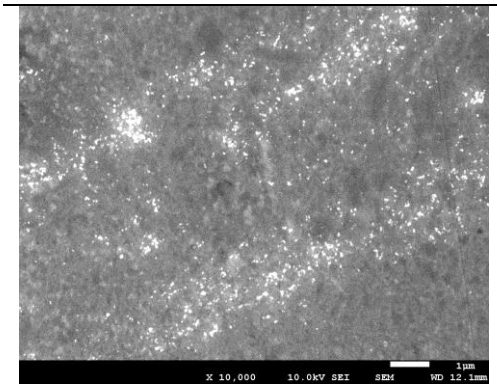

X10000 X30000

Ti + Plasma + APTES + Nano- PHB

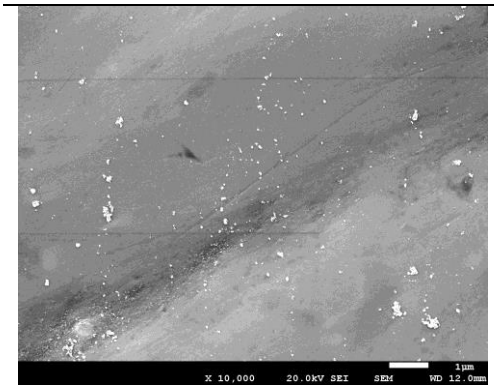

X10000

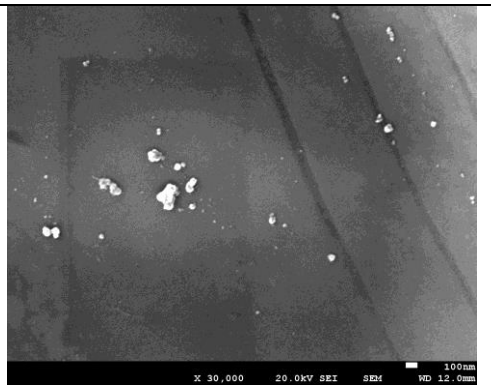

X30000

B) <u>Titanium + Plasma + CPTES + PEG</u>

Ti + Plasma + CPTES + PEG + Micro- PHB + HBTU

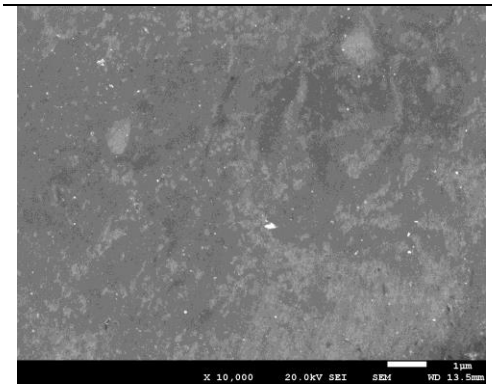

X10000

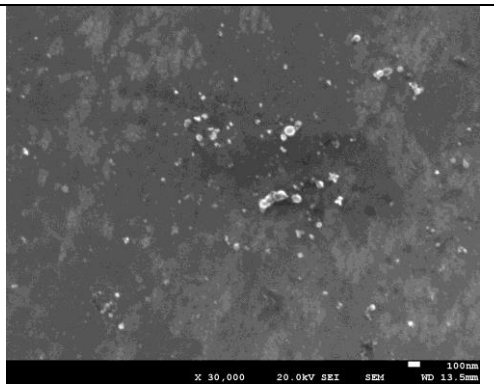

X30000

Ti + Plasma + CPTES + PEG + Micro- PHB

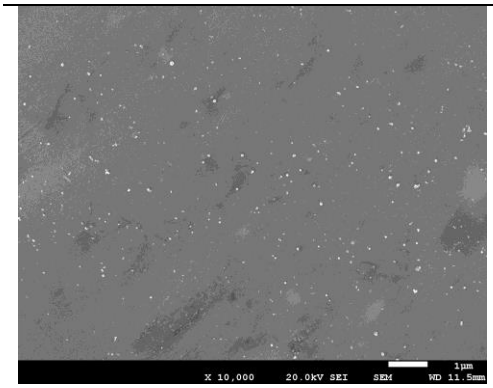

X10000

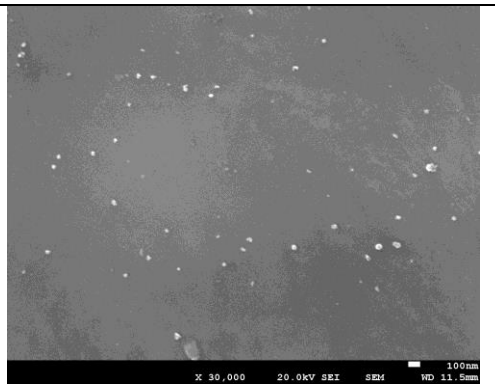

X30000

Ti + Plasma + CPTES + PEG + Nano- PHB + HBTU

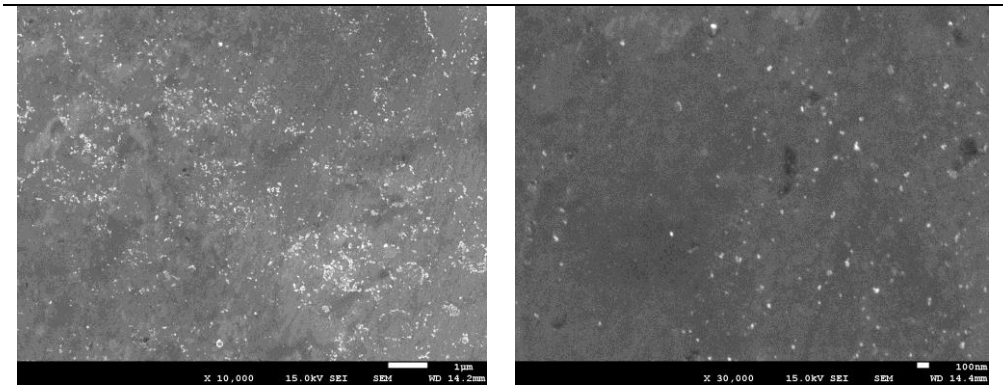

X10000 X30000

Ti + Plasma + CPTES + PEG + Nano- PHB

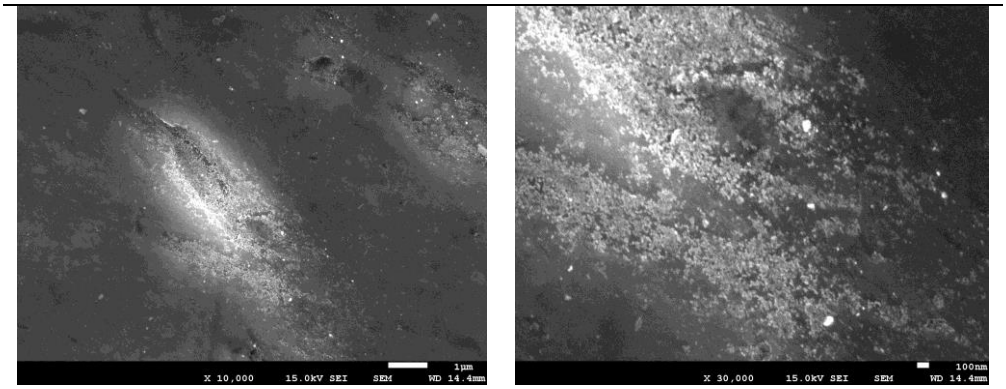

X10000 X30000

Figure 3-6. FESEM Micrographies of A) Ti + Plasma + APTES; B) Ti + Plasma + CPTES + PEG

3.1.3.2. Sodium Hydroxide treatment

Figure 3-7 shows the FESEM micrographies of the samples tested. In general, all samples where the Doxy-loaded PHB spheres were linked using HBTU show slightly better results compared to the samples were no coupling agent was used. These spheres are distributed homogeneously on the entire surface as micrographs at x150 magnifications show. Gathered nano- spheres are detected over the surface of the samples and their size is about 300 nm. Some images at x30000 magnification show some titanium oxide (TiO_2) from the activation treatment. Regarding CPTES treatment only the sample *Ti + NaOH + CPTES + PEG + Micro-PHB* shows spheres on the surface. Most spheres have not linked in the titanium surface, for this reason there is only one image instead of two.

A) *Titanium + NaOH + APTES*

Ti + NaOH + APTES + Micro- PHB + HBTU

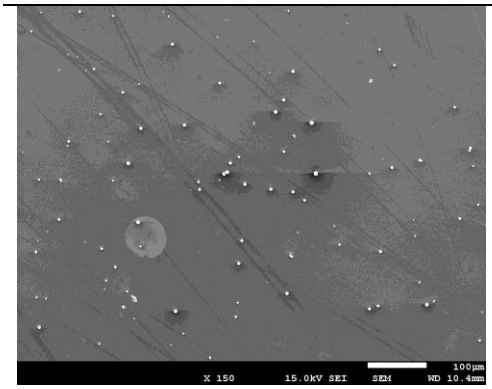

X150

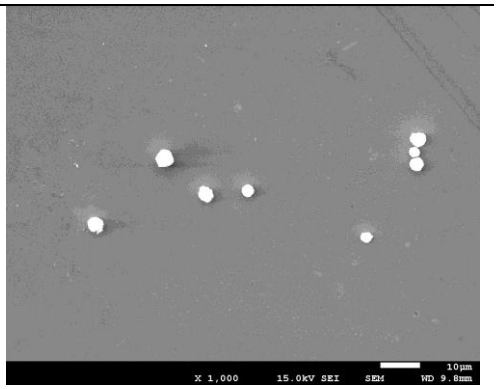

X1000

Ti + NaOH + APTES + Micro- PHB

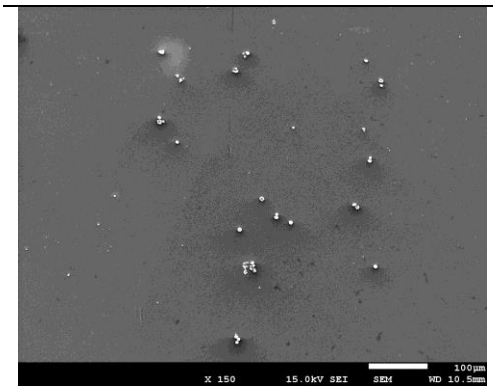

X150

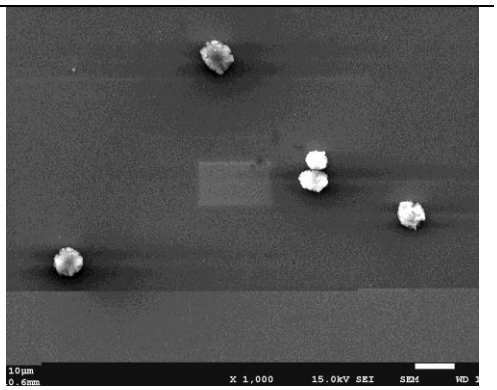

X1000

Ti + NaOH + APTES + Nano- PHB + HBTU

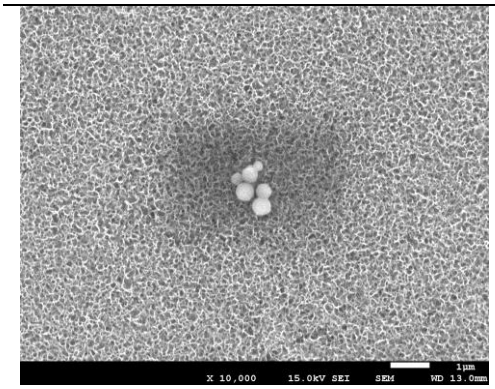

X10000

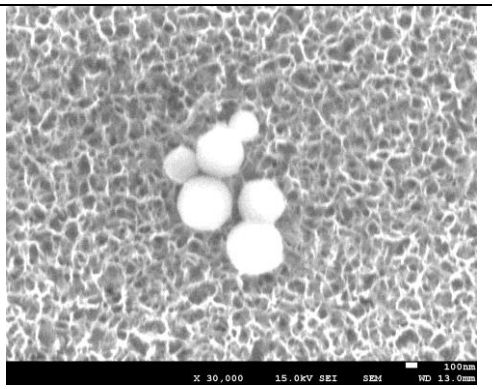

X30000

Ti + NaOH + APTES + Nano- PHB

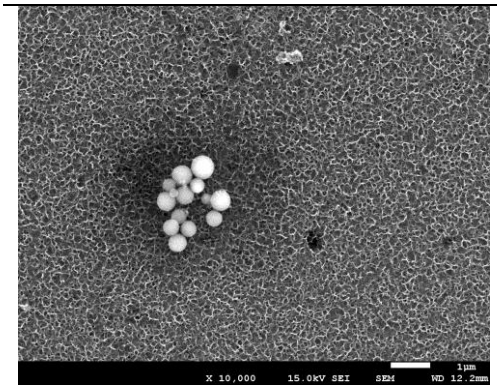

X10000

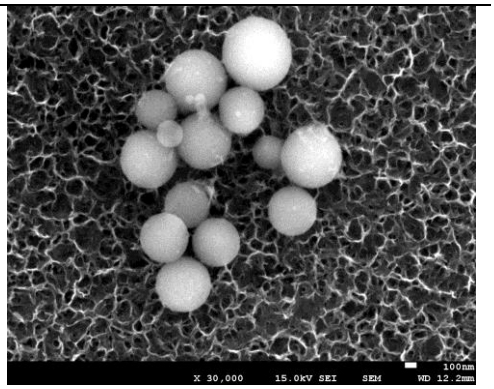

X30000

B) <u>*Titanium + NaOH + CPTES + PEG*</u>

Ti + NaOH + CPTES + PEG + Micro- PHB + HBTU

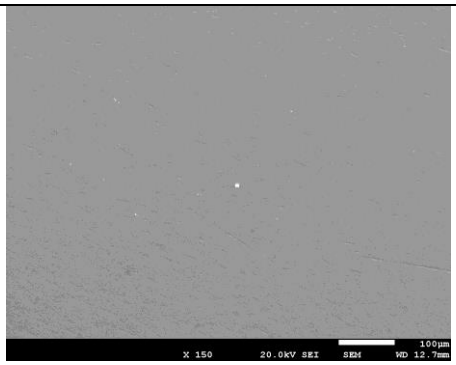

X150

Ti + NaOH + CPTES + PEG + Micro- PHB

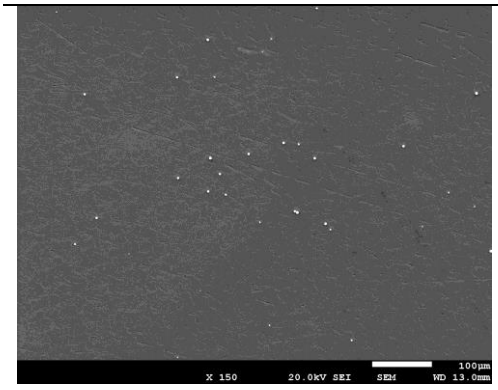

X150

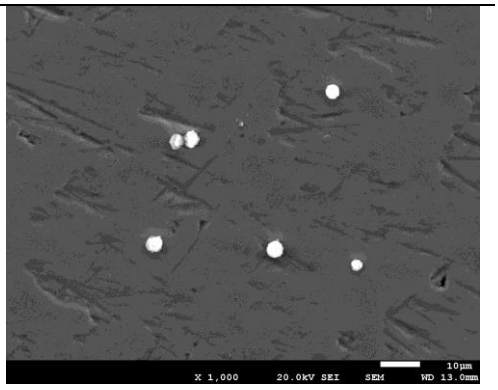

X1000

Ti + NaOH + CPTES + PEG + Nano- PHB + HBTU

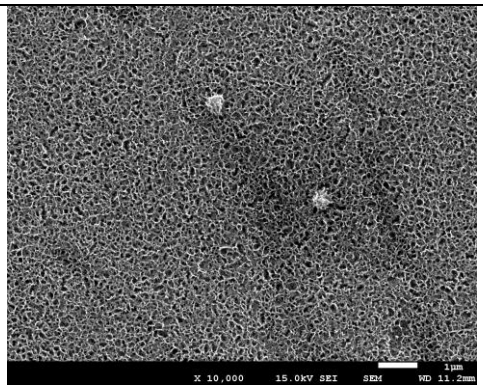

X10000

Ti + NaOH + CPTES + PEG + Nano- PHB

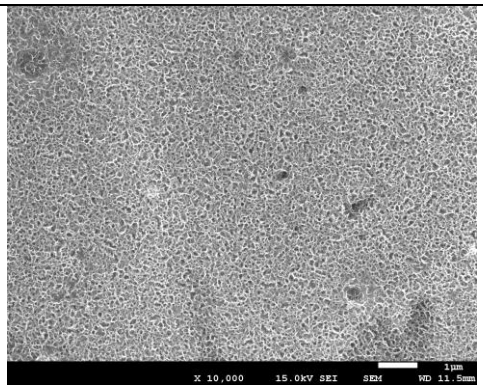

X10000

Figure 3-7. FESEM Micrographies of A) Ti + NaOH + APTES; B) Ti + NaOH + CPTES + PEG

Regarding the EDS results from FESEM, *Figure 3-8* shows the spectrums of each treatment. No differences were seen between plasma and NaOH treatment. The spectra of the samples with APTES show the presence of Nitrogen. Both activation treatments show very similar spectra. The spectra of the samples with CPTES show spectra with the presence of Chlorine (2,62 KeV), that confirm that CPTES reaction has been carry out.

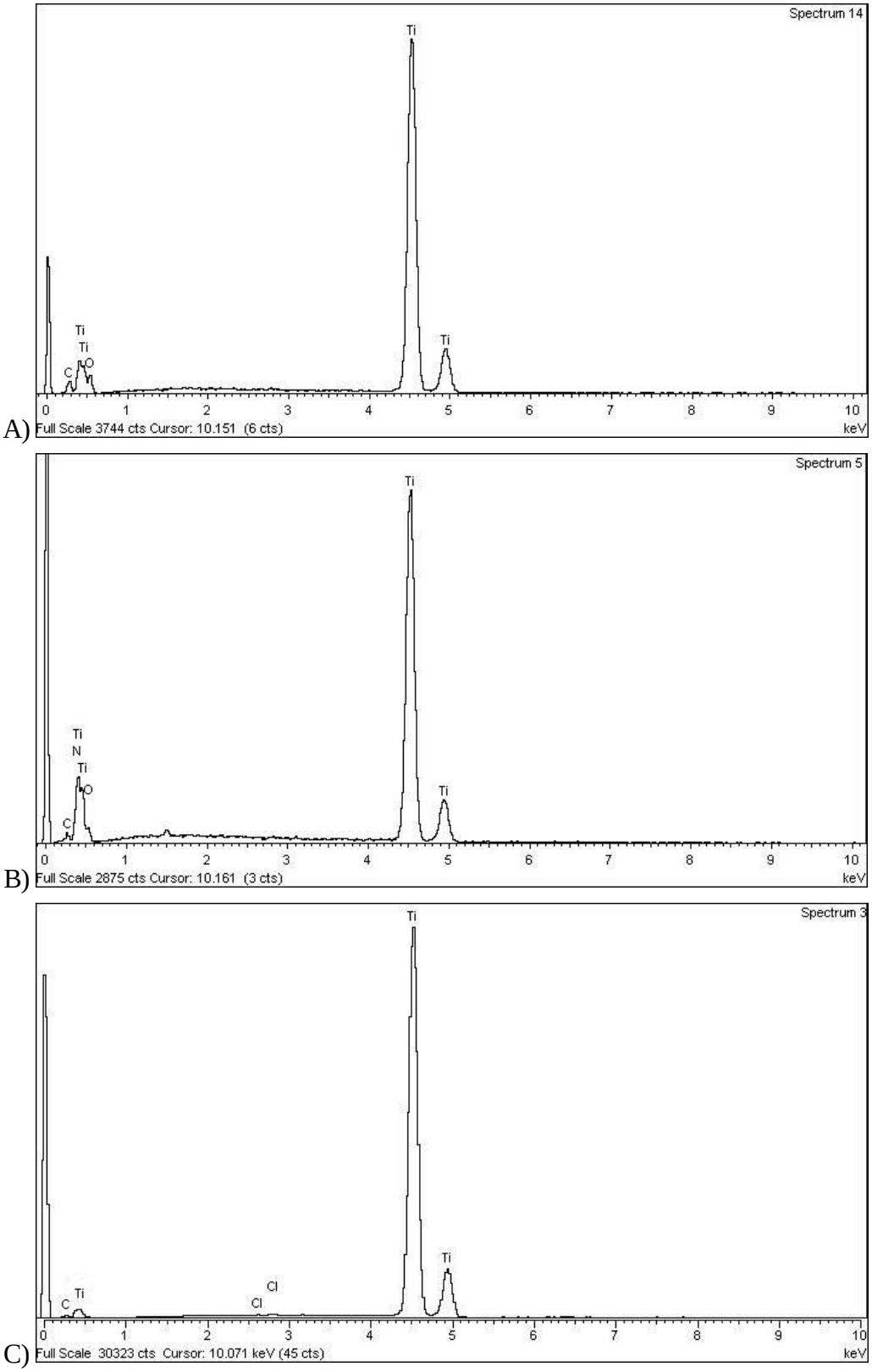

Figure 3-8. EDS results from FESEM. A) Plasma treatment. B) Plasma treatment + APTES. C) Plasma treatment + CPTES. Similar spectrum with NaOH treatment.

3.1.4. In vitro antibacterial Assay

Titanium treated surfaces were in vitro tested with *Escherichia coli* and *Staphylococcus aureus* as a Gram – and Gram + bacteria, respectively. An antibacterial assay was done with the samples of each treatment and PHB activation to compare the results. Figure 3-9 shows an example of the Petri plates with the strain E. *coli* cultivated after 24 hours at 37 ºC in Chromocult(R). The antibacterial assay for sample 37 (Ti + Plasma + CPTES + Micro- spheres + HBTU) shows the countable number of CFU when the dilution was of 10^3. With the dilution of 10^5, the colonies did not grow.

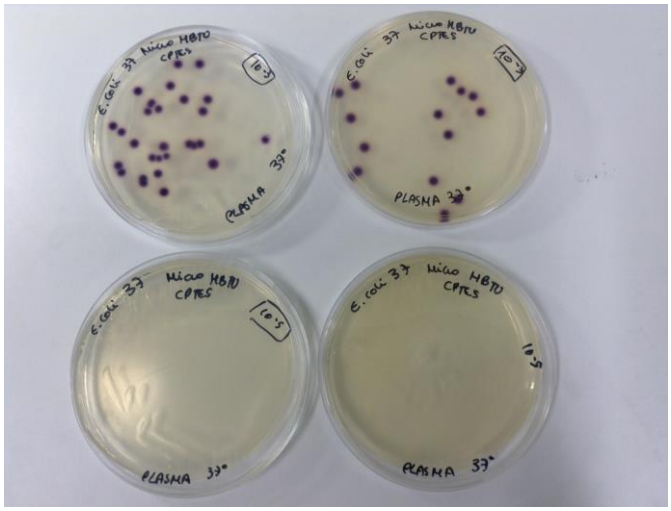

Figure 3-9. Petri plates with bacteria

Following *Figure 3-10* show the bacterial adhesion with a 10^3 and 10^5 dilution for the titanium surfaces with different treatment, but with no Doxy/PHB spheres (Table 3-1).

Treatment	
Titanium	
Ti + NaOH	Ti + Plasma
Ti + NaOH + APTES	Ti + Plasma + APTES
Ti + NaOH + CPTES	Ti + Plasma + CPTES
Ti + NaOH + CPTES + PEG	Ti + Plasma + CPTES + PEG

Table 3-1. Controls

Escherichia coli (G-)

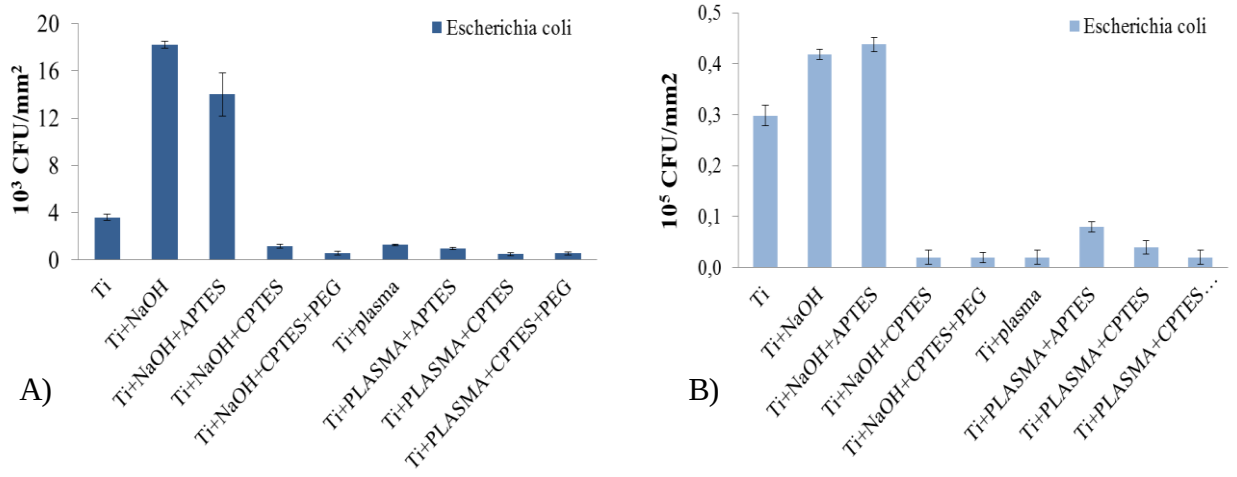

Figure 3-10. Bacterial count from the bacterial adhesion assay. Controls. A) 10^{-3}CFU/mm^2 B) 10^{-5} CFU/mm^2

All samples show less bacterial adhesion than Titanium surface with no treatment. Only the surfaces activated with NaOH with or without APTES show an increase of the microorganisms adhesion (CFU increases). This is due to the increase of the roughness of the samples. Bacterial adhesion decreases for the controls with CPTES at the surface, probably because of the presence of chlorine group on the surfaces. When PEG is added after CPTES, the bacterial adhesion decreases, this could be a confirmation of the presence of PEG as an anti-fouling. In general, all NaOH treated samples show the same tendency with *S. aureus* compared to the samples tested with *E. coli*, but the CFU is lower in all cases. The reason is found in the bacterial type and the sensibility of the Gram + *S. aureus* to Doxycycline. The results of the different assays with 10^3 and 10^5 dilutions show the same profile or bacterial behavior as well as the assays with S.aureus.

Following, *Figure 3-11* shows the bacterial count from the bacterial adhesion assay with the samples treated with Plasma and NaOH.

Staphylococcus Aureus

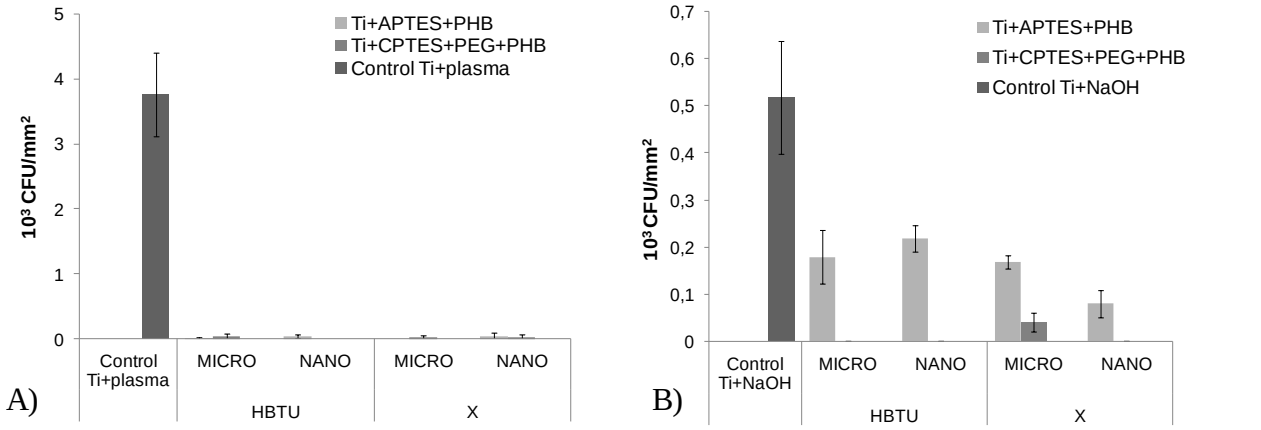

Escherichia Coli

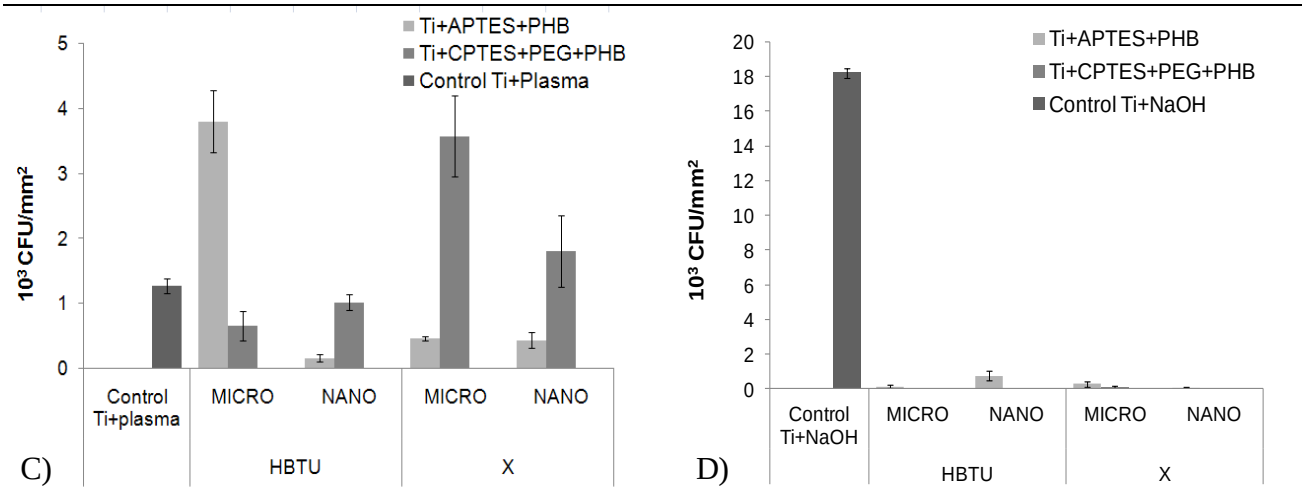

Figure 3-11. Bacterial count from the bacterial adhesion assay: A & C Plasma and B & D NaOH.

3.1.4.1. Staphylococcus aureus (G+)

All samples of titanium surface activated with plasma (*Figure 3-11 A)* show a better antifouling and, therefore antibacterial skills compared to the control.

In general, all samples activated with NaOH treatment (*Figure 3-11 B)* show the same tendency with *S. aureus* compared to the samples tested with *E. coli*, but the CFU is lower.

3.1.4.2. Escherichia coli (G-)

Bacterial adhesion of all samples activated with plasma treatment (*Figure 3-11 C)* and with Ti+APTES+PHB/Doxy is below the control, except the sample with micro-spheres and HBTU. Bacterial adhesion of samples with Ti+CPTES+PEG+PHB/Doxy with HBTU is below the control. However, the samples treated with no HBTU show an increase of the bacterial adhesion compared to the control.

With NaOH Ti-activation treatment (*Figure 3-11 D)*, micro-spheres were possible to be linked on the Titanium surfaces. However neither micro- nor nano-spheres were linked when CPTES was used as an alkoxylane to add PEG. Only in the case where no HBTU was used, micro-spheres were added to the surface. Bacterial adhesion of all samples with Ti+APTES+PHB/Doxy is below the control.

In the bacterial adhesion assay with a 10^5 CFU/mm^2 dilution, only few bacterial colonies were grew obviously following the profile of the bacterial count with a 10^3 CFU/mm^2 dilution.

3.1.5. Atomic force microscopy

The most appealing images resulted from AFM are shown in *Figure 3-12*. Titanium surface activated with plasma clearly shows a superficial coating when the samples were treated with PEG. Titanium surface activated with NaOH do not show that coating so easy.

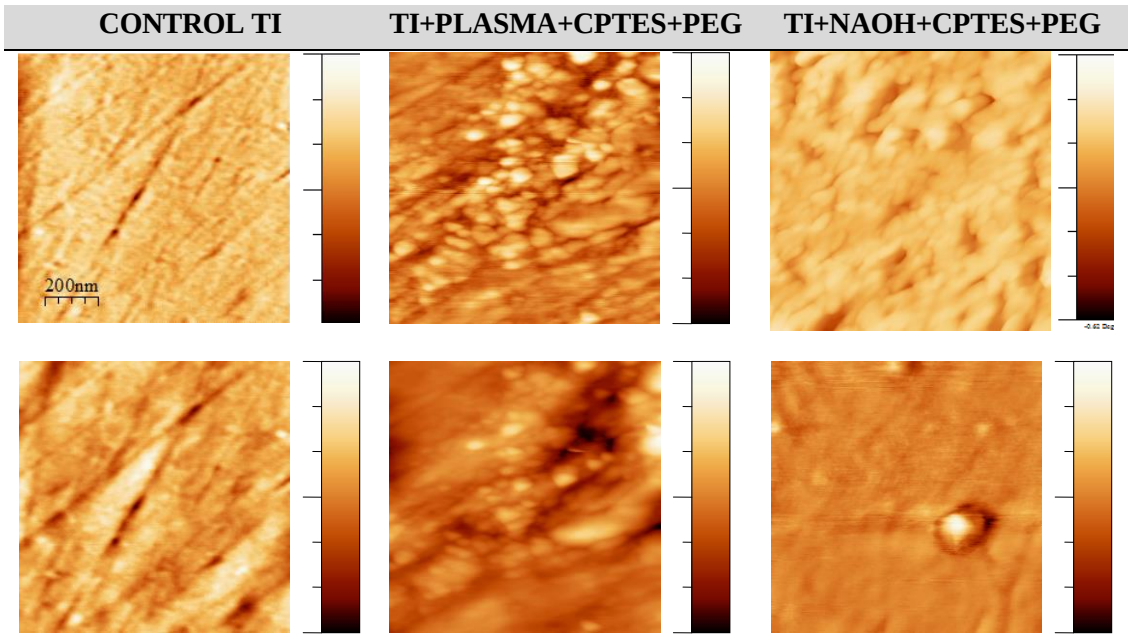

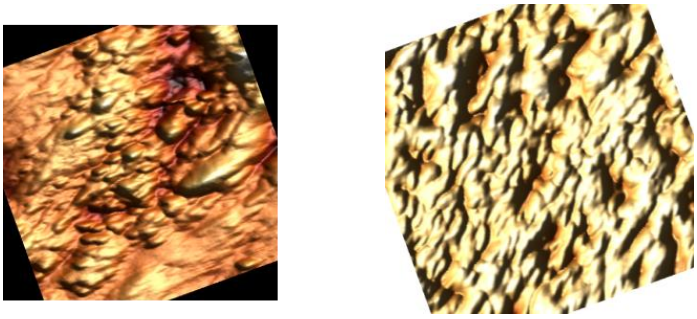

Figure 3-12. AFM images

3.1.6. X-Ray Photoelectron Spectroscopy

Figure 3-13 shows the XPS spectrua of titanium activated. *Graphics A, B* show the general spectrum of the XPS and *C, D* show the deconvulation of the Oxigen (O 1s). Compared *Graphic C* and *D*, the samples with titanium treated with plasma show an increase of the OH group percentage from the total oxigen of the surfaces.

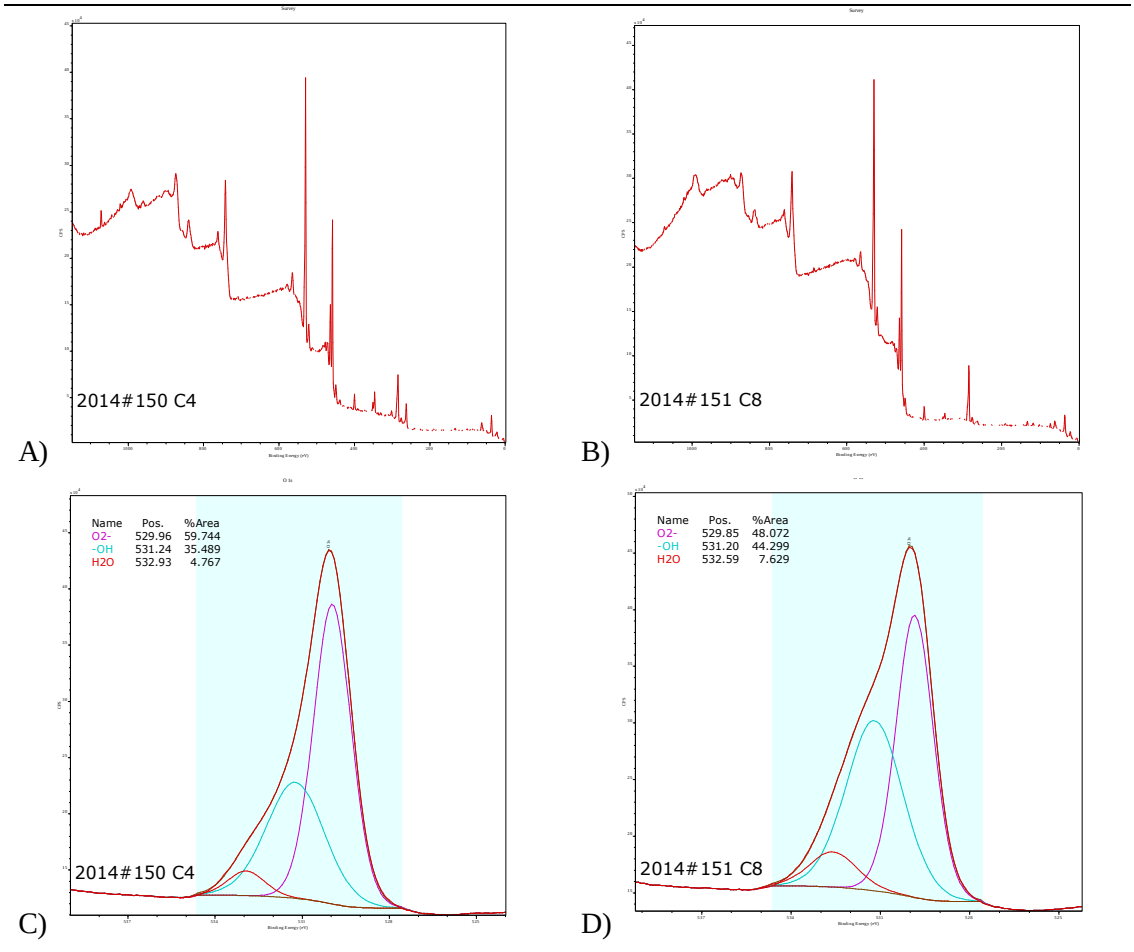

Figure 3-13. XPS. A, C) NaOH Treatment. B, D) Plasma Treatment

Figure 3-14 shows the XPS spectrums of the Titanium activated with CPTES silanization. There is the presence of Chlorine (C,D) and Silice (E,F) on the surfaces. Chloride (Cl^-) is detected but its amount is practically negligible (about 0.149% of the total concentration of Chlorine). *Graphic F* shows that there are more Chlorine organics (CPTES) in the surfaces treated with plasma than in the ones treated with NaOH. This is reasonable due to the higher OH percentage that plasma-treated surfaces show compared to the plasma ones. *Graphics C, D* show silice (O-Si-O) on the surface corresponding to the CPTES molecule.

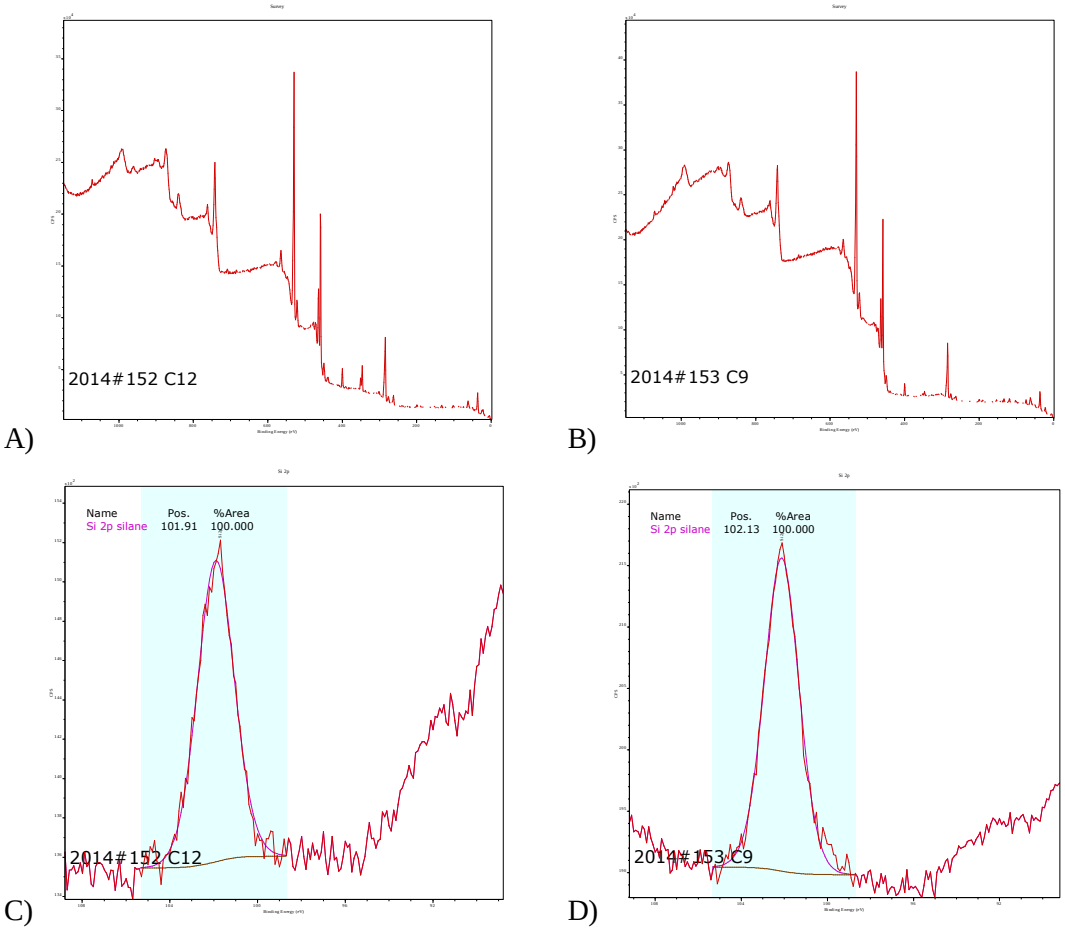

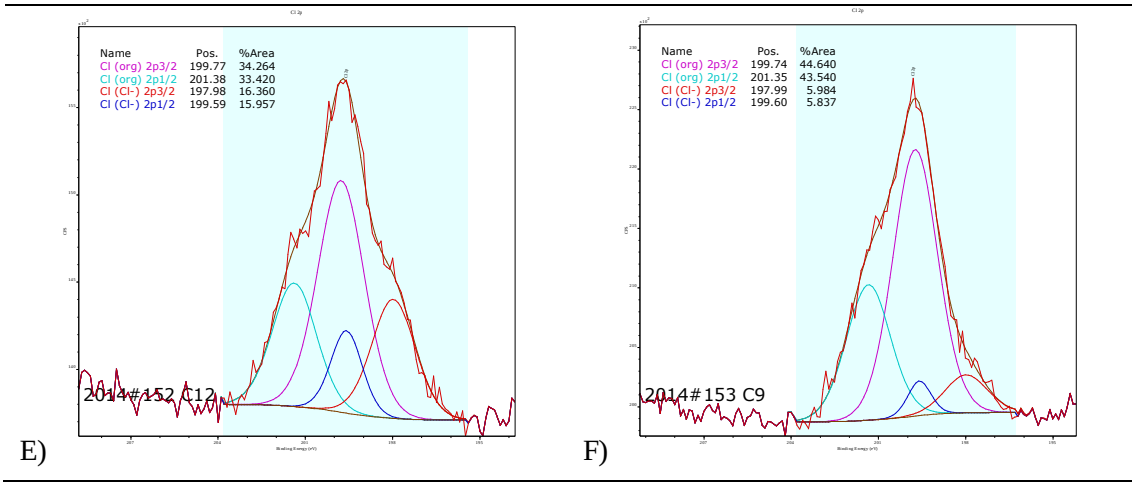

Figure 3-14. XPS. Ti + CPTES. A, C, E) NaOH Treatment. B, D, F) Plasma Treatment

Figure 3-15 shows the XPS spectra of the activated Titanium surfaces functionalised with CPTES, and PEG covalently added. They show the presence of Chlorine and Nitrogen and their deconvulations are shown in the figure (*C, D* and *E, F,* respectively). Chlorine organic is detected but its amount is almos negligible. It is related to unreacted CPTES with the PEG. Two types of Nitrogen are distinguished (graphic E, F): A small one at 401.80 eV corresponding to protonised amines (NH_3^+) and a large peak at 400.70 eV corresponding to a primary free amine non protonised (NH_2) [47][48][49]. These XPS sprectra confirm that the reaction between CPTES and PEG took place.

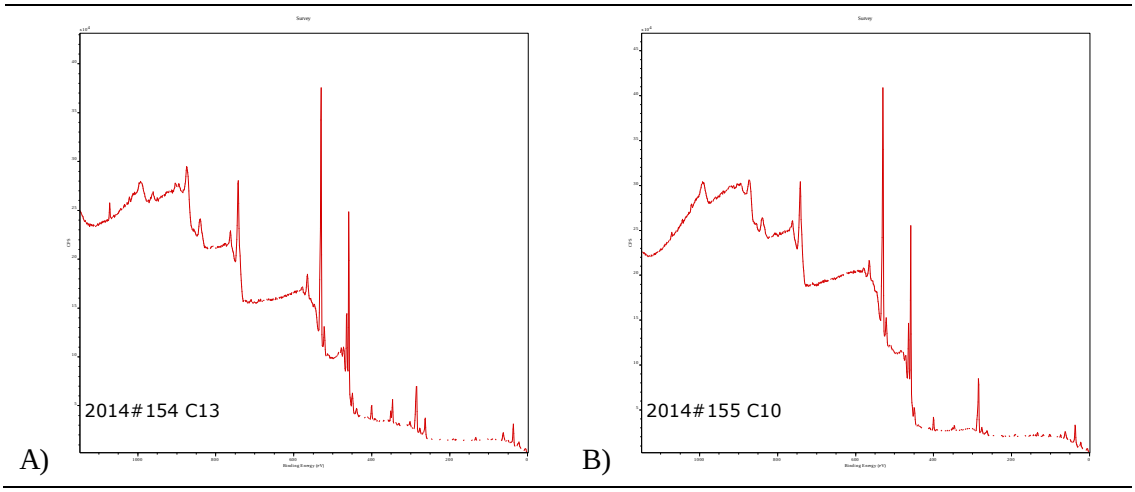

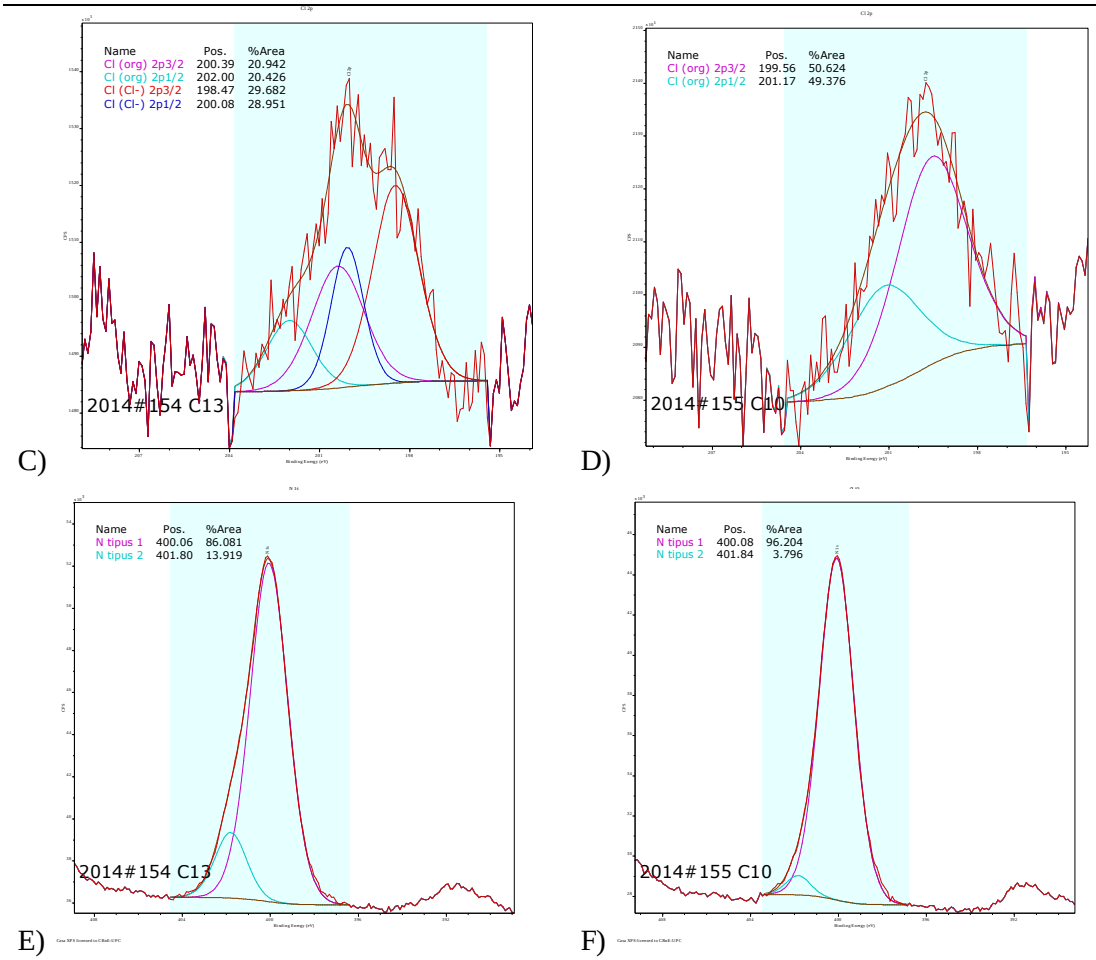

Figure 3-15. XPS. Ti + CPTES + PEG. A, C, E) NaOH Treatment. B, D, F) Plasma Treatment

4. DISCUSSIONS

In order to obtain biomimetic surfaces with antibacterial activity, nano- and micro-spheres of PHB loaded with Doxy as an antibiotic were used to coat Ti surfaces. In the study, PEG was also used as an antifouling agent to cover the Ti surfaces and at the same time connect them with the Doxy-loaded PHB spheres. Thus, the antibacterial activity of the titanium surfaces could be reinforced. The novelty of this study is the combination of these three different materials by means of covalent link via chemical reaction with alkoxysilanes.

Figure 4-1 shows a schema, which summarizes the different steps carried out in order to achieve the main goal of the study.

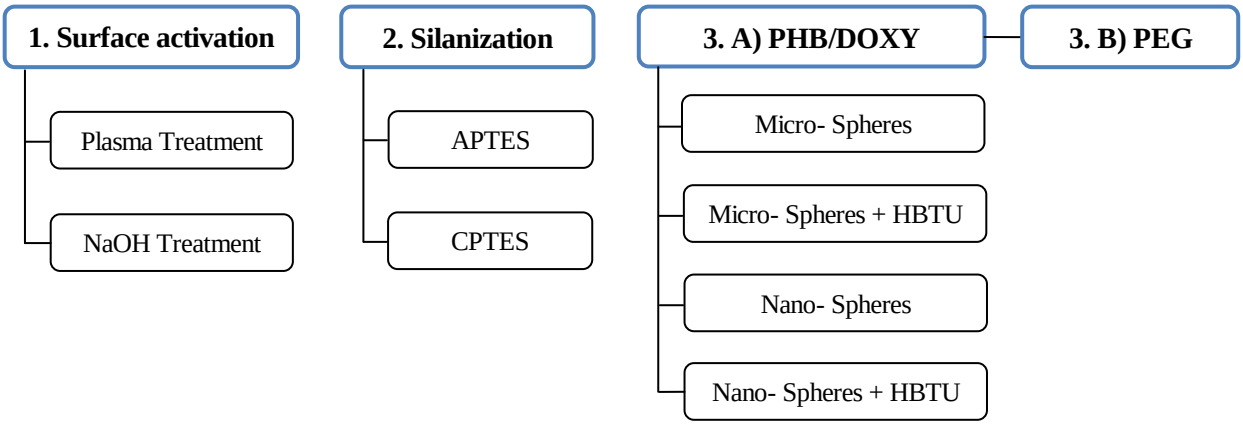

Figure 4-1. Scheme to achieve the main goal of the study

In the first step, two different activation methods have been compared in order to know the best choice for a proper biofunctionalization of titanium surfaces.

Plasma treatment is a method that increases the amount of OH groups on the surface of titanium [16]. OH groups react with the different organosilane structures on the next step and it increases the success probability on the silanization of titanium surfaces. The FESEM images of plasma treatment demonstrated that plasma did not modify the surface topography. However, the hydrophilicity of the surfaces with plasma treatment increased (the contact angle

was reduced) due to the increase of the OH group amount on the surface. This probes that plasma treatment was properly carried out (*Table 4-1*).

It is known that the chemical treatment with NaOH on the titanium surface produces a porous morphology [52]. Effectively, FESEM micrographies of the titanium samples so treated show more roughness and nano- size porous on the surface than the samples treated with plasma. The hydrophilicity increased for surfaces treated using both methods compared with c.p. titanium samples. However, contact angle results show lower hydrophobicity for the samples treated with plasma (*Table 4-1*). XPS results confirm that plasma presents higher amount of OH group on the surface. This explains the increase of the hydrophylicity of these titanium surfaces [18].

	Plasma Treatment	**NaOH Treatment**
OH OH OH TiSURFACE ACTIVATED WITH EITHER PLASMA OR NaOH	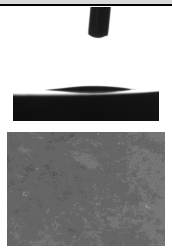	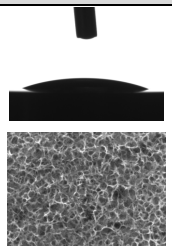

Table 4-1. Plasma and NaOH treatment. Structure, FESEM and Contact Angle

The second step is the functionalization of the titanium surfaces with two alkoxysilanes. Silanization is the most widely used method for the immobilization of biological molecules on model surfaces [33]. 3-Aminopropyltriethoxysilane and 3-Chloropropyltriethoxysilane (APTES and CPTES) were applied as alkoxysilanes on the metal in order to attach the antibiotic-loaded PHB particles and PEG, respectively. The characterization methods show that the APTES and CPTES silanizations took place. *Figure 4-2* shows a scheme of the theoretical reactions with APTES and CPTES.

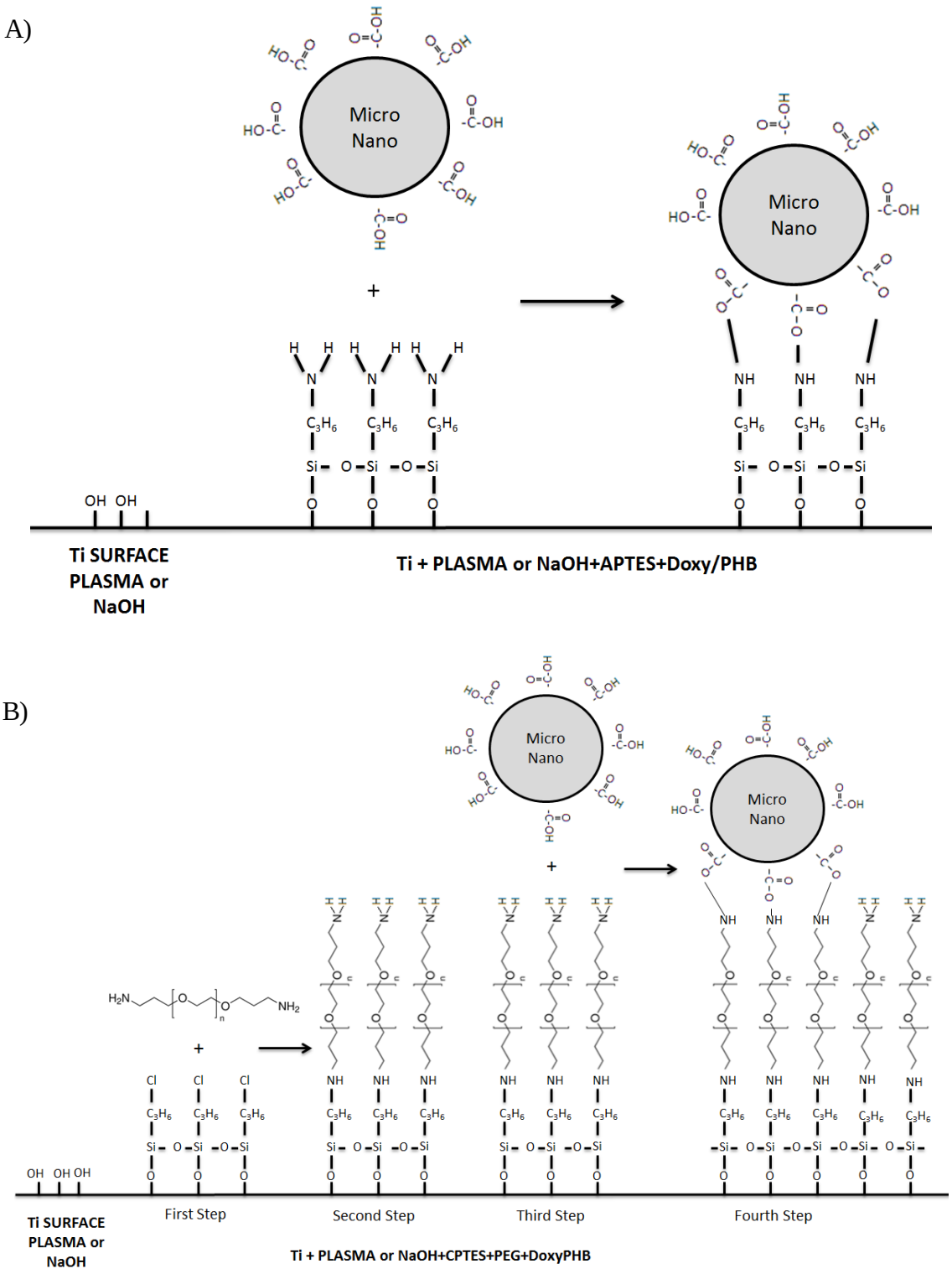

Figure 4-2. Scheme of theoretical reactions. A) APTES; B) CPTES

Figure 4-3 shows a scheme of the chemical reaction of APTES with the Titanium surface activated with either Plasma or NaOH treatment:

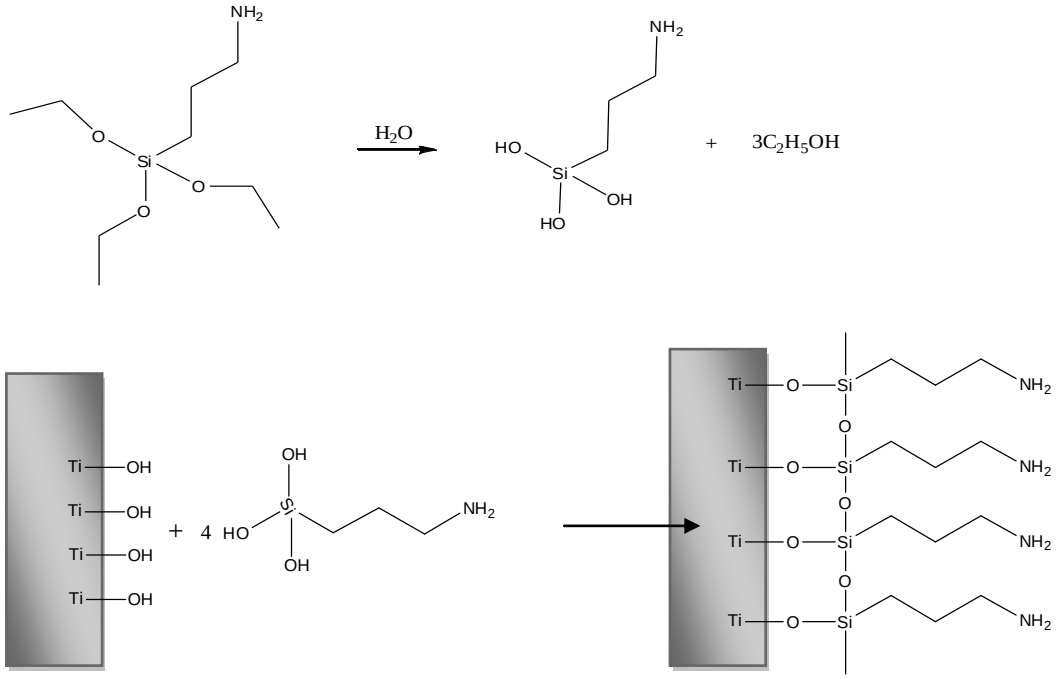

Scheme of the chemical reaction of APTES on the Titanium surface with PHB.

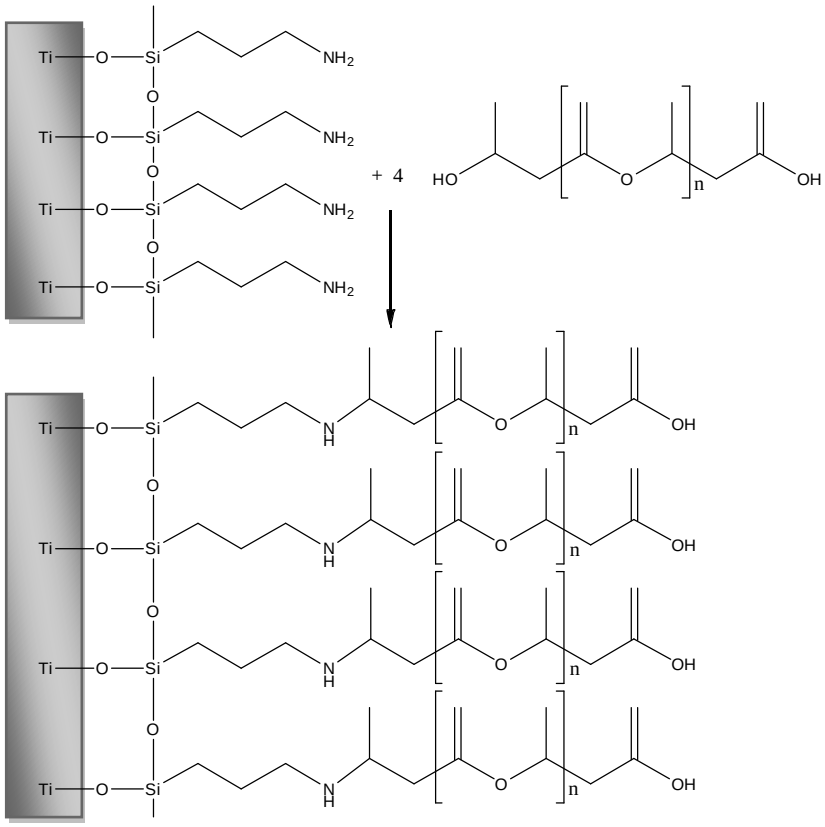

The general reaction is where R_2 can be an H as well:

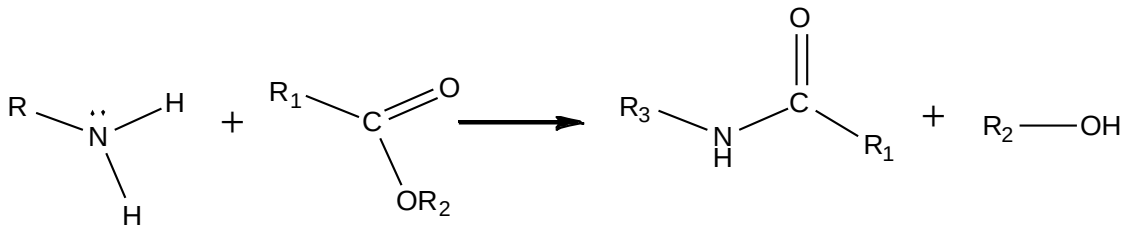

Figure 4-3. Scheme of the chemical reaction of APTES with Titanium surface activated with either Plasma or NaOH treatment

Figure 4-4 shows a scheme of the chemical reaction of CPTES with the Titanium surface activated with either Plasma or NaOH treatment:

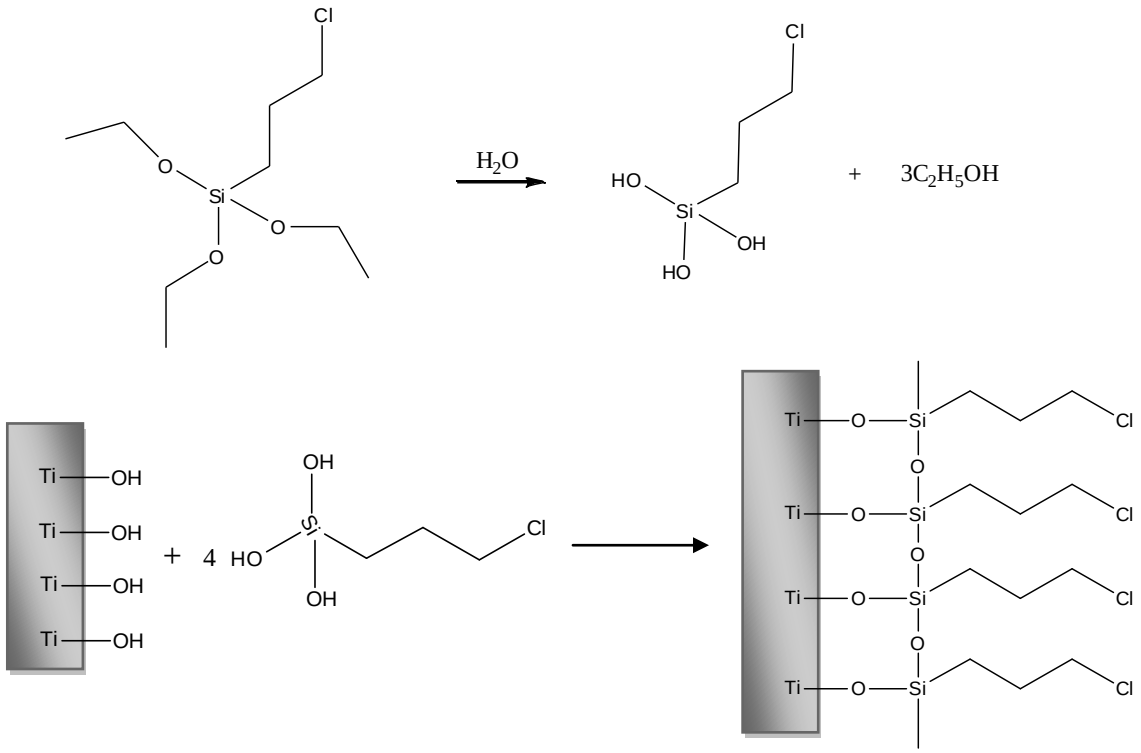

Scheme of the chemical reaction of CPTES on the Titanium surface and afterwards with PHB.

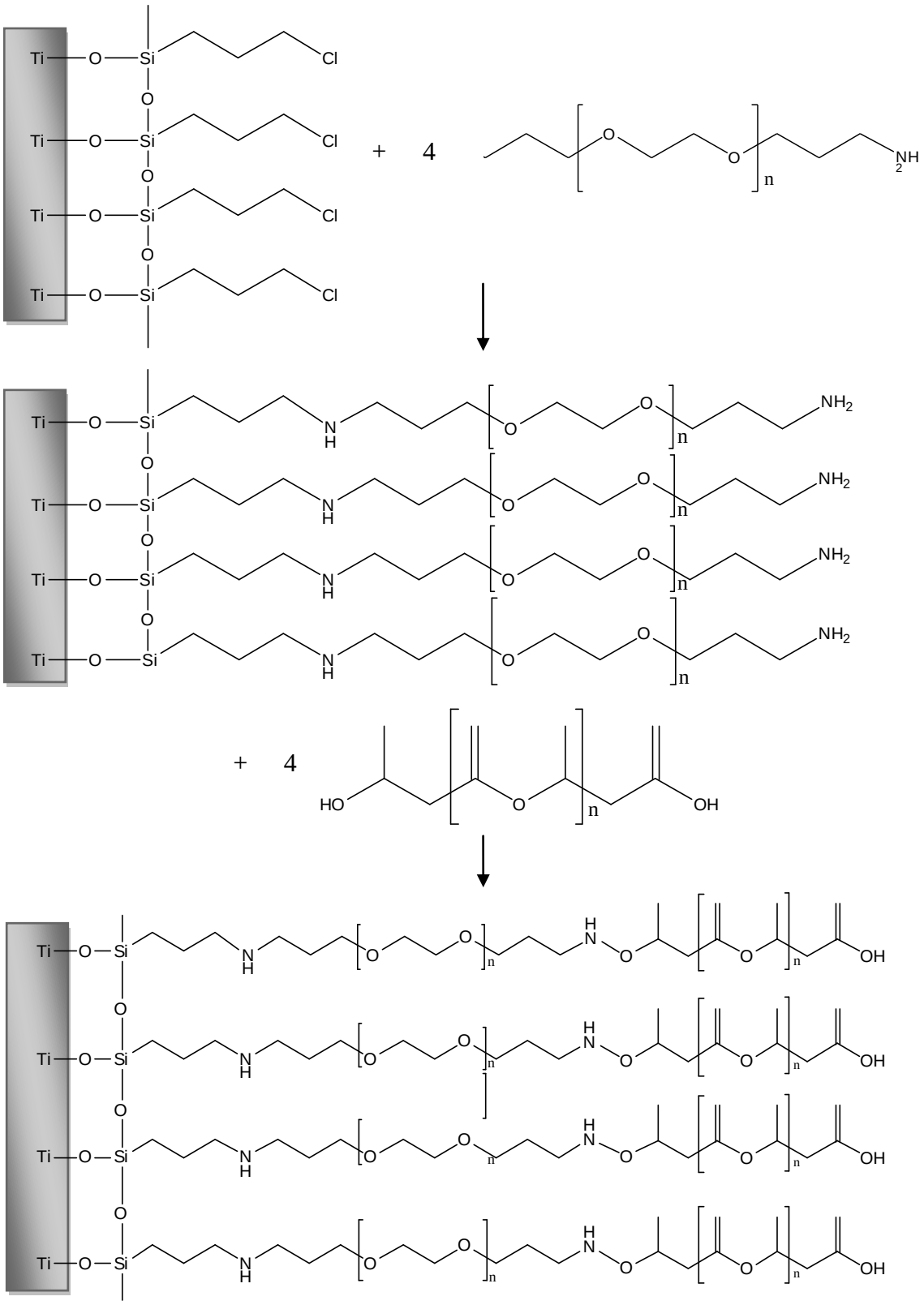

Figure 4-4. Scheme of the chemical reaction of CPTES with the Titanium surface activated with either Plasma or NaOH treatment

An increase in contact angle is a direct evidence for surface modification on the substrates. The contact angle of the titanium surface was increased by both APTES and CPTES. But the higher contact angle was with APTES silanization, the reason is that surfaces acquire different hydrofobicity depending on the chemicals groups deposited on them. In these cases, chlorine groups for CPTES is less hydrophilic than the primary amine group in APTES [17][33]. This is a first confirmation that both silanizations took place. Also, the presence of Nitrogen and Chlorine in the FESEM and XPS spectra, confirm the silanization reaction with APTES and CPTES respectively. A summary of all these evidences are shown in *Table 4-2*.

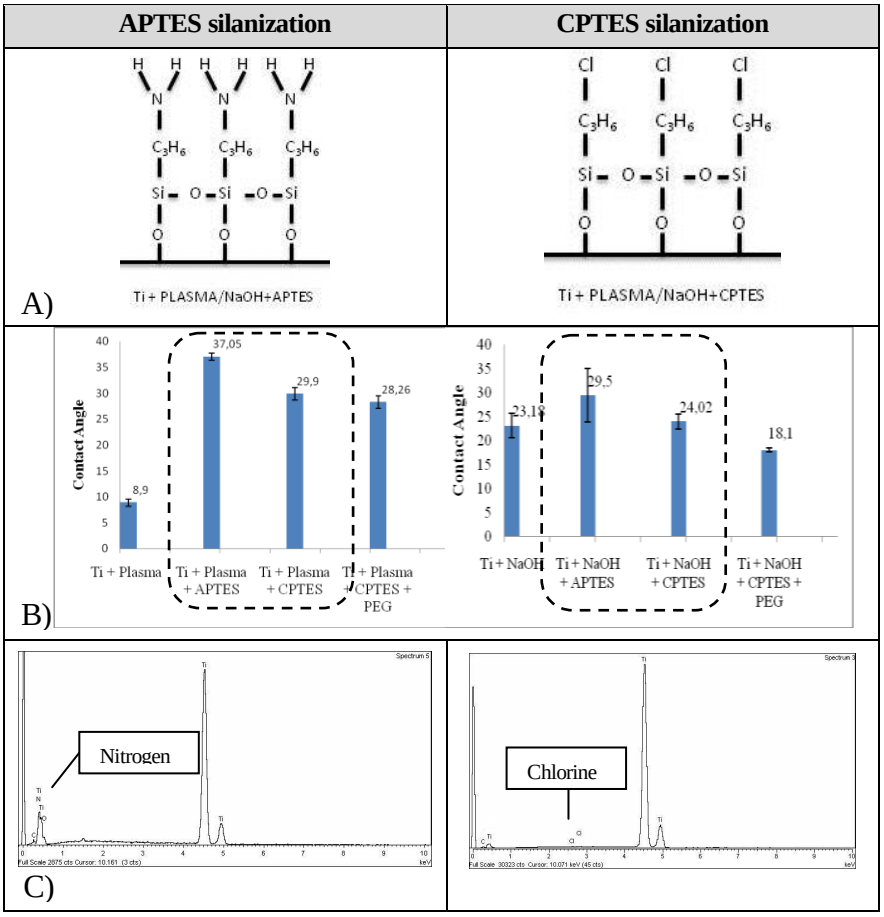

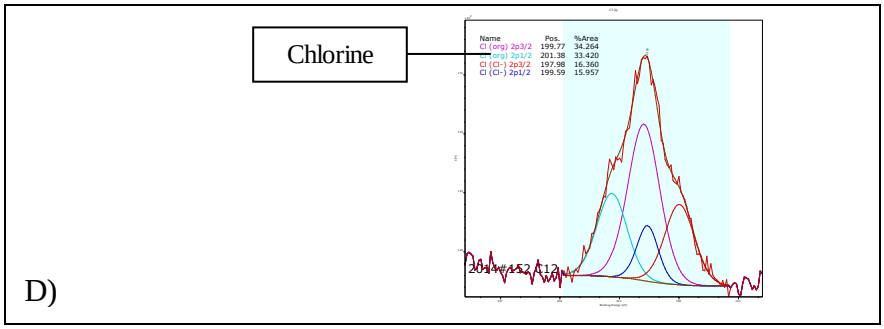

Table 4-2. APTES and CPTES Silanization. A) Chain. B) Contact angle. C) EDS spectrum. D) XPS

The novelty of this study is focused in the third step. After the titanium surfaces functionalization with two different alkoxysilanes, the addition of Doxy-loaded PHB spheres and PEG took place. This is the first time that this combination is arranged. FESEM micrographies give a qualitative evaluation of the amount of spheres attached on the surface of the samples. All samples were observed under FESEM and spheres were detected in practically all the surface of the samples, so the experimental attachment of the Doxy-loaded PHB spheres via APTES and CPTES with PEG was successful.

Regarding the functionalization with APTES, micro-particles were not linked to plasma treated titanium surfaces, and only nano-size particles were observed on these samples. The presence of nano-size particles is explained by the high particle-size dispersion of the Doxy-loaded PHB micro-particles. However, micro-spheres were possible to be attached on the titanium surfaces activated with NaOH. Maybe, the attachment reaction between the carboxylic acid of the PHB particles and the primary amines of the surfaces (whether APTES or difunctionalised PEG as well) is related to the specific surface and the roughness. In general, nano-sized spheres were better linked on the titanium surfaces than the micro-ones. They have more specific surface and are therefore more stable. Also, they show less size dispersion and the amount of them is higher [17][33].

HBTU is a coupling agent that is used for peptide synthesis in *Solid* phase. For this reason, it was used in this study instead of other coupling agents such as N-Hydroxysuccinimide, which is used in aqueous phase reactions [18]. In general, all samples where the Doxy-loaded PHB spheres were linked using HBTU show slightly better results compared to the samples were no coupling agent was used.

Figure 4-5 shows the scheme of the reaction with PHB, where R=PHB.

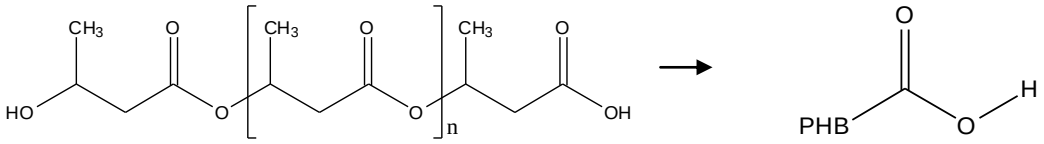

Figure 4-5. Scheme of the reaction with PHB

Then, the reaction of the PHB + HBTU with a primary amine is shown in the *Figure 4-6*

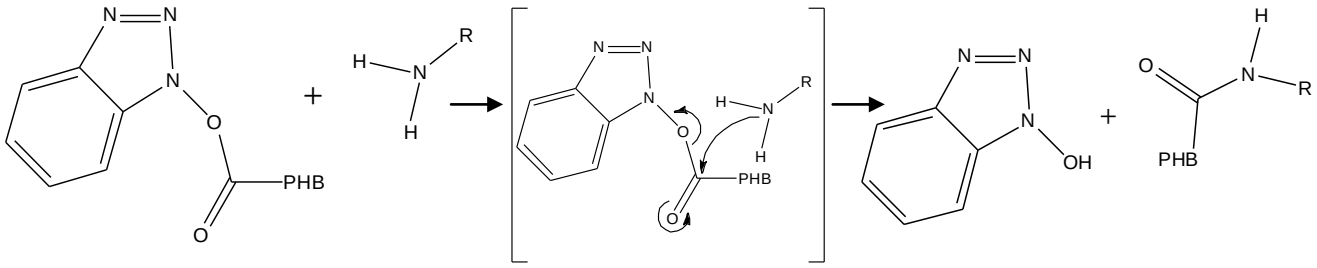

Figure 4-6. Reaction of the PHB + HBTU with primary amine

PHB reaction with the primary amine from APTES or from the difunctionalized PEG without HBTU:

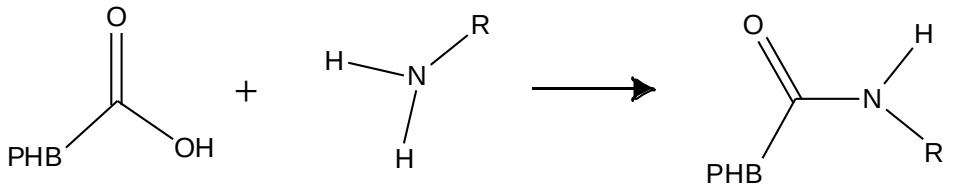

Figure 4-7. PHB reaction with the primary amine from APTES or from the difunctionalized PEG Carboxylic acids and primary amines condense to form an amide bond (condensation reaction). One reactant contains a carboxylic acid group (-COOH), this is the case of PHB, and the other reactant an amine group (-NH_2), this is the case of APTES or difuntionalised PEG. In this reaction the carboxylic acid loses its –OH group and the amine loses its –H. The lost atoms form H_2O and the nitrogen bonds to the carbon. The product of this reaction is an amide covalent bond.

On Titanium surfaces activated with NaOH treated, silanized with CPTES and PEG was successfully added. However, further attachment of the Doxy-loaded PHB spheres was not achieved for all samples. Only the sample Ti + NaOH + CPTES + PEG + Micro PHB shows spheres on the surface.

Regarding the functionalization with CPTES, the presence of PEG decreases the hydrophobicity compared to the treatments without it (CPTES control). This is because the chlorine at the end of the chain of CPTES links less with H_2O, and the NH_2 at the end of PEG bounds better with the H_2O molecules. This is an evidence of the surface changes by means of both reactions; with CPTES and with CPTES plus PEG. XPS and AFM analyses also give evidences of the presence of PEG in these samples. On one hand, AFM results show a coating above the titanium surface when samples with PEG were tested. This verifies that CPTES and PEG reaction took place. On the other hand, XPS shows the presence of Chlorine and Nitrogen peaks of the Titanium surfaces spectra. It is important to highlight that the two peaks visible in the deconvulation of the Nitrogen 1S (free amine -NH_2 and protonised amine NH_3^+) point out that the PEG chains are in the required and expected position for further PHB attachment [47][48][49]. The hydrophobicity of the samples corroborates this fact, since the samples with PEG are more hydrophilic than the ones with just CPTES (figure 4-3 B). Thus, is possible to dismiss the possibility of the double bonding of the difunctionalised PEG with the chlorine groups of the CPTES (figure 4-3 A).

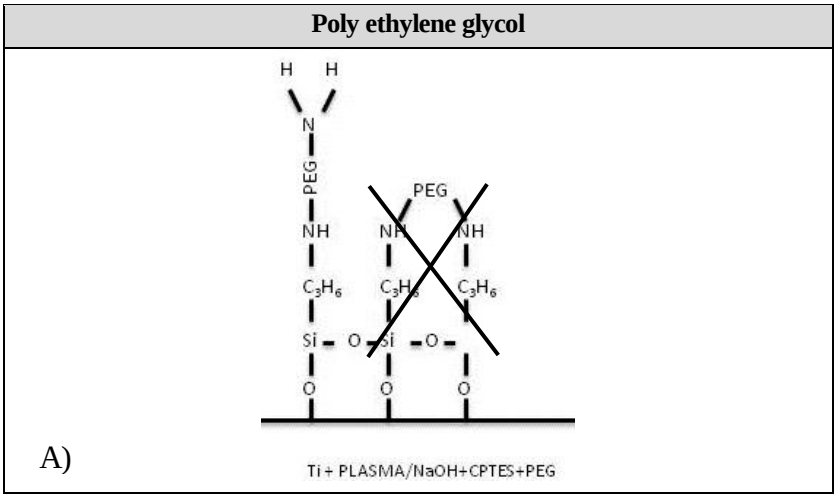

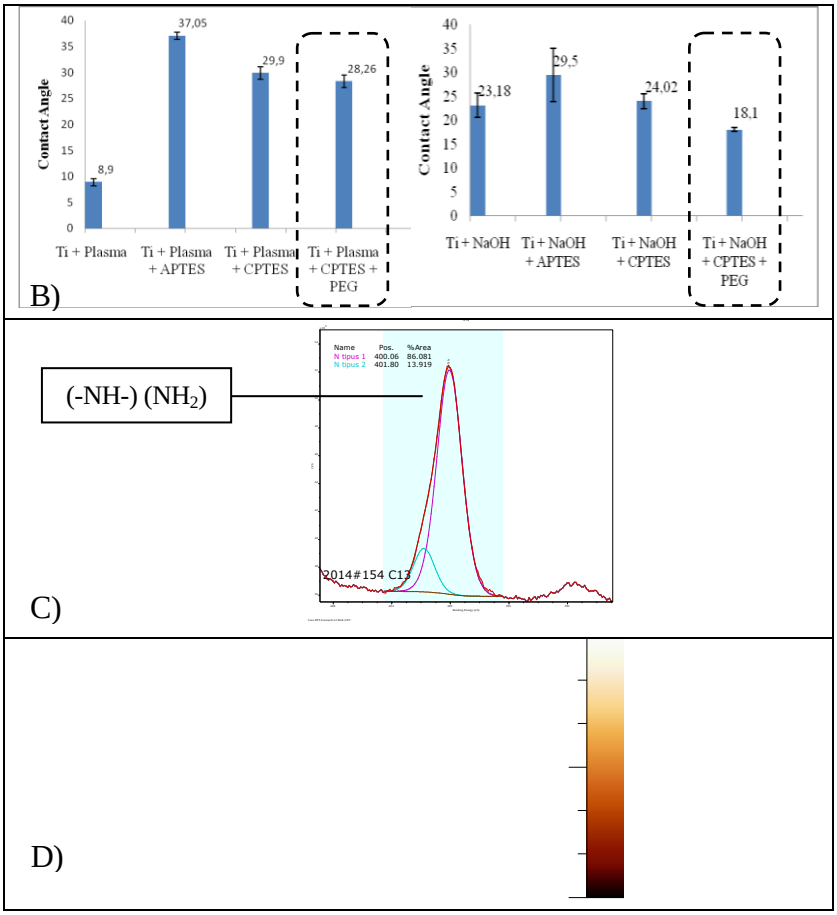

Table 4-3. PEG reaction. A) Chain. B) Contact angle. C) XPS. D) AFM

Ones the treatment was carried out and Doxy-loaded PHB particles were attached to the titanium surface together or not with PEG, Titanium treated surfaces were *in vitro* tested with *Escherichia coli* and *Staphylococcus aureus* as a Gram – and Gram + bacteria, respectively. An antibacterial assay was done in order to corroborate the antibacterial activity of the Titanium treated surfaces [51].

As it was commented on before, bacterial adhesions of all plasma treated samples with Ti+APTES+PHB/Doxy are below the control, except the sample with micro- spheres and HBTU. For this last sample, could be possible that less spheres where linked to the surface since only the smaller ones were finally attached. Thus, the presence of antibiotic on the surface was less.

Bacterial adhesions of samples with Ti+CPTES+PEG+PHB/Doxy with HBTU are below the control, indicating that the samples so treated improve the antifouling skill of the surfaces. On

one hand, because of the Doxy-loaded PHB spheres and its antibacterial activity, and on the other hand due to the PEG presence and its antifouling skills. However, the samples treated with no HBTU show an increase of the bacterial adhesion. Probably, the absence of this coupling agent provoked a lesser attachment of Doxy-loaded PHB spheres to the titanium surfaces and, thus, these samples show less antibacterial skills. (*Figure 4-8*).

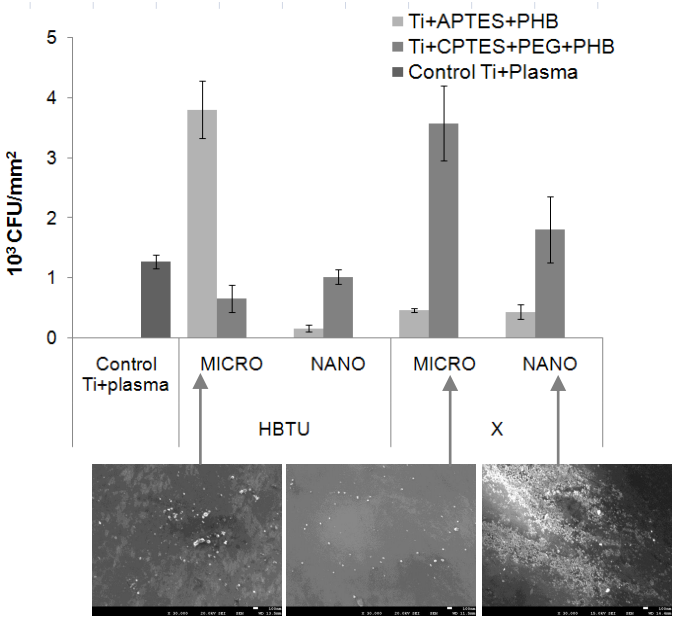

Figure 4-8. Bacterial count from the bacterial adhesion assay and microstructures. Plasma treatment. Bacteria: Escherichia Coli.

With NaOH Ti-activation treatment, micro- spheres were possible to be linked on the Titanium surfaces. However neither micro- nor nano-spheres were linked when CPTES was used as an alkoxsilane to link PEG. Only in the case where no HBTU was used, micro-spheres were added to the surface.

Bacterial adhesions of all samples with Ti+APTES+PHB/Doxy are below the control. The Doxy-loaded PHB spheres inhibit the bacterial proliferation and adhesion, specially the samples which show better sphere distribution as FESEM micrographs show (*Figure 4-9)*.

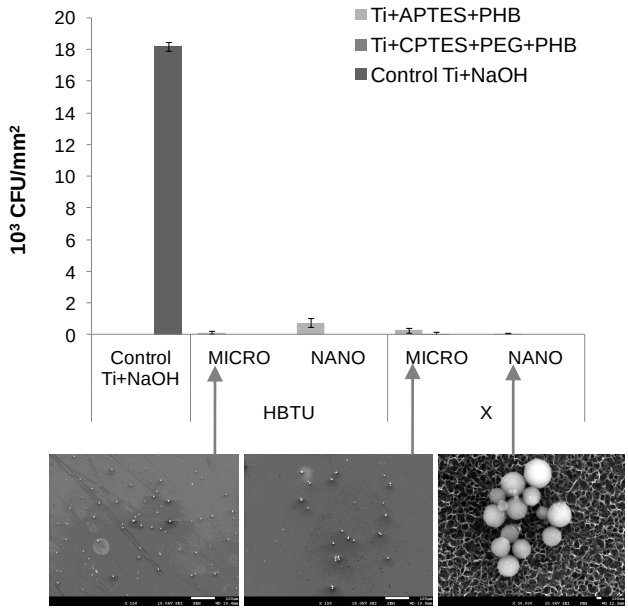

Figure 4-9. Bacterial count from the bacterial adhesion assay. NaOH treatment. Escherichia coli.

All plasma treated samples show a better antifouling and, therefore antibacterial, skills compared to the control. This is possible since *S. aureus* is more sensible to Doxycicline than *E. coli* [34]. Therefore, this assay could be considered to control the efficiency of the method.

CONCLUSIONS

The general objective of the study was successful achieved since a new method to combine the antibacterial properties of antibiotic-loaded Poly(3-hydroxybutyrate) particles and the antifouling ones of poly(ethylene)glycol with titanium has been developed.

The following secondary conclusions can be taken from the study:

- Optimal activation of the titanium surfaces with plasma and NaOH treatments was achieved. However, plasma treatment shows better activation capacity than NaOH.

- Optimal functionalization of the activated titanium surfaces with both alkoxysilanes, APTES and CPTES was achieved. Different characterization methods such as contact angle and XPS, confirm the presence of the alkoxysilanes.

- Covalent attachment of Doxycycline-loaded PHB spheres was successfully achieved by using APTES as an alkoxysilanes. In this case, plasma treatment for the activation of titanium surfaces can be considered a good alternative to attach nano-PHB particles, while NaOH treatment can be used for the attachment of both micro- and nano- spheres of PHB.

- The use of HBTU as a coupling agent show slightly better results compared to the samples were no coupling agent.

- Optimal covalent attachment of difunctionalised PEG was achieved. Different characterization methods such as contact angle, AFM, XPS, as well as the antibacterial assay confirm the presence of this antifouling agent.

- Covalent attachment of PHB spheres on the difunctionalised PEG was successfully achieved in the titanium surfaces activated with plasma. Titanium surfaces activated with NaOH show no attachment of the PHB particles when difunctionalised PEG was used.

- When the bacterial adhesion assay was carried out with *Staphilococos aureus* and *Escherichia coli,* all the titanium surfaces treated which showed antibiotic-loaded PHB spheres show good antifouling and, therefore, antibacterial skills compared to the raw titanium. To highlight, this results are clearer for *Staphilococos aureus* since it is more sensible to Doxycicline than *Escherichia coli.*

AKNOWLEDGEMENTS

No hagués estat possible que aquest projecte sortís a la llum sense l'ajut d'algunes persones.

Agrair a José Maria Manero, el director de projecte, per haver-me donat l'oportunitat de realitzar aquest projecte final de màster en el grup de biomaterials.

Vull agrair a una persona que ha sigut el meu pilar imprescindible en aquest projecte, la Sandra Rodríguez, sense ella no hauria pogut tirar endavant aquest tipus de treball. M'ha ajudat, ensenyat, aconsellat, animat, recolzat, corregit… gràcies a ella, a la seva comprensió, aportacions i gran entusiasme tinc aquest projecte finalment a les mans. Gràcies Sandra!

Agrair també a tota la meva família que m'estima incondicionalment i sempre m'ha estat recolzant, ajudant i animant a que seguís endavant sense rendir-me. Als meus pares, que no han deixat de confiar en mi en cap moment. A la Lidia, que m'ha recolzat i ajudat en el que ha pogut. A la meva iaia Rosa, que creu amb mi i em dona ànims per seguir endavant. Als meus tiets i cosins. Al Jordi, que sempre està al meu costat i m'ajuda a seguir endavant en tot moment. I al Màgnum. Amb ells tot és més fàcil!

I a totes aquelles persones que d'una manera o altre m'han anat ajudant al laboratori, Casimir, Judit, Meritxell... i als companys de feina, com la Míriam que m'ha animat i ajudat amb tot el que ha pogut.

Gràcies a tots!

REFERENCES

[1] DAROUICHE RO. *Treatment of infections associated with surgical implants*. England. 2004.

[2] ALCANTAR, ERAY S. AYDIL, JACOB N. Polyethylene glycol–coated biocompatible surfaces Journal of Biomedical Materials Research. 2000.

[3] BANERJEE I, PANGULE R C, KANE RS. Antifouling coatings: recent developments in the design of surfaces that prevent fouling by proteins, bacteria, and marine organisms. 2011.

[4] RATNER, D., HOFFMAN, S., SCHOEN, J., LEMONS, E. *An Introduction to Materials in Medicine*. USA, Elsevier Academic Press, 2004.

[5] BLACK, J. *Biological Performance of Materials*. New York, USA, Marcel Dekker, Inc. 3rd ed., 1999.

[6] BANDYOPADHYAY, A., BOSE, S. *Characterization of biomaterials.* USA, Elsevier, 2013.

[7] PROUBASTA, I., GIL MUR, J., PLANELL, J.A. *Fundamentos de Biomecánica y Biomateriales.* Madrid, Ediciones Ergon, 1997. p.291

[8] PARK, J., LAKES, R.S. *Biomaterials. An introduction.* New York, USA, Springer, 3rd ed., 2007.

[9] BERGERET A. *Environmental-friendly biodegradable polymers and composites, integrated waste management.* Volume I. Sunil Kumar. 2011

[10] MUDGAL S. *Plastic waste in the environment*. European Commission DG ENV. BIO Intelligence Service Report. 2011.

[11] HENESS, G., BEN-NISSAN, B. *Innovative Bioceramics.* USA, Vol. 27, 2004.

[12] MICHAEL M. DOMACH. *Introduction to Biomedical Engineering.* New Jersey, Pearson Prentice Hall, 2004.

[13] RAKHORST, G., PLOEG, R. *Biomaterials in Modern Medicine.* Singapore, World Scientific, 2007.

[14] KATSUBE, N., SOBOYEJO, W.O., SACKS, M. *Functional biomaterials.* Switzerland, Trans Tech Publications Ltd, 2001.

[15] TEXTOR, SITTING, FRAUCHIGER, TOSATTI, BRUNETTE. *Titanium in Medicine.* Berlin, Springer, 2001. *Pp 171-230.*

[16] BOEHM, H.P. *Discuss Faraday*. 52, 1971. 264.

[17] W. W. BALWANZ. *Plasma Cleaning of Surfaces.* Springer US. Alexandria, USA. 1979.

[18] SEVILLA P. *Functionalization of titanium surfaces with TGF-β inhibitor peptides.* PhD thesis dissertation. Barcelona, 2013.

[19] LIU, CHU, DING. *Surface modification of titanium, titanium alloys, and related materials for biomedical applications.* City University of Hong Kong. 2004.

[20] WANG, X., HAYAKAWA, S., TSURU, K., OSAKA, A. *Improvement of the bioactivity of H2O2/TaCl5-treated titanium after a subsequent heat treatment*. J. Biomed. Mater. 2000.

[21] HENDRICH, V.E. Rep. Prog. Phys. 48, 1965, 177.

[22] PARKS, G.A. Chem. Rev. 65. 1965. 177

[23] KURRAT, R., WÄLIVAARA, MARRTI, TEXTOR, TENGALL, RAMSDEN, SPENCER. *Biointerfases. Colloid. Spencer. 1998.*

[24] WILLIAMS, BROWN, MERRITT. *Biomaterials 9.* 1988. 181

[25] KNOB L.J., OLSON D.L. *Metals handbook: Corrosion.* Ninth ed. Vol 13. 1987, p. 669

[26] LUTJERING, WILLIAMS, GYSLER. *Microstructure and Mechanical Properties of Titanium Alloys.* Germany. Spencer. 1999.

[27] XIONG YC, YAO YC, ZHAN XY, CHEN GQ. *Application of polyhydroxyalkanoates nanoparticles as intracellular sustained drug-release vectors.* J Biomater Sci Polym. 2010.

[28] MADISON LL, HUISMAN GW. *Metabolic engineering of poly(3-hydroxyalkanoates): From DNA to plastic*. Microbiol Mol Biol Rev 63. 1999.

[29] WILLIAMSON DH, MELLANBY J, KREBS *HA Enzymic determination of D(-)-β-hydroxybutyric acid acetoacetic acid in blood*. 1961

[30] SUDESH K, ABE H, DOI Y. *Synthesis, structure and properties of Polyhydroxyalkanoates: biological polyesters*. Prog Polym Sci. 2000.

[31] KOLLER M, SALERNO A, DIAS M, REITERER A, BRAUNEGG G. *Modern Biotechnological polymer synthesis: A review. Biotechnological Polymer Synthesis, Food Technol Biotechnol*. 2010

[32] TRECCANI, KLEIN, MEDER, PARDIN, REZWAN. *Functionalized ceramics for biomedical, biotechnological and environmental applications.* Elsevier. Germany. 2012.

[33] LI D, TEOH WY, GOODING JJ, SELOMULYA C, AMAL R. *Functionalization strategies for protease immobilization on magnetic nanoparticles.* Funct Mater. 2010

[34] RODRIGUEZ, A., CANAL, C., CALAFELL, M., GINEBRA, M.P., JULIO, G., MARQUES, M. *Methods for the preparation of doxyxyxline-loaded PHB micro- and nano- spheres.* European Polymer Journal. 2013

[35] SHETH, LECKBAND. *Measurements og attractive forces between proteins and end grafted poly ethylene glycol chains.* Proc Natl Acad Sci, USA. 1997.

[36] BUDDY, ALLA, FREDERICK, JACK, JOSEPH. *Biomedical Engineering Desk Reference.* Elsevier. Oxford, UK. 2009

[37] GOLDSTEIN, J. *Scanning electron microscopy and x-ray microanalysis*. Kluwer Adacemic/Plenum Pulbishers, p. 689. 2003

[38] EGERTON, R. F. *Physical principles of electron microscopy: an introduction to TEM, SEM, and AEM.* Springer, p202, 2005

[39] FREEMAN-COOK, L., FREMAN-COOK, K. *Staphylococcus Aureus Infections.* Kuorkor Dzani. USA. 2006.

[40] HOWARD C. BERG. *E. Coli in Motion.* Springer. USA. 2004.

[41] SUSSMAN MAX. *Escherichia Coli. Mechanisms of virulence.*Cambridge University Press. UK. 1997.

[42] MORITA, WIESENDANGER, MEYER. *Noncontact Atomic Force.* Springer. Germany. 2002.

[43] EATON, P., WEST, P. *Atomic Force Microscopy.* Oxford University Press. 2010.

[44] WIESENDANGER, R. *Scanning Probe Microscopy and Spectroscopy: Methods and Applications.* Oxford University Press. 2010

[45] SMART, R. *X-ray Photoelectron Spectroscopy,* City University of Hong Kong. 2004

[46] YANWEI, Z. *Microstructural study by XPS and GISAXS of surface layers formed via phase separation and percolation in polystyren/tetrabutyl titanate/alumina composite films,* Materials Science and Engineering, 2006.

[47] TRUICA-MARASESCU, F., WERTHEIMER, M. *Nitrogen-rich plasma-polymer films for biomedical applications.* Interscience. Weinhelm, 2008.

[48] GRAF, YEGEN, GROSS, LIPPITZ, WEIGEL, KRAKERT, TERFORT, UNGER. *XPS and NEXAFS studies of aliphatic and aromatic amine species on functionalized surfaces.* Elsevier. Germany, 2009.

[49] ACRES, ELLIS, ALVINO, LENAHAN, KHODAKOV, METHA, ANDERSSON. *Molecular structure of 3-aminopropyltriethoxysilane layers formed on silanol-terminated silicon surfaces.* ACS Publications. Australia, 2011.

[50] WAGNER, RIGGS, DAVIS, MOULDER, MUILENBERG. *Handbook of X-Ray Photoelectron Spectroscopy.* Perkin-Elmer Corporation. Minnesota. 1979.

[51] RODRIGUEZ-HERNANDEZ, JUAREZ, ENGEL, GIL. *Streptococcus sanguinis adhesion on titanium rough surfaces: effect of shot-blasting particles.* Springer. Barcelona. 2011

[52] WANG, Z L. *Characterization of nanophase materials.* Wiley-VCH. Michigan. 2000

ANNEX

Summery all the assays

The next *Table 0-1* shows all the assays with the amount of samples for each method. The amounts of PHB + Doxycycline spheres and HBTU for each sample are described below:

ASSAY	SAMPLE NUM	PHB SPHERES	Ti ACTIVATION	PHB + Doxy (g)	HBTU (g)
TI + APTES + PHB	**1**	MICRO	Plasma	0,0091	0,3417
	2	MICRO	Plasma	0,0091	0,3417
	3	MICRO	Plasma	0,0091	0,3417
	4	MICRO	Plasma	0,0091	-
	5	MICRO	Plasma	0,0091	-
	6	MICRO	Plasma	0,0091	-
	7	NANO	Plasma	0,0093	0,3446
	8	NANO	Plasma	0,0093	0,3446
	9	NANO	Plasma	0,0093	0,3446
	10	NANO	Plasma	0,0089	-
	11	NANO	Plasma	0,0089	-
	12	NANO	Plasma	0,0089	-
	13	MICRO	NaOH	0,0099	0,3449
	14	MICRO	NaOH	0,0099	0,3449
	15	MICRO	NaOH	0,0099	0,3449
	16	MICRO	NaOH	0,009	-
	17	MICRO	NaOH	0,009	-
	18	MICRO	NaOH	0,009	-
	19	NANO	NaOH	0,0097	0,3477
	20	NANO	NaOH	0,0097	0,3477
	21	NANO	NaOH	0,0097	0,3477
	22	NANO	NaOH	0,0092	-
	23	NANO	NaOH	0,0092	-
	24	NANO	NaOH	0,0092	-
	25	MICRO	Plasma	0,01	0,3414
	26	MICRO	Plasma	0,01	0,3414
	27	MICRO	Plasma	0,01	0,3414
	28	MICRO	Plasma	0,0099	-
	29	MICRO	Plasma	0,0099	-

	30	MICRO	Plasma	0,0099	-
	31	NANO	Plasma	0,01	0,3411
	32	NANO	Plasma	0,01	0,3411
	33	NANO	Plasma	0,01	0,3411
	34	NANO	Plasma	0,0099	-
	35	NANO	Plasma	0,0099	-
	36	NANO	Plasma	0,0099	-
TI + CPTES + PEG + PHB	**37**	MICRO	Plasma	0,0089	0,3415
	38	MICRO	Plasma	0,0089	0,3415
	39	MICRO	Plasma	0,0089	0,3415
	40	MICRO	Plasma	0,0073	-
	41	MICRO	Plasma	0,0073	-
	42	MICRO	Plasma	0,0073	-
	43	NANO	Plasma	0,0101	0,3409
	44	NANO	Plasma	0,0101	0,3409
	45	NANO	Plasma	0,0101	0,3409
	46	NANO	Plasma	0,005	-
	47	NANO	Plasma	0,005	-
	48	NANO	Plasma	0,005	-
	49	MICRO	NaOH	0,008	0,3403
	50	MICRO	NaOH	0,008	0,3403
	51	MICRO	NaOH	0,008	0,3403
	52	MICRO	NaOH	0,0081	-
	53	MICRO	NaOH	0,0081	-
	54	MICRO	NaOH	0,0081	-
	55	NANO	NaOH	0,0051	0,34
	56	NANO	NaOH	0,0051	0,34
	57	NANO	NaOH	0,0051	0,34
	58	NANO	NaOH	0,0053	-
	59	NANO	NaOH	0,0053	-
	60	NANO	NaOH	0,0053	-
TI + APTES + PHB	**61**	MICRO	Plasma	0,0106	0,345
	62	MICRO	Plasma	0,0106	0,345
	63	MICRO	Plasma	0,0106	0,345
	64	MICRO	Plasma	0,0104	-
	65	MICRO	Plasma	0,0104	-
	66	MICRO	Plasma	0,0104	-
	67	NANO	Plasma	0,014	0,3457
	68	NANO	Plasma	0,014	0,3457
	69	NANO	Plasma	0,014	0,3457
	70	NANO	Plasma	0,015	-

	71	NANO	Plasma	0,015	-
	72	NANO	Plasma	0,015	-
	73	MICRO	NaOH	0,0106	0,3409
	74	MICRO	NaOH	0,0106	0,3409
	75	MICRO	NaOH	0,0106	0,3409
	76	MICRO	NaOH	0,0111	-
	77	MICRO	NaOH	0,0111	-
	78	MICRO	NaOH	0,0111	-
	79	MICRO	NaOH	0,0097	0,3414
	80	NANO	NaOH	0,0097	0,3414
	81	NANO	NaOH	0,0097	0,3414
	82	NANO	NaOH	0,0101	-
	83	NANO	NaOH	0,0101	-
	84	NANO	NaOH	0,0101	-
TI + CPTES + PEG + PHB	**85**	MICRO	Plasma	0,0102	0,3423
	86	MICRO	Plasma	0,0102	0,3423
	87	MICRO	Plasma	0,0102	0,3423
	88	MICRO	Plasma	0,0102	-
	89	MICRO	Plasma	0,0102	-
	90	MICRO	Plasma	0,0102	-
	91	NANO	Plasma	0,0114	0,343
	92	NANO	Plasma	0,0114	0,343
	93	NANO	Plasma	0,0114	0,343
	94	NANO	Plasma	0,0106	-
	95	NANO	Plasma	0,0106	-
	96	NANO	Plasma	0,0106	-
	97	MICRO	NaOH	0,0107	0,349
	98	MICRO	NaOH	0,0107	0,349
	99	MICRO	NaOH	0,0107	0,349
	100	MICRO	NaOH	0,0111	-
	101	MICRO	NaOH	0,0111	-
	102	MICRO	NaOH	0,0111	-
	103	NANO	NaOH	0,0102	0,3433
	104	NANO	NaOH	0,0102	0,3433
	105	NANO	NaOH	0,0102	0,3433
	106	NANO	NaOH	0,0107	-
	107	NANO	NaOH	0,0107	-
	108	NANO	NaOH	0,0107	-

Table 0-1. General information of the samples

The following *Table 0-2* shows the control samples with each method in order to compare the results with the others methods.

CONTROLS	**C1**	TI	**C18**	TI+NaOH
	C2	TI+PLASMA	**C19**	TI+NaOH+APTES
	C3	TI+PLASMA+APTES	**C20**	TI+PLASMA
	C4	TI+NaOH	**C21**	TI+PLASMA+CPTES
	C5	TI+NaOH+APTES	**C22**	TI+ PLASMA+CPTES+PEG
	C6	TI+PLASMA	**C23**	TI+NaOH
	C7	TI+PLASMA+APTES	**C24**	TI+PLASMA+CPTES
	C8	TI+PLASMA	**C25**	TI+PLASMA+CPTES+PEG
	C9	TI+PLASMA+CPTES	**C26**	TI+PLASMA+PHB MICRO
	C10	TI+PLASMA+CPTES+PEG	**C27**	TI+ PLASMA+PHB+NAN
	C11	TI+NaOH	**C28**	TI+PLASMA+PHB MICRO+HBTU
	C12	TI+NaOH+CPTES	**C29**	TI+PLASMA+PHB NANO+HBTU
	C13	TI+NaOH+CPTES+PEG	**C30**	TI+NaOH+PHB MICRO
	C14	TI+PLASMA+PHB	**C31**	TI+NaOH+PHB NANO
	C15	TI+NaOH+PHB	**C32**	TI+NaOH+PHB MICRO HBTU
	C16	TI+PLASMA	**C33**	TI+NaOH+PHB NANO HBTU
	C17	TI+PLASMA+APTES		

Table 0-2. General information of the controls

X-ray Photoelectron Spectroscopy

The next Table 0-3 shows the results of the characterization with XPS.

		Ti+NaOH				**Ti+Plasma**	
		POSITION	STD DEV	AREA (%)	STD DEV	POSITION	AREA (%)
C 1s		284,82	0,11			284,83	
	C-C, C-H	284,80	0,01	63,94	8,84	284,8	62,094
	C-O, C-N	286,24	0,06	18,60	3,15	286,14	18,956
	C=O	288,05	0,04	17,47	5,70	288,15	18,95
O 1s		530,02	0,11			530,03	
	O^{2-}	529,92	0,06	57,73	2,85	529,85	48,072
	Ti-O-Si, OH^-	531,25	0,01	34,25	1,75	531,2	44,299
	H_2O	532,87	0,08	8,02	4,60	532,93	7,629
Ti 2p		458,42	0,11			458,43	
	TiOX 2p3/2	458,45	0,06	51,14	0,23	458,47	51,261
	TiOX 2p1/3	464,15	0,07	48,86	0,23	464,17	48,739

		Ti+NaOH+CPTES		**Ti+plasma+CPTES**	
		POSITION	AREA (%)	POSITION	AREA (%)
C 1s		284,89		284,91	
	C-C, C-H	284,81	64.127	284,80	64,78
	C-O, C-N	286,19	18.950	286,20	19,63
	C=O	288,02	16.923	288,13	15,59
O 1s		529,99		530,01	
	O^{2-}	529,85	58.379	529,86	49,95
	Ti-O-Si, OH^-	531,16	36.593	531,23	44,17
	H_2O	532,79	5.028	532,64	5,87
Ti 2p		101,7			
	TiOX 2p3/2				
	TiOX 2p1/3				
Si 2p		101,7		102,11	
	O-Si-O	101,91	100	102,13	100,00
Cl 2p		199,601		199,81	
	Cl org 2p3/2	199,77	34.264	199,74	44,64
	Cl org 2p1/2	201,38	33.420	201,35	43,54
	Cl^- 2p3/2	197,98	16.360	197,35	5,98
	Cl^- 2p1/2	199,59	15.957	199,60	5,84

		Ti+NaOH+CPTES+PEG		Ti+PLASMA+CPTES+PEG	
		POSITION	AREA (%)	POSITION	AREA (%)
C 1s		285,01		284,86	
	C-C, C-H	284,82	55,49	284,80	61,99
	C-O, C-N	286,22	27,13	286,22	21,96
	C=O	287,98	17,39	288,14	16,05
O 1s		530,01		529,96	
	O^{2-}	529,92	61,47	529,87	51,45
	Ti-O-Si, OH^-	531,12	32,29	531,17	40,69
	H_2O	532,81	6,25	532,64	7,86
Cl 2p		200,01		199,76	
	Cl org 2p3/2	200,39	20,94	199,56	50,62
	Cl org 2p1/2	202,00	20,43	201,17	49,38
	Cl^- 2p3/2	198,47	29,68		
	Cl^- 2p1/2	200,08	28,95		
N 1S		400,12		400,06	
	-NH-, NH2	400,06	86,08	400,08	96,20
	NH_3^+	401,80	13,92	401,84	3,80

Table 0-3. XPS Results